INFLUENCE OF WEATHERING AND STRESS RELIEF ON GEOTECHNICAL PROPERTIES OF ROADCUT MASS AND EMBANKMENT FILL ON ST. VINCENT AND ST. LUCIA

CHISHALA MULENGA
March, 2015

SUPERVISORS:
DR. H.R.G.K. HACK
PROF. DR. V.G. JETTEN

INFLUENCE OF WEATHERING AND STRESS RELIEF ON GEOTECHNICAL PROPERTIES OF ROADCUT MASS AND EMBANKMENT FILL ON ST. VINCENT AND ST. LUCIA

CHISHALA MULENGA
Enschede, The Netherlands, March, 2015.

Thesis submitted to the Faculty of Geo-Information Science and Earth Observation of the University of Twente in partial fulfilment of the requirements for the degree of Master of Science in Geo-information Science and Earth Observation.
Specialization: Applied Earth Sciences (Engineering geology)

SUPERVISORS:
Associate Professor, DR. H.R.G.K. HACK
Professor, DR. V.G. JETTEN

THESIS ASSESSMENT BOARD:
Professor, DR. F.D. VAN DER MEER (Chair)
DR. IR. S. (SIEFKO) SLOB (External Examiner, Witteveen + Bos Raadgevende ingenieurs B.V., Deventer, The Netherlands)

ABSTRACT

Weathering and stress relief can have a profound influence on geotechnical properties of rock and soil masses of volcanic origin within the engineering lifetime. When an exposure is made in a rock mass, discontinuities develop due to stress relief. Weathering starts from the surface of the exposure and from the surface of discontinuities penetrating the rock inside with time. Slopes and embankment failures have been widely reported in the steep and rugged volcanic terrains of St. Vincent and St. Lucia. Hence, the need to investigate the influence of weathering and stress relief on deterioration of geotechnical properties of volcanic rock and soil masses in road cuts and embankments, and establish how weathering and stress relief impact the stability.

The "simple means" methods and SSPC system are used to determine the basic geotechnical parameters important for slope stability and deterioration assessment in cut slopes. The BS standards are used to determine properties important for geotechnical parameters in both slopes and embankments. In cut slopes, analyses showed that the intact rock strength (SIRS), Cohesion (SCOH), and angle of internal friction (SFRI), deteriorated as the degree of weathering and exposure time increases. Assessments of future stability also showed that almost all units will become unstable before the end of engineering lifetime. The engineering lifetime is taken as 50 years.

Embankments are constructed using cut and fill methods. Analyses showed that these were constructed at heights beyond which the shear strength parameters could sustain the embankments, and hence, were only supported by artisanal retaining structures. The presence of kaolinite, chlorite, and montmorilonite clay minerals in fill materials suggested that weathering could have contributed to deterioration in shear strength, leading to failures. Another possible cause of failure is reported or assumed by many to be ground water recharge due to higher precipitation levels in the area in recent times. However, for this no evidence has been found.

ACKNOWLEDGEMENTS

I express gratitude to the Dutch government through NUFFIC, for the opportunity granted to me to pursue my MSc study at the University of Twente, Faculty ITC. My sincere gratitude also goes to my employers the Zambian government for granting me study leave without hesitation.

My sincere and profound gratitude goes to my first supervisor Dr H R G K Hack for his vivid and critical comments and provision of scientific direction towards my thesis. I also extend my gratitude to my second supervisor Prof. Dr V G Jetten for his valuable comments despite his extremely busy schedule. I am grateful to Drs B D smith for his help in laboratory work and his critical advice on the results. My appreciation also goes to Dr Liz Holcombe of the University of Bristol for her support.

My humble thanks goes to the staff of AES and ESA departments, my colleagues and the ladies in student affairs, for all the support they gave me during my stay and stride to achieve this goal.

Special thanks go to my wife: Kasonde and son: Emmanuel, who had to move miles to come and give me support and for their patience throughout. I am indebted to you.

Above all I thank the almighty God for bringing me this far, and to him I give all the glory. For I can only do all things through Christ who strengthens me (Philippians 4:13).

TABLE OF CONTENTS

LIST OF FIGURES

LIST OF TABLES

1. INTRODUCTION

1.1. Research background

Natural and man-made slopes exist in all parts of the world. However, countries that are located in mountainous regions continuously face slope stability challenges when constructing infrastructure, e.g., roads. In Saint Vincent and Saint Lucia islands which are of volcanic origin, roads constructed along the hill slopes act as the only means for motor vehicle transportation. Therefore, when road-cuts are made on the slopes of these mountains, instabilities occur. Thus, the resulting failures are often an economical nuisance (Hoek et al., 2000). However, to ensure the safety of citizens and road traffic from failure of the slopes and embankments, an assessment of the geotechnical properties governing stability of mass in the road corridor is necessary (Kainthola et al., 2014).

Failure of cut slopes and embankments before the end of their engineering lifetime sometime after construction have been attributed to the deterioration of rock and soil masses, resulting from weathering and stress relief (Hack & Price, 1997; Tating *et al.*, 2013). In addition, poor compaction and differential settlement of fill materials may also lead to instability of embankments (Price et al., 2009). The stability of these structures generally depends upon the shear strength of materials, geometrical and strength characteristics of discontinuities, degree of weathering, slope geometry, pore water pressures or seepage forces, loading, and environmental conditions (Homand and Souley, 1996; Hack et al., 2003). The influence of these geotechnical properties and factors to stability in volcanic formations is governed by the composition and mass characteristics of rocks and soils. This characteristic behaviour is controlled by the nature of in-situ weathering conditions in which they are formed (Anderson & Holcombe, 2013).

A number of studies have been done on the effect of weathering on slope mass and its assessment methodologies in volcanic rocks, (Schmidt, 1981; Tuğrul & Gürpinar, 1997; Karpuz, 1997; Rijkers & Hack, 2000; Orhan et al., 2006; Vallejo *et al.*, 2007; Arıkan *et al.*, 2007; del Potro & Hürlimann, 2008; Crosta *et al.*, 2012 ; Pola *et al.*, 2014). Of these, only a few researches have been conducted in the study area. Anderson & Kneale (1980, 1985) examined and derived empirical relationships between precipitation and pore water pressure with ultimate slope stability in Saint Lucia. Further, Anderson (1982, 1983) formulated two pore water pressure prediction models, reported as capable of predicting pore-water pressures to an acceptable level of accuracy from the knowledge of only storm precipitation, material permeability and topography in road cut slopes. This study also confirmed that by use of stability envelopes, topography, which is reported to be a controlling factor for soil-water potential in slopes, loses its control as permeability of the material decreases. Furthermore, Anderson et al., (2007, 2011) and

Anderson & Holcombe, (2013) assessed slope stability and landslides directed at unplanned settlements and communities only. However, with regard to these previous researches in the study area, none has directly addressed the influence of weathering to geotechnical properties of materials in the road corridors. Only brief references have been made to the subject in these tropical volcanic rocks of Saint Vincent and Saint Lucia.

1.2. Research problem

Road alignments and embankments in both flat and mountainous areas are planned for a certain engineering life time (Price *et al.*, 2009; Tating *et al*, 2013), and thereafter maintained to re-achieve the allowable design safety factor (US Army Corps, 2010). However, if failure of the structure occurs before its envisaged lifetime, it becomes an economical constraint especially in developing nations were resources are scarce. In this case, the Caribbean Islands of Saint Vincent and Saint Lucia having rugged and steep mountainous terrain face the challenge of road-cut slope failures. The islands' routes for the road alignments are strictly limited because of terrain, which is associated with steep slopes. Therefore, when failures occur, they typically affect road operations and can be costly to repair. If near the streams and channel crossings, they have an added risk of impact to water quality and marine reserve. As a way to mitigate these hazards, this research is aimed at helping the designers of future roads in this region to develop an optimal plan that address maintenance of slope stability. Bell (1992) and Huisman (2006) described weathering as one of the prominent factors that could reduce the stability of a slope by weakening (via extension, solution, alteration) of a rock mass in terms of its geotechnical applications. Therefore, the optimal plan could be achieved by incorporating in the initial road design, the influence of weathering and future weathering on geotechnical properties of engineering materials. The resulting safety factor should enable designed structures to be stable in their envisaged engineering lifetime.

Thus, this research seeks to relate the influence of weathering on geotechnical properties of exposed volcanic rock masses and embankment fill materials, to potential causes of slope failures along the road corridor. In establishing this relation, future stability on rock mass in Saint Vincent and Saint Lucia transport corridors will be forecast.

1.3. Research objective

This research work will address the following main and specific objectives.

1.3.1. Main objective

To determine the influence of weathering and stress relief on deterioration of geotechnical properties of volcanic rock and soil masses in roadcut slopes and embankment fill, and establish how this impacts the stability.

1.3.2. Specific objectives

- Characterize and classify the geotechnical properties of roadcut mass and embankment fill material.
- Compare minerals, texture, and structure important for geotechnical properties of source quarry material and embankment fill.
- Determine the correlation between weathering and changes in geotechnical properties of roadcut mass and embankment fill at various degrees of weathering.
- Determine time related deterioration of geotechnical properties of roadcut mass and embankment fill material to forecast future stability.

1.4. Research questions

- Specific objective one
    - What are the geotechnical properties of the slope mass and embankment material?
    - Which clay mineralogical units are identified in rock mass and embankment material?

- Specific objective two
    - What type of clay mineralogy, texture and structure important for geotechnical properties constitutes the borrow pit and embankment material?

- Specific objective three
    - What is the degree of weathering in slopes and embankment materials?
    - What is the change in geotechnical properties of rocks and soils in each weathering class?

- Specific objective four
    - What is the relation between the degree of weathering and change in geotechnical properties of rock mass and fill?
    - What is the underlying mechanism of weathering and weathering susceptibility in slope mass?
    - What is the link between the changed geotechnical properties of rock mass and fill material due to weathering with slope stability of the assessed slopes?

1.5. Data sources

The geotechnical data was collected from previous and present relevant available data from literature, fieldwork, and laboratory analysis.

1.6. Thesis structure

- Chapter one covers the general introduction
- Chapter two covers the literature review
- Chapter three describes the study area
- Chapter four covers the overall research methods
- Chapter five covers field data description
- Chapter six covers analyses, results and discussion
- Chapter seven conclusions and recommendation

2. LITERATURE REVIEW

2.1. Rock mass deterioration in cut slopes

Deterioration of an excavated slope occurs within its engineering lifetime. Therefore, understanding the deterioration and degradation processes of rock masses in time is important as these processes lead to reduced future stability of cut slopes (Nicholson, 2000; 2003). Cut slopes may be referred to as excavated slopes. Their stability is very much governed by the state of rock mass geometry and strength of discontinuities. A rock mass is described by ISO (2003) as "rock together with its discontinuities and weathering profile". While Hack (1998) gave a detailed description as "a mass of rock blocks with or without discontinuities and or inhomogeneity and with anisotropy". Rock mass deterioration in cut slopes starts immediately after excavation by exposure to influence of local atmospheric agents (air and water). This process starts on both the slope surface and rock inside. Deterioration is a time dependent process resulting from stress relief and weathering (Hack & Price, 1997). Its controls and influences at the rock mass scale include the nature of the rock mass in terms of its discontinuity network and structure. These are the static and dynamic stress conditions such as residual and gravitational stresses, and quarry blasting, the atmospheric environment of exposure in terms of climatic regime, and fluctuations in temperature and moisture, the engineering design factors like the slope geometry and stabilisation measures, and the time since excavation (Nicholson, 2000; Hack, 2008; Tating *et al.*, 2013).

2.1.1. Stress relief

When a natural slope is excavated, the confining pressure and stress regime in the slope rock mass changes. The release and variation in confining pressure provoked by removal of material during excavation causes development of new joints and opening of existing discontinuities (Hencher and Knipe, 2007; Miščević & Vlastelica, 2014). The variation in stress increase and concentration may lead to rock fracturing and loss of structure (Price et al., 2009). Thus, the development of new joints and fractures speeds up physical weathering and enables deeper penetration of chemical weathering effects on a rock mass (Hack,1998; Huisman, 2006).

2.1.2. Weathering of rocks and rock masses

Weathering is the mechanical and chemical process that causes the disintegration and decomposition of rocks, and is responsible for the formation of residual soils which control surface morphology (Hack & Price, 1997). Price (1995) described weathering as "the irreversible response of soil and rock materials and masses to their natural or artificial exposure to the near-surface geomorphologic or engineering environment". This implies that weathering of a rock mass affect significantly the integrity and durability of a rock slope after excavation. It further affects the rock mass through weakening of engineering properties, i.e., intact rock strength, fabric and strength of discontinuities (De Mulder et al., 2012).

Weathering processes of rocks and rock masses depends upon local conditions such as surface and ground water, local climate, and to an extent land use. The susceptibility to weathering of rocks and rock masses depends upon their composition; and in general, the more clayey the rock, the greater is its susceptibility. For instance, if Shale and sandstones are found in an interlayered rock mass exposure, and Shale is considered more susceptible than sandstone, differential form of weathering could occur on such an exposure, as the weathering in shale would be more than that of sandstone (Hack, 1998). Therefore, three processes involved in rock weathering are discussed as follows:

- Physical (mechanical) weathering
- Chemical weathering
- Biological weathering

Physical weathering leads to the opening and propagation of discontinuities by intact rock fracturing, and progressively breaking down the original rock mass to residual material. These mechanical processes dominate in cold and dry climates and occur in two forms, freeze-thaw weathering, and exfoliation as shown in figure 1.

Chemical weathering, however, results in chemical changes in mineralogy, texture and structure (Price et al., 2009). This form of weathering involves the processes of carbonation, hydrolysis, oxidation and reduction, as presented by Selby (1993), Price et al. (1995) and the Geological Society (1995). Biological weathering processes are caused by the presence of vegetation through root wedging and production of organic acids, and to lesser extent by animals. Both chemical and biological weathering processes tend to be more active in warm and humid climates. Below is some of the representative chemical weathering reaction equations 2.0, 2.1, 2.2, and 2.3:

"Carbonic acid" reactions

Involve dissolved atmospheric CO_2 or CO_2 respired by plants

$$CO_2 + H_2O \Leftrightarrow \underset{\text{"carbonic acid"}}{H_2CO_3} \Leftrightarrow \underset{\text{"bicarbonate"}}{H^+ + HCO_3} \quad (2.0)$$

$$2\,KAlSi_3O_8 + H_2O + 2\,H_2CO_3 \rightarrow Al_2Si_2O_5(OH)_4 + 2\,K^+ + 2\,HCO_3^- + 4\,SiO_2 \quad (2.1)$$

K-feldspar -> kaolinite (clay)

Oxidation reactions

"Oxidation" is removal of an electron from an ion (e.g. $Mn^{2+} \rightarrow Mn^{3+} + e^-$)

$$\underset{\text{from silicate}}{2\,Fe^{2+}} + \underset{\text{dissolved } O_2}{1/2\,O_2} + 2\,H_2O \rightarrow \underset{\text{hematite } (Fe^{3+})}{Fe_2O_3} + 4\,H^+ \quad (2.2)$$

Hydration / hydrolysis reactions

Depend on pH - acid vs. alkaline conditions

$$NaAlSi_3O_8 + H^+ + H_2O \rightarrow Al_2Si_2O_5(OH)_4 + Na^+ + 3\,SiO_2 \quad (2.3)$$

Na-feldspar (albite) -> kaolinite (clay)

A combination of these three weathering processes explained above leads to a general weakening of rocks, owing to alteration of minerals, the growth of voids, and disintegration (Ebuke et al., 1993). Thus, basically the consequences of weathering are dependent on climate, lithology, mineralogy, microtexture and structure of the original rock as well as the various processes and rates (Bell, 1992; Geological Society of London, 1995). Therefore, several researchers have studied the effect of weathering on engineering properties of rocks and rock masses (Ruxton and Berry, 1957; Saunders and Fookes, 1970; Onedera et al., 1974; Saito, 1981; Ramana & Gogte, 1982; Bell, 1992; Irfan, 1996; Tugrul, 2001; Lee et al., 2004; Borrelli et al., 2007; Calcaterra and Parise, 2010). These have reported that weathering involves important processes and its effect on rock mass generally decreases with depth, although differential weathering can occur in some zones which results into modification of simple layered sequence of weathering. They have further suggested that beyond a specific degree of weathering, there is substantial degradation and alteration in the initial basic mineralogical and fabric characteristics of original geomechanical index properties of intact rocks that make up a rock mass. Their results furthermore affirm that quantitatively, weathering of a rock mass can be assumed as a predisposing factor to slope instability.

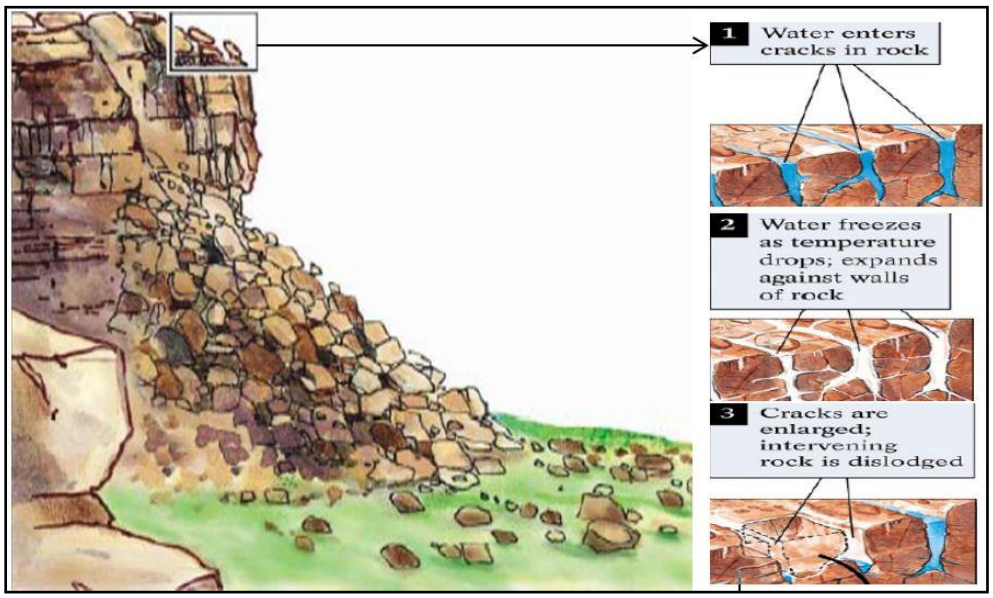

Figure 1: Rock fracturing and progressive breakdown stages of freeze-thaw cycles (after Martinati, 2003).

2.1.3. Weathering of volcanic rocks and rock masses

The geotechnical behaviour, nature of formation, and weathering of volcanic rocks and materials differ significantly with respect to non-volcanic materials and rocks (Serrano, A., Olalla, C., & Hernandez-Gutierrez, 2007). Thus, knowledge of the style of volcanic rocks weathering is required in order to interpret correctly the nature of mass weathering of exposed slopes in volcanic formations. The susceptibility of volcanic rocks to weathering and their rate of decomposition depends on the rock composition stability conditions and climate at the time of formation (Goldich, 1938). The temperature, pressure, and other environmental conditions such as water and air, that are present at time of rock

crystallisation play a critical role (del Potro & Hürlimann, 2009). Volcanic rocks formed at the surface are mostly at equilibrium with surface conditions, and are less susceptible to weathering, such as the felsic rocks. Volcanic rocks that solidify underground at high temperatures are not at equilibrium and are more susceptible to weathering on exposure to surface conditions as shown in table 1 below. All rock types (table 1) on weathering eventually form clay minerals of varying character, table 2.

Table 1: Susceptibility of igneous rock-forming minerals to weathering (Fell et al., 2005)

Temperature of formation	Susceptibility to weathering	Mineral	Common igneous Rock types
Highest	Highest	Olivine	
			Basalt, dolerite, gabbro
		Calcic Feldspar	
		Augite	Andesite, diorite
		Hornblende	
		Sodic feldspar	
		Biotite	
			Rhyolite, granite
		Muscovite	
Lowest	Lowest	Quartz	

Table 2: The susceptibility of other common minerals to weathering (Fell et al., 2005)

Group	Mineral	Effects of weathering
Carbonates	Calcite	Readily soluble in acidic waters
	Dolomite	Soluble in acidic waters
Evaporites	Gypsum	Highly soluble
	Anhydrite	Highly soluble
	Halite (common salt)	Highly soluble
Sulphides	Pyrite and various other pyritic minerals	Weather readily to form sulphates, sulphuric acid and limonite
Clay minerals	Chlorite	Weathers readily to other clay minerals and limonite
	Vermiculite	Weathers to kaolinite or montmorillonite*
	Illite	Weathers to kaolinite or montmorillonite*
	Montmorillonite	Weathers to kaolinite
	Kaolinite	Stable**
Oxides	Haematite	Weathers to limonite
	Ilmenite	Stable
	Limonite	Stable

When volcanic rocks are exposed by excavation, discontinuities may develop because of stress regime changes (chapter 2.1.1). Weathering penetrates and eats into the rock material beginning at the joints. The zone of weathered material increases and widens around joints until rounded corestones of almost fresh rock begin to float in a matrix of fine to coarse-grained material. Weathering of volcanic deposits produces various types of clay minerals (table 2). Pyroclastic ash and basalts of vesicular nature, on weathering, produces halloysite a clay mineral which replaces etched plagioclase crystals with a sharp contact and may

occur as vermicular, or as massive cavity filling or replacement in fractures and joints (Hay, 1959b; Bates, 1962). Thus, due to the complex nature of volcanic rock mass weathering, investigating weathering through visual field mapping and laboratory may offer a good opportunity for better results. Although using borehole data may also be appropriate, it is likely to give a lot of uncertainties (BS 10-5930:1999, 1999). This is asserted that a rock mass may wrongly be classified as fresh when a drill core has penetrated through sequential corestones, or as weathered when drilled through the matrix (figure 2). Thus, a number of researchers have studied weathering and its effects on volcanic rock masses, (Schmidt, 1981; Tuğrul & Gürpinar, 1997; Karpuz, 1997; Rijkers & Hack, 2000; Orhan *et al.*, 2006; Vallejo *et al.*, 2007; Arıkan *et al.*, 2007; del Potro & Hürlimann, 2008; Crosta *et al.*, 2012 ; Pola *et al.*, 2014). They have reported that due to the nature of formation of volcanic rock masses, which could be matrix or clasts supported or may occur as massive lava flows, discontinuities are a major influence to spatial distribution of weathering profiles and stability. They have further indicated that some volcanic materials are already weathered at time of deposition, resulting from denudation, erosion, or mass wasting. This has been reported to complicate the definition of weathering profiles. However, defining the weathering intensity has been reported as being done by using the weathering grade and type clay mineral products. Other indicators used are the mobile oxides (MgO, CaO, and Na2O) which have been found to decrease, while iron oxides and the loss on ignition percentage have been seen to increase in most volcanic rocks. They furthermore report that by use of geomechanical laboratory tests, the strength of most volcanic rocks has been found as generally controlled by weathering. Observations conducted in the field as well as laboratory mineralogical analyses have established that the effect of weathering and its penetration was critical to slope stability. This is due to the substantial degradation in geotechnical properties of volcanic rocks, reported to occur beyond a certain degree of weathering.

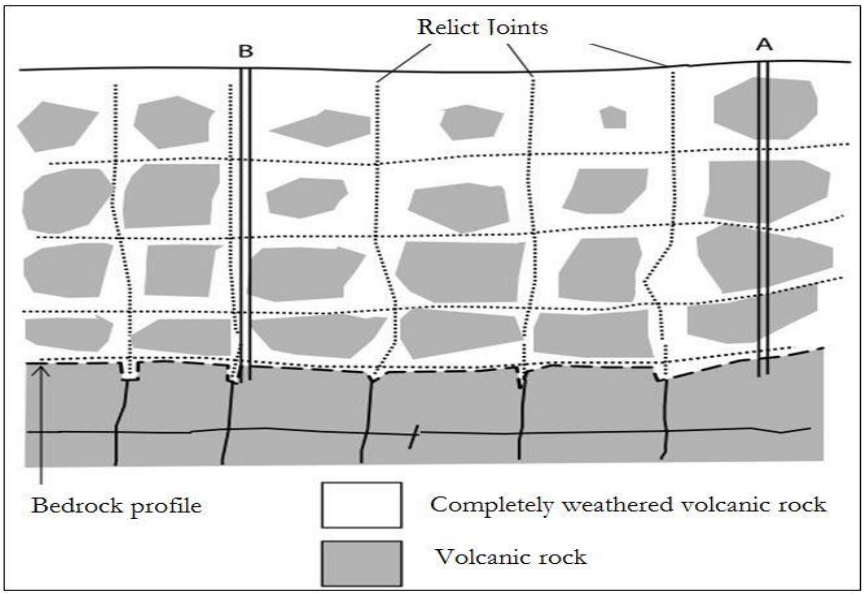

Figure 2: Corestones weathering in volcanic rocks. Borehole A would appear to be in almost solid rock; borehole B in volcanic matrix (Modified after Price, 1995)

2.1.4. Weathering in time; weathering rates

Weathering rate could be looked upon as a measure of loss of material per unit area over a certain amount of time (Thomas, 1994; Thomas et al., 2005). In many cases the erosional transfer of sediments and solutes are therefore used as an approximation for the weathering rate. Phillips (2005) defines weathering rate as the rate at which parent material is converted to weathering products and residuals. The thickness and degree of weathering is a product of the rate and duration (Taylor & Eggleton, 1992), and the depth of regolith is the product of a balance between the rate of production by weathering processes and the rate at which products of weathering are removed by erosion (Hachinohe et al., 2000; White & Brantley, 2003). In cut slopes, these processes normally happen when a natural slope is excavated and the rock mass is exposed to the surface environment (Pacheco & Alencoão, 2006). The rock mass and minerals in it are out of equilibrium and will tend to interact with available physical and chemical agents for geomorphic stability. Hence, due to the heterogeneity mineralogical character of most rocks and rockmasses, quantification of the physical and chemical weathering processes and rates is difficult (Fookes et al, 1988); thus, these processes and rates are most commonly expressed empirically as logarithmic time functions (Colman 1981). Therefore, Bland & Rolls (1998), and Huisman (2006) suggested an interactive set of factors that are said to determine the intensity of weathering in artificial slopes as falling into three categories:

1. Internal: rock and soil material and mass properties such as permeability, discontinuities, and material composition.
2. External: parameters like topography, vegetation, and climate, which are related to the weathering environment.
3. Geotechnical: parameters related to slope design such as aspect, slope angle, height, method of excavation, and drainage measures.

The internal and external parameters are both functions of time and to an extent, some geotechnical parameters are likely to change over time on site. This makes weathering to be a dynamic process. Some of the controlling factors to which the type, rate and extent of weathering depend upon (Goldich, 1938), are explained as follows:

- **Rock Type:** determines the resistance of the rock to the weathering processes that operate in that particular environment. Different rock types are composed of unique set of minerals. These minerals are joined together by chemical bonding, crystallisation, and or cementation. Weathering begins the moment these rocks are exposed to the atmosphere from the subsurface environment in which they have been formed.
- **Rock Structure**: highly jointed or faulted rocks present many planes of weakness along which weathering agents (e.g. water) can penetrate into the rock mass
- **Climate:** dictates the type of weathering processes that operate in a particular area, and largely determines the amount of weathering agents (i.e. water, temperature) available at which the

processes occur. Chemical reactions are enhanced by higher temperatures, and frost wedging usually occurs in colder climates.

- **Topography**: the slope angle determines the energy of the weathering system by controlling the rate at which water passes through the rock mass profile. In general, dynamic weathering systems are more pronounced in higher and tectonically active areas having steeper slopes, while weathering systems in flat plains are slower.
- **Erosion:** the effectiveness and dynamic state of erosion determines how rapidly any weathered material is removed, how frequently fresh rock is exposed to weathering, and if deeply weathered profiles are preserved.
- **Time:** time frame or duration in which the same type of weathering has been operating, uninterrupted by climatic change, earth movements, and other factors, determines the degree and depth to which the rocks have been weathered.

2.1.5. Fill material and weathering

BS 10-5930:1999 (1999) describes fill as "made ground in which the material has been selected, placed and compacted in accordance with an engineering specification". It may be pieces of intact rock, or if soil-grained, it may be described as soil, and if larger, it may exhibit the characteristics of a rock mass. However, for most highway constructions, stable granular materials are used as fill, although economy often dictates the placement of the closest available material, regardless of their composition, except they contain highly compressible organic constituents (Terzaghi, K., Peck, B. R., Gholamreza, 1996). Nevertheless, weathering has a profound effect on roughness of the circumference of fill material grains. It causes material grains to become smoother with time and thus reducing their angle of internal friction (Hack & Price, 1997). Reduction in angle of internal friction results in reduced shear strength (Price et al., 2009). During the weathering action, the particle sizes are reduced forming clay minerals and fine clayey materials which cause a decrease in permeability and subsequent increase in pore water pressure (Anderson, 1982; Nishiyama & Matsukura, 2006). The clay fraction affects the soil compressibility or its consolidation under load as it depends on the permeability; the compression rate depends on the rate of moisture release from the soil. Thus, decrease in permeability and rise in pore water pressure may also lead to dissolution of cement materials and reduced cohesion and tensile strength (Rao, 1996). These mechanisms may cause instabilities as the original slope or embankment cannot sustain the material anymore.

Further, the mechanism of material weathering and particle-size reduction leads to increased susceptibility to erosion (Holtz & Kovacs, 1981). Erosion may cause undercutting of slopes and embankments, and may lead to daylighting of water fissures especially along the contact between fill and slope profile. Resulting is the instability of cut slopes and embankments infrastructure (US Army Corps, 2010). Although in mountainous areas, cut and fill methods are widely used for construction of road embankments, the durability of materials, which is governed by texture, porosity or permeability and mineralogical

composition, is not guaranteed. Therefore, the mixture of soils and rocks is expected to exhibit a differential form of weathering due to variations in material properties, mineralogy and particle sizes (Bell, 1992).

2.1.6. Assessment of weathering

The complex and heterogeneous nature of rocks and rock masses, especially those of volcanic origin, makes the assessment of weathering a complex phenomenon (Marinos & Hoek, 2001; Moon & Jayawardane, 2004). This has led to difficulties in the quantification of weathering processes, rates and sequences in various rocks and rock masses, and thereby attracting various researches in the recent past. Nevertheless, most studies have given particular attention to the strength, the character and distribution of discontinuities, and the weathering grade (Dearman, 1976). Although the strength and discontinuities may be dealt with in isolation for a part of the rock mass being described, the same is not the case for weathering grade. Weathering grades are determined by comparing the attributes of a particular grade with those of grades lower in the standardized scale. Therefore, a number of methods and standards exist for assessment of weathering. These may be expressed as:

- Chemical indices comparison method ((Aires-Barros, 1978 and Hodder 1984)
  - Weathered material and unweathered parent rock material (Moses *et al.,* 2014)
  - Geochemically mobile to relatively immobile elements (Hodder 1984, Thomson *et al*., 2014)
  - Mineralogy in weathered material and unweathered parent material (Gupta & Rao, 2001;Duzgoren-Aydin *et al*., 2002)
- Standardized classification and rating systems often referred to as verbal descriptive approach. This approach uses reduction values for geotechnical parameters and slope stability assessment depending on the expected weathering degree at end of engineering life time. These standards fall in a category of (BS 10-5930:1999, 1999), SSPC (Hack et al., 2003), Mining Rock Mass Rating MRMR (Laubscher, 1990) and Q-system (Barton et al., 1974).
- Mechanical index properties methods: tests done by strength estimates using the geological hammer, Schmidt hammer, pocket knives, hands, and index property tests (Schmid, 1981; Karpuz , 1997; Pola et al., 2014).

2.2. Mineralogy, lithology and weathering

A slope may not homogenously be made up of a single lithological body that represents one physical and genetic unit. Usually, in most cases slopes are made from a lithological complex of rocks of different geological origin or scale. Thus, each unit may have rock material properties controlled by varying mineral composition, texture, fabric and the weathering state (Irfan, 1996). For instance, in the research areas of Saint Lucia and Saint Vincent, rock formations are basalts, andesites, agglomerates, pyroclastics and tuffs. These rock units may react differently to local conditions on exposure to the surface environment, since

they are formed at varying temperatures and pressure fig (2-2). Other studies conducted elsewhere in similar types of geological formations, have observed that due to susceptibility variances, differential form of weathering in such environments is often the case (Gabler *et al.*, 2009; Admassu et al., 2012). Different rock type materials and their alteration products have inherently different weaknesses and strengths resulting from their origin and conditions during formation, and subsequent history (Piteau, 1975). Thus, the most important aspect of the rock properties is its natural mineral assemblage and the strength of constituent minerals. Rocks are not stronger if the bond between mineral constituent assemblages is weak (Anon, 1961). The strength of the rock depends not only on the strength of mineral component, but also on the character of the bond between the mineral constituting the rock unit (Savanick & Johnson, 1974).

2.3. Geotechnical parameters

Before any geotechnical analysis can be performed, the parameter values required for analysis must be determined. These geotechnical parameters may be grouped as mass and material characteristics, and secondary exposure characteristics. For this research, however, most of these parameters will be obtained by simple means field methods proposed by among others Hack (2003). The importance of rock mass geotechnical properties is recognized in geotechnical engineering as paramount in controlling slope stability (Bray & Hoek, 1981). Therefore, during site investigations, the data collected included:

- Mass characteristics

  Weathering state, geometrical and strength characteristics of rock mass discontinuities
- Material characteristics

  Nature, strength and state of rocks and soil masses, which may include intact rock strength (IRS), texture and structure, colour, particle and grain size, rock or soil type and its accessibility; and
- Secondary exposure parameters

  Date and method of excavation, geology, and external influences

These characteristics and parameters have a considerable engineering value and are relevant to stability analysis of cut slopes (Hack, 1998; Hack, et al., 2003). The intact rock strength of a material can be a good indicator to its susceptibility to weathering, for example, while fractures may act as lines which promote preferential weathering and release surfaces for the generation of rock falls and frequently control the precise nature of rock block detachments or slope failures (Bell, 1992).

2.4. Slope stability analysis

The study and analysis of slopes are essential for understanding their performance and in particular their stability, reliability and deformations. Therefore, geotechnical engineers often seek to calculate values of quantitative indicators of performance such as the factor of safety (FoS) against failure, the magnitude of vertical or lateral deformation and the probability of failure. Thus, many techniques for slope stability assessment have been developed over the years. Pantelidis, (2009) reviewed a number of rock mass slope

stability assessment classification systems and reported that each of the existing rock mass classification systems deals with specific type of failures. An observation, however, was made that for slope cuts along highways, specific or unique classification systems could be used which are able to encompass all or most of the common types of failures. A further recommendation was made that such a system should be able to handle or examine each type of failure independently, since each particular slope could be governed by specific instability factors. In the study of slope stability evolutions conducted by Aryal (2006), the principal difference between Limit equilibrium methods (LE) and finite element methods (FE) methods was analysed and it was found that the LE methods are based on the static of equilibrium whereas FE methods utilise the stress-strain relationship or constitutive law. Further, Pourkhosravani & Kalantari, (2011) and Nuric et al., (2013) in their analysis of methods reported that the accuracy and choice of method for slope stability analysis using the Limit equilibrium methods, Numerical methods, Limit Analysis methods or the Artificial Neural Network method only depends on few important factors, which are the location of the slope and the shape of a probable slip surface. Therefore, in adopting a classification system and software package that fits with the methodology and technics of this research, the analyses of the methods made above are adopted in this thesis. As such, it should be noted that the main objective of the study is not to review assessment methods but rather to determine the influence of weathering on geotechnical properties of volcanic rocks and soil masses in slopes and embankment fill materials, and then assess the impact of this influence on the selected slope stability.

3. DESCRIPTION OF STUDY AREA

3.1. Location and topography

Saint Vincent and Saint Lucia are located within the Caribbean Windward Islands of the Lesser Antilles arc which extend south from 15° 45' to 11° 45' North latitude and from 60° 45' to 62° 00' West longitude (figure 3 and 4). It stretches about 850 km long from the South American Venezuela boundary to the north Anegada passage boundary of the Greater Antilles, and has an approximate curvature radius of 450 km (Bouysse, 1984). Saint Vincent has area of 389 km^2 and Saint Lucia 616 km^2. Their topography is rugged with steep slopes, on average 20 percent of the area has slopes less than 20 degrees. The average heights above sea level are 950m and 137m respectively. Structurally the islands are aligned along a north-south axis on the subduction zone boundary between the North American and Caribbean plates (Lindsay et al., 2005). In both islands, slope gradients falling along the west of the central axis are significantly greater than gradients on the east. Numerous sharp lateral ridges radiate from these steep highlands of the central range. Deep-cut Valleys and high vertical coastal cliffs characterize the leeward side (west coast) of the islands, while on the windward coast the valleys tend to be wider and flatter, opening into a fairly flat coastal plain. Although no field evidence of faulting has been found, almost all the major river courses on the island appear to be structurally controlled (Lindsay *et al.*, 2002).

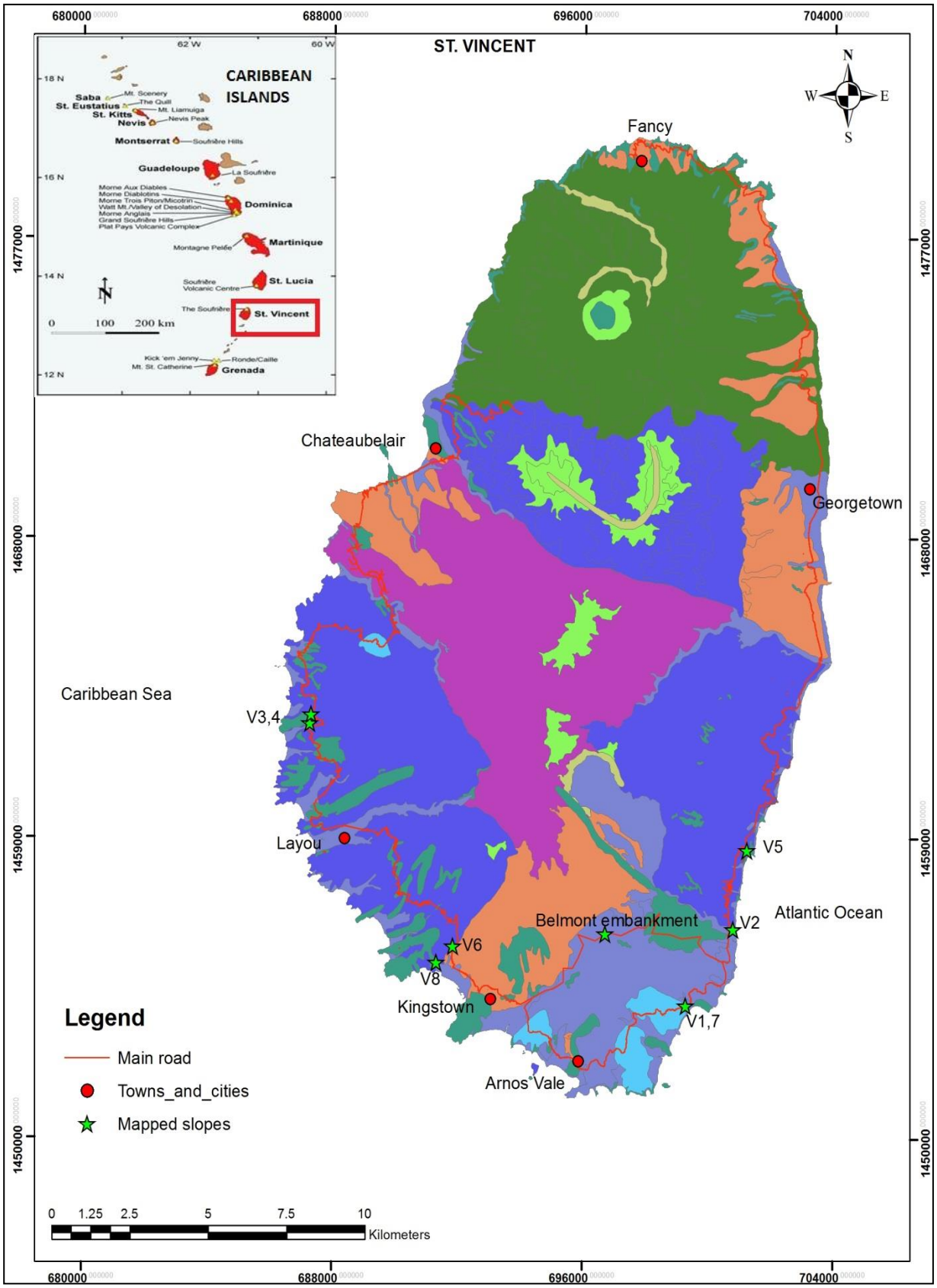

Figure 3: Location of the research area – St. Vincent (after Lindsay et al, 2002)

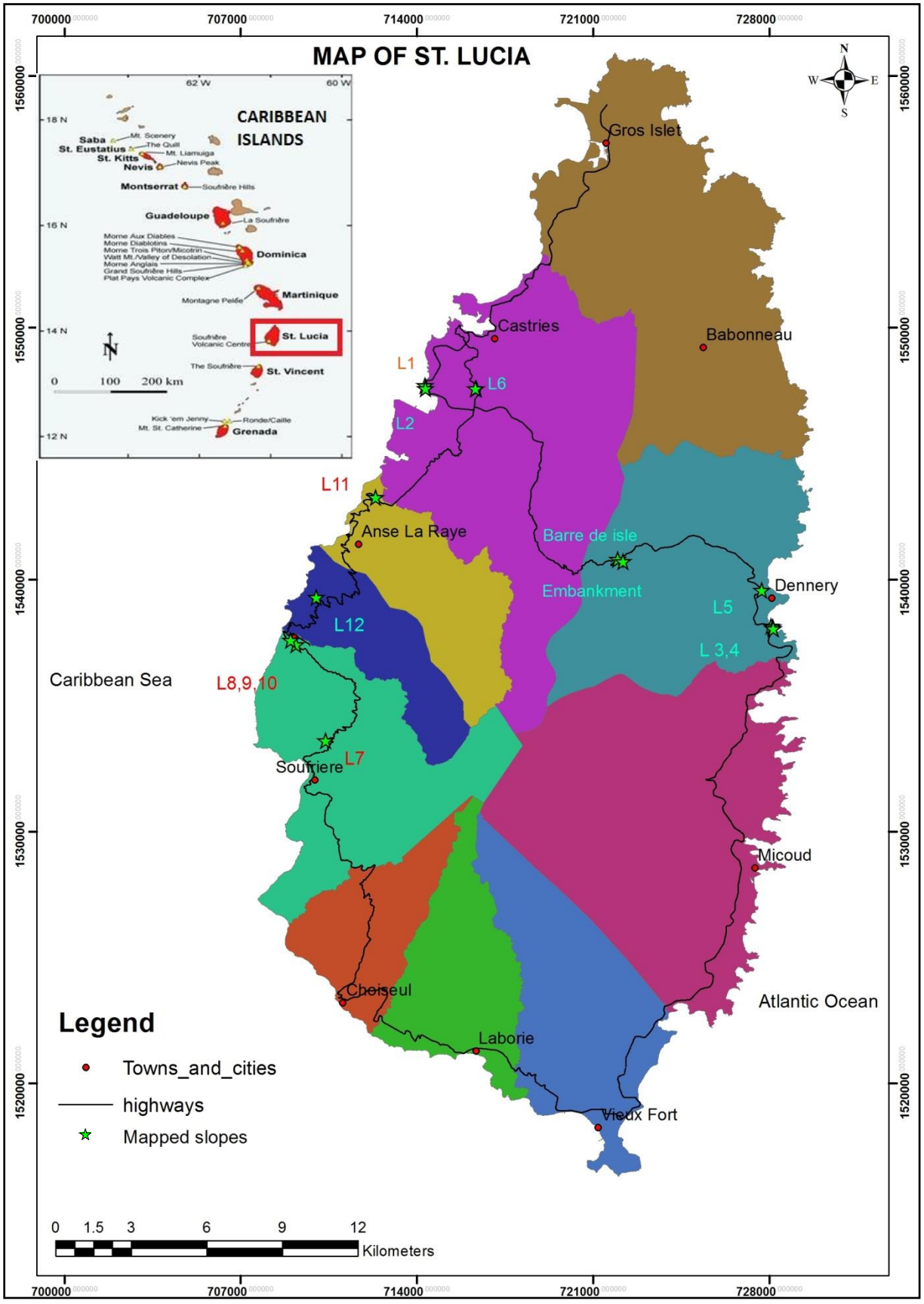

Figure 4: Location of the research area – St. Lucia (after Lindsay et al, 2002)

3.2. Climate

Saint Vincent and Saint Lucia are in the tropical zone, although their climate is moderated by northeast trade winds. Since they are fairly close to the equator, the temperature does not fluctuate much between winter and summer. Rainy seasons are from June to November, and dry seasons run from December to June. On average, daytime temperature is around 27 °C (80.6 °F), and average night time temperatures are around 18 °C (64.4 °F). Average annual rainfall ranges from 1,300 mm (51.2 in) on the coast to 3,810 mm (150 in) in the mountain rainforests (figure 5).

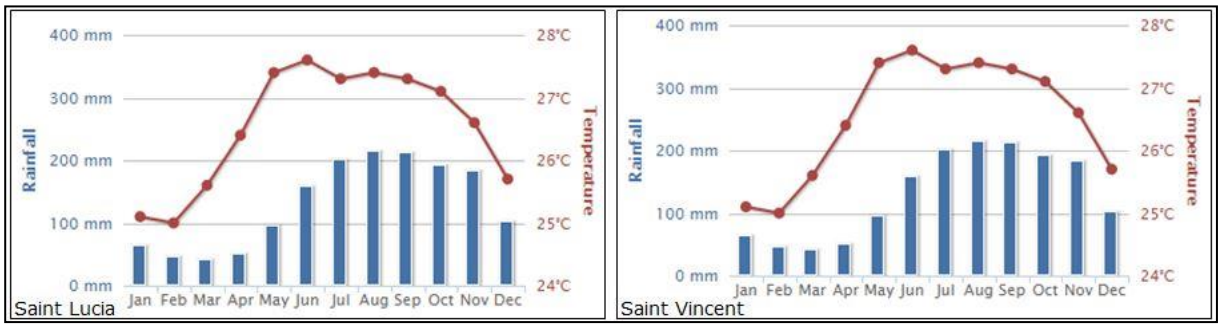

Figure 5: Average monthly rainfall and temperature for Saint Lucia and Saint Vincent (1900-2009) (after Climate Change Knowledge Portal, http://sdwebx.worldbank.org/climateportal/index.cfm?)

3.3. Geology

The Antillean arc of islands in the Caribbean is geologically young, probably not exceeding 50 million years, and is predominantly volcanic in origin. The geology of the study area is presented in categories of St. Vincent, St. Lucia and the lithological units. Despite the categorisation, the rock types exposed on both islands fall in the same compositional group of basalts, andesites, agglomerates, tuffs and pyroclastics.

3.3.1. Saint Vincent

The geology of St. Vincent is entirely volcanic with the southern part consisting of weathered and deeply dissected eroded volcanic breccias and basaltic lava flows, in some cases occurring as dykes; the northern part consisting of relatively fairly weathered andesite lavas, interbedded with pyroclastic deposits of the Soufriere eruptions (RL Hay, 1959b). The island has generally an even distribution of porphyritic and olivine bearing andesite lava flows and pyroclastics (Hay, 1959a; Rowley, 1978a). In some centres (fig. 4) like the South-East Volcanics, lavas are dominate, while at others like the Grand Bonhomme Volcanic Centre, the distribution of volcaniclastic is predominate (Robertson, 2014). Pyroclastics ash deposits are the most abundant volcanic products on the island, include particles varying in fragment size from fine to coarse, and in some places consist of lapilli, bombs, and blocks. It is estimated that 55% of the island is mantled by well-bedded pyroclastic ash fall deposits of the yellow tephra formations, resulting from the Soufriere volcano eruptions during the late Pleistocene, Rowley (1978b). The deposits are generally andesitic with varying compositions of lithic and vitric, at variable degrees of weathering. Other common rock types present include agglomerate which is principally andesitic and basaltic in composition, alluvial and reworked deposits of the nature of pyroclastic, agglomerates, volcaniclastic, volcanic ash and scoria

(Robertson, 2014). A description of rock types is given in chapter 3.3.3. Studied slopes (figure 3) on the east and west coasts of the island fall in geological formations shown in figure 6.

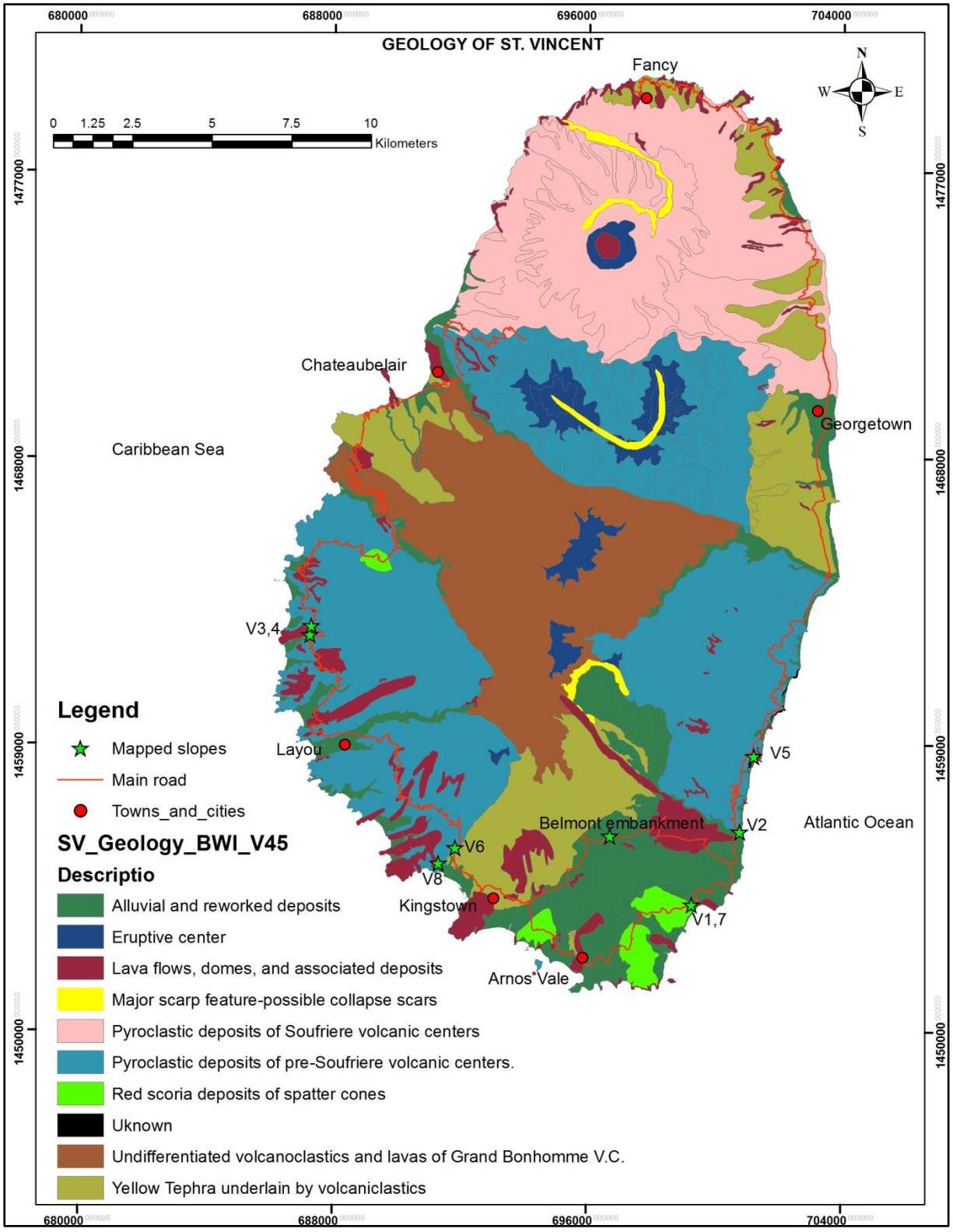

Figure 6: Geology of volcanic centres (after Robertson, 2003)

3.3.2. Saint Lucia

Saint Lucia is almost entirely volcanic with the oldest rocks, largely rhyolite, andesite and various basalt lavas, dating from the early tertiary period about 50 million years ago, with an exception of some minor sedimentary rocks of lower Miocene age cropping out on the east coast. Newman, (1965) divided the volcanic rock formations of Saint Lucia into three broad categories, from oldest to youngest, namely: the Northern Series, the Central Series and the Southern Series, with respect to their predominant locations in the northern, central and southern parts of the island as shown in figure 7. Lindsay et al., (2002) noted that subsequent age dating of these rocks showed several centres in the Southern Series to be more likely to corresponding to older centres in the Northern Series. Therefore, for purposes of volcanic hazard assessment, Lindsay et al., (2002) preferred to use a revised grouping of volcanic rocks for Saint Lucia as below:

- eroded basalt and andesite centres (a revision of the Northern Series of Newman, 1965), this is subdivided into northern and southern series;
- dissected andesite centres (Central Series of Newman, 1965); and
- Soufriere Volcanic Centre (a revision of the Southern Series of Newman, 1965).

Thus, for the purpose of weathering and slope stability assessments, the three broad categories (oldest to youngest) of Newman, (1965) are adopted, since the revised grouping made by Lindsay et al., (2002) does not change anything geologically. The Newman, (1965) series are summarised as follows:

- **The Northern Series**

The deposits of the northern series consist of deformed and eroded basalts and andesite lavas with pyroclastic deposits. The oldest of these represent the earliest volcanic activity on this island. Much of the northern parts of the primary road network, around Morne Fortune to upper Castries, are within the Northern Series. Small areas of outcropping northern series are also present on the western coast around Anse La Raye and Canaries, and in the southern parts of the island. A part of the Morne Fortune on the map is shown to fall on altered andesite porphyry and agglomerates.

- **The Central Series**

The Central Series is mainly around the central part of the island is associated with andesite lavas and clastic deposits. They extend along the southeast coast, Dennery to Micoud and appear to be younger than the deformed basaltic rocks in the northern series but are not of recent origin. The rocks of this series were deposited following an increase in sea level across the Lesser Antilles approximately 25 million years ago. During this period of general submergence, there was a development of coral reefs, which were later uplifted above sea level (Newman, 1965). These are present as small outcrops of limestone in the northeast of the island. The primary road network is not shown to encounter any limestone bedrock on the published mapping. The Barre de I'sle and majority of the east coast road are within the Central Series. The Barre de I'sle is shown on the published map to be within andesite ash and altered andesite deposits, and the east coast road mainly within andesite agglomerate and mud flow deposits.

- **The Southern Series**

Much of the west coast road is within the Southern Series. The series consists mainly of small basaltic andesite lava deposits, which were deposited 5 – 10 million years ago (Newman, 1965). The relatively young age and limited uplift and erosion have led to the subdued topography of the landforms in this series. There are hot fumaroles associated with this series and several instances of 'cold' fumarolic activity and gas vents located in areas of highly altered rock within the southern series exist. The southern series is the most recent centre of volcanic activity in the Island and hosts what appears to be a remnant of a caldera in the south of the town of Soufriere. It consists of a series of volcanic vents and a vigorous high temperature geothermal field associated with a large acute structure (Qualibou depression) in the southwest Saint Lucia about 300 thousand years ago, formed as a result of a huge landslide or structural collapse (Lindsay et al, 2002).

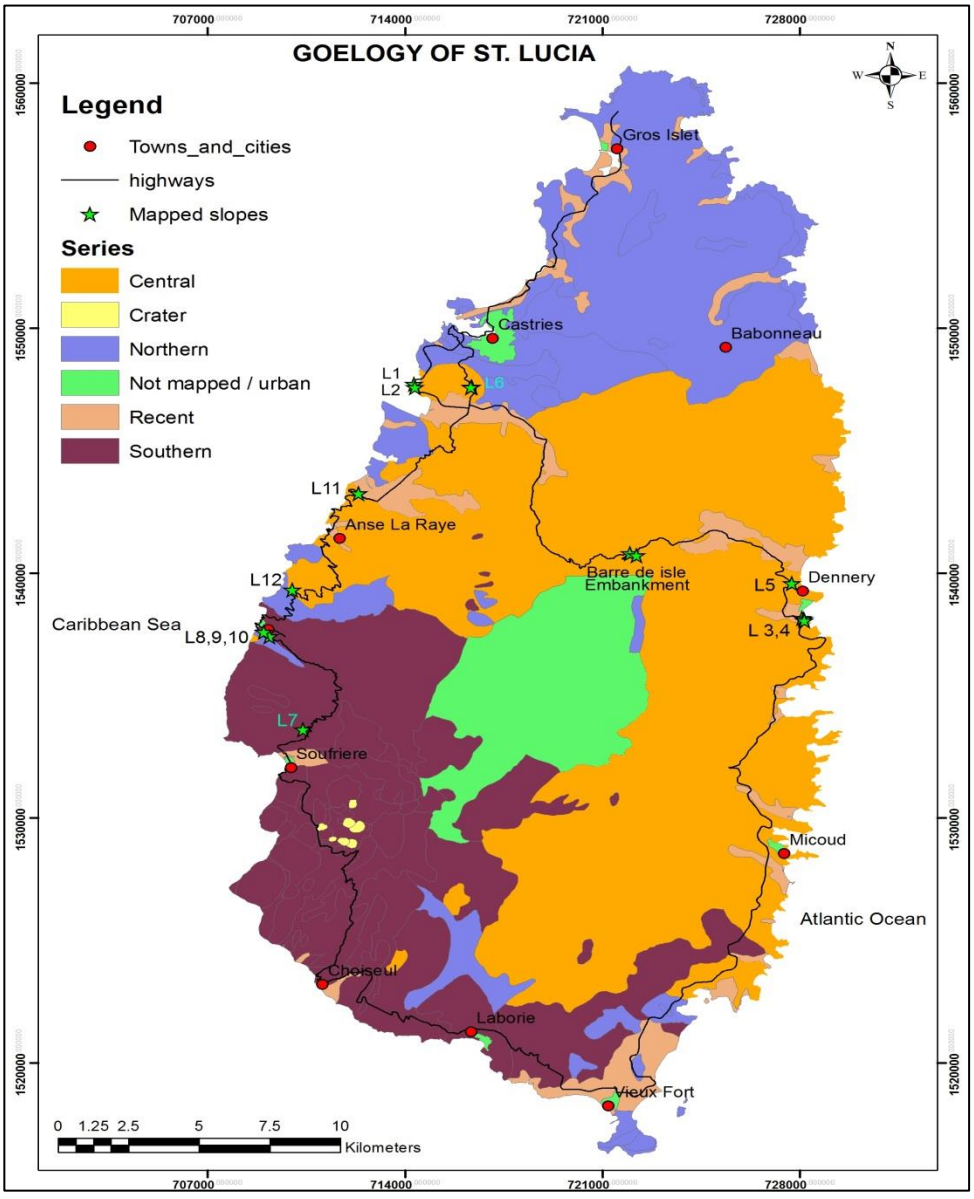

Figure 7: St. Lucia geology and rock formations (after Newman, 1965)

3.3.3. Geological descriptions of lithological units

1. ***Basalts***

Basalts are basic igneous rocks, fine-grained and extrusive (volcanic) products resulting from the flow of lava on the surface until it cools or the volcanic emission stops. The magma's composition and topography in which the lava flows determines, among others, the length and thickness, and morphology of the deposit (Vallejo et al., 2007). Its mineralogical structure is a fine interlocking crystal mosaic with no textural orientation. It may have open vesicles or mineral-filled amygdales (old gas bubbles), with about 50% feldspar and 50% mafics (Waltham, 1993). Differential cooling process related with the progression of viscous basaltic lava flow results in layers of bedded sequences. Structurally, sheets or lenses maybe interbedded with ash or tuff, and commonly with weathered or vesicular scoria tops on each flow. Scoria is a general term for a porous, dark, and glassy pyroclast of basaltic composition. Young lavas may have smooth pahoehoe or clinkery surfaces, and if compact, may have columnar jointing (from cooling contraction)(del Potro & Hürlimann, 2008). Basaltic lava weathers with rust and maybe spheroidal, and decays to clay soils. One of the main characteristics of the lava flows is the presence of discontinuities.

2. ***Pyroclastic rocks***

Pyroclastic rocks are also known as volcaniclastic. They are formed of material collectively known as tephra, which are fragmental rocks ejected from volcanic vents during explosive eruptions (Vallejo et al., 2007). These solid fragments deposit and accumulate forming volcanic cones and deposits of layered sequence, because of eruptive processes. Most of these tephra material is cooled in flight, and land forming various types materials (i.e. tuff and agglomerate), all with the properties of sedimentary rocks (Waltham, 1993). Tephra that erupts in turbulence at high temperature as pyroclastic flow lands hot and welds into ignimbrite, or welded tuff. Thus, pyroclastic rocks maybe divided into strongly welded, and weakly welded and/or interlocked pyroclastic rocks (del Potro & Hürlimann, 2008). These deposits maybe poor to very poorly sorted, consisting of angular to sub-rounded grains of pumice, scoria, and lapilli. Depending on the size of the fragments, pyroclasts may be classified into bombs or blocks (grain size >64 mm) – volcanic breccia deposits, lapilli (2–64 mm) - lapilistone and ash (<2 mm) – tuff.

3. ***Tuffs***

Tuff is an explosively erupted volcanic material, which has consolidated and lithified after deposition. It is a pyroclastic rock formed by lithification of lapilli and ash deposits (Vallejo et al., 2007). Lithification is a process by which weak, loose sediment is turned into a stronger sedimentary rock. The composition of the lapilli and ash fragments determines the classification of tuffs, either as medium, fine grained, very fine grained, and basic or acidic (Anon, 1981). Tuffs that are formed from pyroclastic fall resulting from hydrovolcanic eruptions have their fragments mostly compacted and consolidated in the form of post-sedimentary process (Vallejo et al., 2007).

4. ***Agglomerates***

Agglomerate is basically a pyroclastic rock composed of coarse grained angular to sub-angular igneous rock (lava) fragments of varying size and shape in a matrix of volcanic ash, and typically occurring in volcanic vents (Gabrieli et al., 2012). It forms from pyroclastic eruptions and generally fills in the vents of volcanoes during explosive activity or during caldera collapse (del Potro & Hürlimann, 2008). The term agglomerate can also be used to describe deposits which are vent breccias or debris flows like lahars (Vallejo et al., 2007). An agglomerate is often composed of a variety of igneous materials of different composition, along with large, coarse, rock fragments associated with lava flow that are ejected during explosive volcanic eruptions. These fragments usually are poorly sorted and are in form of a matrix of tuffaceous nature or may occur in lithified dust or ash of volcanic nature.

5. ***Andesites***

Andesite is a fine-grained extrusive volcanic rock intermediate in composition between rhyolite and basalt. It is characterized by the presence of plagioclase feldspars (oligoclase-andesine) with some combination of pyroxene and amphibole (Patino et al., 2003). Its lava's moderate viscosity results in thick lava flows forming domes. It is often associated with subduction magmatism, besides being the result of the mixture of acidic and basic magmas likely coexisting within a stratified magma chamber. Classification of andesites is mostly refined according to the abundance of phenocryst, and is often red brown when weathered (Karpuz & Pa¸samehmetog˘lu, 1997).

4. RESEARCH METHODS

4.1. Introduction

This research work comprises of three main phases: data collection, data analysis and slope stability modelling (fig.8).

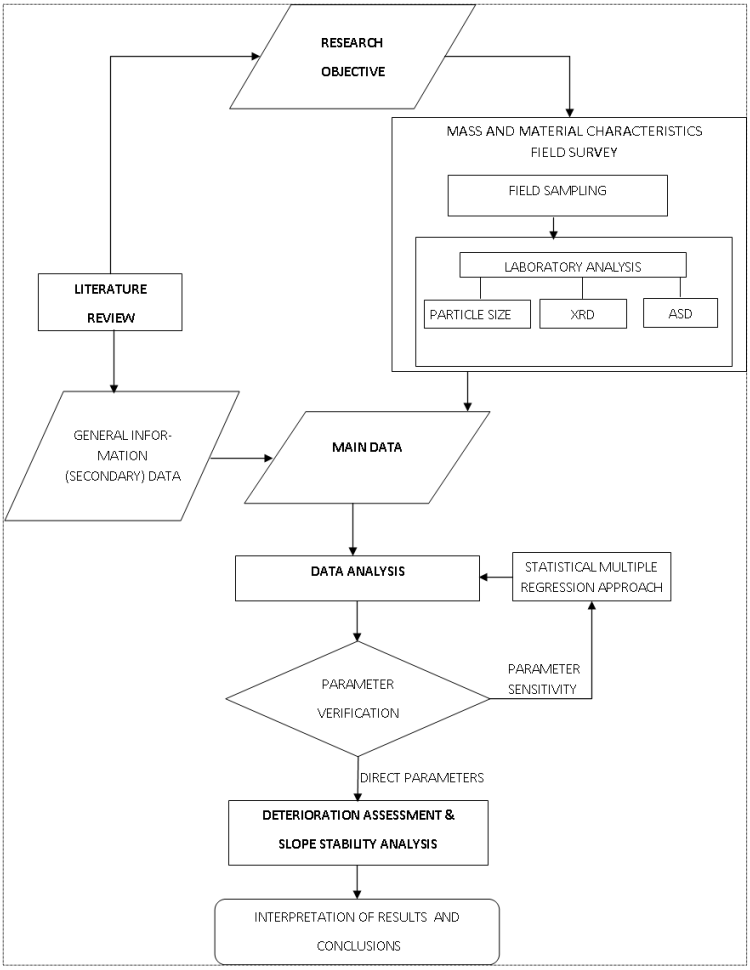

Figure 8: Thesis flow chart

4.2. Data collection

Fieldwork for data collection was carried out from September 25, 2014 to October 16, 2010 in both St. Vincent and St. Lucia. During this period, the weather conditions were mostly dry and bright in the morning, and rainy and cloudy in the afternoons, coupled with tropical high temperatures during daytime.

4.2.1. Field investigation

Geological field mapping for acquisition of basic geotechnical parameters were conducted by 'simple means' , which are elaborated in the following chapters and described by among others Hack & Huisman, (2002), Hack et al., (2003) and according to BS, ISRM and ISO standards. The following steps were followed:

- Identification of slopes (see chapter 4.2.2)
- The exposed rock mass of any rock slope being assessed is divided into geotechnical units
- The intact rock strength, discontinuity orientation, spacing, and condition parameters of rock mass for each geotechnical units` are determined using a geological hammer, Schmidt hammer and geological compass, and then classified (see chapter 4.2.3).
- The rock mass weathering classification for each geotechnical unit are evaluated and graded based on the scale of BS 5930: 1999 specifications as used in SSPC system (Hack, 1998; Hack et al., 2003) (chapter 4.2.3).
- The cohesion and internal friction angle values (c, Φ), are derived from intact rock strength, spacing and condition of discontinuities as elaborated by Hack, (1998, 2003).

The factors considered for fill slopes included the following:

- Structure of the fill slope and its foundations, and that of borrow pit; i.e. the foundation and drainage conditions, method of fill placement or dumping and materials used in embankment construction.
- Observation of external factors influencing weathering and stability
- Disturbed grab sampling from slopes, embankment fill and borrow pit for clay mineralogy analysis (Duzgoren-Aydin et al., 2002).

4.2.2. Cut slope and embankment site identification

The criteria used for identification of cut slopes was an overall Island's reconnaissance taking into consideration the following factors; priority or critical spots, accessibility, size of exposures, fresh (recent) and old exposures. A total of twenty cut slopes and four embankments were marked and investigated for both St. Vincent and St. Lucia, distributed as eight cut slopes and one embankment in St Vincent, and twelve slopes and three embankments in St Lucia. All the selected slopes are considered for analysis in this study.

4.2.3. Cut slope exposure and specific parameters

The exposure and slope specific parameters for the investigated slopes are described in terms of mass and material characteristics, and general information as specified by BS 5930 (1999) for description of excavations. These parameters are collected for both the identified cut slopes and embankment fill material slopes. The cut slopes and embankments are described. Representative samples are collected insitu at time of investigation, from both the failed embankment slopes and fresh material being used for rehabilitation construction.

4.2.3.1. Mass characteristics

This involved obtaining data on the rock mass state of weathering, geometrical, and strength characteristics of discontinuities. These parameters are the degree of weathering (WE), slope geometry

(height, dip and dip direction), discontinuity orientation (dip and dip direction), discontinuity spacing, and the condition of discontinuities. The degree of weathering was obtained by observation (table 3), use of hand pressure, and geological hammer; the slope geometry, spacing, and orientation of discontinuities were obtained using the geological compass, measuring tape and punto inclinometer, while the parameters for condition of discontinuities were obtained through tactual and observation. All these parameters obtained were classified according to (BS5930, 1981/99) and as used and described in SSPC classification system (Hack, 1998: Hack et al., 2003).

Table 3: Scale of weathering grades classification for uniform materials, according to BS5930 (1981), incorporating SSPC system (Hack, 1998), as used in the field.

Term	Description	Grade	WE
Fresh	No visible sign of rock material weathering; perhaps slight discoloration on major discontinuity surfaces.	I	1
Slightly weathered	Discoloration indicates weathering of rock material and discontinuity surfaces. All the rock material may be discoloured by weathering.	II	0.95
Moderately weathered	Less than half of the rock material is decomposed or disintegrated to a soil. Fresh or discoloured rock is present either as a continuous framework or as core stones.	III	0.90
Highly weathered	More than half of the rock material is decomposed or disintegrated to a soil. Fresh or discoloured rock is present either as a discontinuous framework or as core stones.	IV	0.62
Completely weathered	All rock material is decomposed and/or disintegrated to soil. The original mass structure is still largely intact.	V	0.35
Residual soil	All rock material is converted to soil. The mass structure and material fabric are destroyed. There is a large change in volume, but the soil has not been significantly transported.	VI	

4.2.3.2. Material characteristics

This involved obtaining data on the nature, strength, and state of rocks and soil masses for the investigated exposures. These parameters are the intact rock strength, texture, and structure, colour, grain size and rock name. The intact rock strength was obtained by use of hand pressure, Schmidt hammer and geological hammer (table 4); texture was obtained by tactile and hand lens, and structure by observation. Colour for both slope surface and slope inside was obtained using the colour charts. Grain size was obtained by sand ruler (disc), and rock name from rock identification and geological map. Overall, visual inspection was done on almost all parameters except the intact rock strength. All the parameters observed and obtained were classified according to (BS5930, 1981/99) and as used and described in SSPC classification system (Hack, 1998; Hack et al., 2003).

Table 4: Intact rock strength field classification (BS 10-5930:1999, 1999)

Term	Field definition	Unconfined compressive strength(MN/m^2)
Very weak	Gravel size lumps can be crushed between finger and thumb.	<1.25
Weak	Gravel size lumps can be broken in half by heavy hand pressure.	1.25 to 5
Moderately weak	Only thin slabs, corners or edges can be broken off with heavy hand pressure	5 to 12.5
Moderately strong	When held in the hand, rock can be broken by hammer blows.	12.5 to 50
Strong	When resting on a solid surface, rock can be broken by hammer blows.	50 to 100
Very strong	Rock chipped by heavy hammer blows.	100 to 200
Extremely strong	Rock rings on hammer blows. Only broken by sledgehammer	>200

4.2.3.3. General information

This involved obtaining information and observations not included in the mass and material characteristics but important for the study. These included the methods of excavation observed on site and classified according to SSPC classification system (Hack, 1998) (table 5), accessibility and observed stability (stability tick), external influences (.i.e. slope surface run-off and erosion state, drainage, vegetation etc.) observed insitu. The dates of excavations were obtained through enquiries from local population and appropriate government ministries and agencies on the two islands, and the geological formations from desk study.

Table 5: Method of excavation classification as used in the field, according to SSPC system (Hack, 1998)

METHOD OF EXCAVATION (ME)	
(tick)	
natural/hand-made	1.00
pneumatic hammer excavation	0.76
pre-splitting/smooth wall blasting	0.99
conventional blasting with result:	
good	0.77
open discontinuities	0.75
dislodged blocks	0.72
fractured intact rock	0.67
crushed intact rock	0.62

.

4.2.4. Embankment characteristics and parameters

This involved obtaining data on the state of embankments, mode of construction and method of dumping (current methods and practices), type of fresh material being used, existing material in the failed embankments, drainage channels, clay mineralogy test (specifically for expansive clays), and grain size distribution.

The road embankment height to valley bottom was obtained. The geology and fill material type is noted. The method of embankment construction, with the type of fill material insitu and geology (rock types) at the location is obtained.

Soil samples from borrow sources (currently in use for rehabilitation works) are obtained and taken for laboratory testing to determine the suitability of the material for reconstruction and rehabilitation of the embankments.

The designated tests for soil investigation of both the embankment fill material and borrow sources material were the clay mineralogy, and particle size distribution analyses.

The above tests results, together with strength parameters obtained from literature are used for the embankment stability modelling, using Culmann's 1875 method.

It should be important to note that parameters collected for analysis are coupled with alot of limitations, and thus, the level of uncertainties in the results may be quiet high.

All observations and parameters obtained were done according to the BS 5930, (1999), Montana Department of Transport, (2008), and US Army Corps, (2003, 2010) standards.

4.3. Data analysis

Analyses of field and laboratory data are carried out for cut slope and road embankment analyses.

4.3.1. Cut slopes

In order to forecast future stability of cut slopes, the future geotechnical properties have to be known. The data obtained in both field and laboratory investigations are analysed using multiple regression analysis statistical methods to find correlations for deterioration in time of geotechnical properties with degree of weathering. The time related deterioration of geotechnical parameters is determined using the exposure and reference rock mass parameters as determined in the SSPC system (Hack, 1998; Hack et al., 2003) and the equations from Colman (1981), simplified by Huisman (2006) and Tating et al. (2013; 2014).

4.3.1.1. Determining of geotechnical parameters

Geotechnical parameters are required in weathering and deterioration assessment and slope stability analyses (Wyllie and Mah, 2004). In this research, the basis for obtaining and deriving geotechnical parameters for the twenty slopes investigated, are the 'simple means' described by among others Hack & Huisman (2002) and the 'Slope Stability Probability Classification' (SSPC) system (Hack, 1998; Hack et al., 2003). The SSPC system was developed and validated in sedimentary formations, but also, it was applied successfully in volcanic formations on Saba, Netherlands Antilles, Caribbean (Rijkers and Hack, 2000). Three sets of parameters are derived from the SSPC:

1. The exposure rock mass parameters "parameters of the rock mass in the exposure"
2. Reference rock mass parameters "parameters of an imaginary unweathered and undisturbed rock mass prior to excavation"

3. Slope rock mass parameters "parameters of the rock mass in which a new slope is to be made"

Since in this research existing slopes are examined, the exposure rock mass parameters and slope rock mass parameters are considered the same (Hack, 1998). The three step SSPC system concept is illustrated in figure 9.

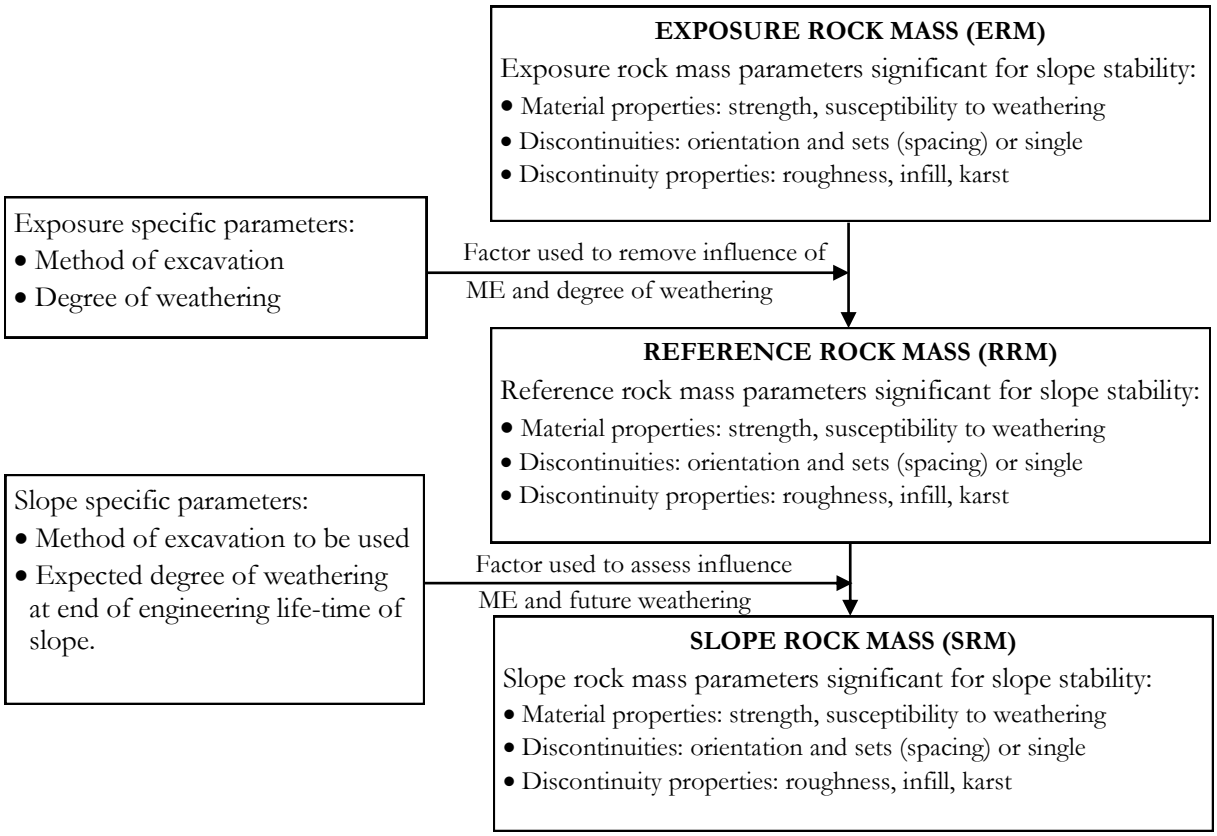

Figure 9: Flow chart of three step concept of the SSPC system (Hack, 1998).

4.3.1.2. Determining the exposure rock mass parameters

A number of parameters significant for slope stability are determined for the exposure rock mass in the SSPC system per geotechnical unit (Figure 9). In this chapter, only exposure rock mass parameters significant for deterioration assessment are explained as given in SSPC. The intact rock strength (IRS), spacing (DS) and condition properties (i.e., persistence, roughness, infill, and presence of karst) of discontinuities are determined in the field (chapter 4.2.3.1 and 4.2.3.2). These are input parameters for the SSPC, spacing parameter (SPA), discontinuity condition (CD), internal friction angle of the rock mass (FRI), cohesion of rock mass (COH) and the intact rock strength (IRS). Values for the spacing parameter (SPA) and condition of discontinuity parameter (CD) are determined using equations (4.1) and (4.2); the values for cohesion (COH) and internal friction angle (FRI) are obtained by equations (4.4) and (4.5).

Determination of the spacing parameter (SPA), is done by using the values for the spacing factors for discontinuity sets which are calculated from a series of formulas determined by Taylor (1980), used in the SSPC system. Graphically these are shown in figure 10. Where three or more discontinuity sets exist, all the three factors (i.e. maximum, intermediate, and minimum) are determined for sets with minimum spacing. If only two discontinuity sets exist, two factors (minimum and maximum) are determined; and if only one set is present, a single factor is determined (eqn. 4.1).

$$SPA = factor_{maximum} * factor_{intermediate} * factor_{minimum}$$
$$SPA = factor_{maximum} * factor_{minimum}$$
$$SPA = factor \quad (4.1)$$
$$SPA = spacing\ parameter$$
$$factor_x = determined\ by\ graph \text{ (figure 10)}$$

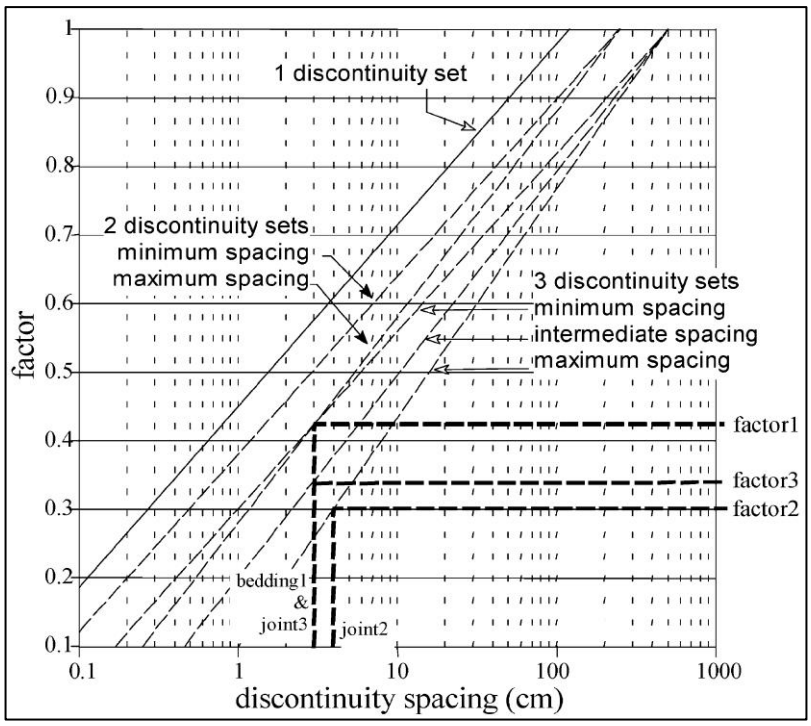

Figure 10: Spacing factor vs. discontinuity spacing for 1 through 3 discontinuity seats

Determining the total condition of discontinuities (TC); used as input in calculating the CD factor. The TC factor (eqn. 4.2) is calculated by using factors for condition of discontinuities obtained in the field using table 6, as shown:

$$TC = Rl \times Rs \times Im \times Ka \quad (4.2)$$

Where:

Rl and Rs are factors for large and small-scale roughness, Im is infill material and Ka is karst.

Determining the overall condition of discontinuities (CD): The CD factor is calculated by the mean of the condition of discontinuities (TC) of three sets with minimum condition values weighted by spacing (DS), as shown (eqn. 4.3).

$$CD = \frac{\frac{TC_1}{DS_1} + \frac{TC_2}{DS_2} + \frac{TC_3}{DS_3}}{\frac{1}{DS_1} + \frac{2}{DS_2} + \frac{3}{DS_3}} \tag{4.3}$$

Where:

$TC_{1, 2, 3}$ are the total conditions of discontinuities

$DS_{1, 2, 3}$ are the spacing of discontinuity set 1, 2, and 3 respectively.

Table 6: Factors for condition of discontinuities as used in SSPC system

Roughness large scale **(Rl)** (on an area between 0.2x0.2 and 1x1 m2)	wavy		1.00
	slightly wavy		0.95
	curved		0.85
	slightly curved		0.80
	straight		0.75
Roughness small scale **(Rs)** (on an area of 0.2x0.2 m2)	rough stepped		0.95
	smooth stepped		0.90
	polished stepped		0.85
	rough undulating		0.80
	smooth undulating		0.75
	polished undulating		0.70
	rough planar		0.65
	smooth planar		0.60
	polished planar		0.55
Infill material **(Im)**	cemented / cemented infill		1.07
	no infill - surface staining		1.00
	non-softening & sheared material, e.g. free of clay, talc, etc.	coarse	0.95
		medium	0.90
		fine	0.85
	soft sheared material, e.g. clay, talc, etc	coarse	0.75
		medium	0.65
		fine	0.55
	gouge<irregularities		0.42
	gouge>irregularities		0.17
	flowing material		0.05
Karst **(Ka)**	none		1.00
	karst		0.92

Deriving the unit rock mass angle of internal friction (FRI) and cohesion (COH): These parameters are determined in SSPC system by the effective use of Mohr – coulomb failure criterion, utilising the condition of discontinuities (CD), intact rock strength (IRS), and spacing parameter (SPA). Resulting equations 4.4 and 4.5 follows:

$$\varphi'_{\text{mass}} = IRS * 0.2417 + SPA * 5212 + CD * 5.779 \tag{4.4}$$

$$coh'_{\text{mass}} = IRS * 94.27 + SPA * 28629 + CD * 3.593 \tag{4.5}$$

Where:

φ'_{mass} = angle of internal friction of the rock mass (in degrees)

coh'_{mass} = rock mass cohesion (in MPa)

SPA = Spacing parameter

CD = Condition of discontinuity

(If IRS > 132MPa; IRS =132 MPa)

4.3.1.3. Determining reference rock mass parameters

The reference rock mass is an imaginary unweathered and undisturbed rock mass that is in existence prior to excavation and unweathered. The reference rock mass parameters are determined from the exposure rock mass parameters by using correction factors for the influence of local weathering (WE) (table 3) and method of excavation (ME) (table 5; figure 9). The outline for the calculation as given in SSPC system (Hack, 1998) follows;

Determine the reference intact rock strength (RIRS), by correction for local weathering (WE).

$$RIRS = IRS / WE \tag{4.6}$$

Where:

IRS is the intact rock strength (in MPa) as obtained in the field.

WE is the degree of weathering (refer to chapter 4.2.3.1)

Determine the reference overall discontinuity spacing (RSPA), by correction for local weathering (WE) and method of excavation (ME)

$$RSPA = SPA/(WE \times ME) \tag{4.7}$$

Where:

The SPA values are derived from equations (4.1) and the method of excavation (ME) and degree of weathering (WE) are obtained in the field.

Determine the reference overall weighted discontinuity condition (RCD), by correction for local weathering. Using equation (4.3) for the discontinuity condition (CD), the RCD is derived. But where a single discontinuity exists, (RTC) is used to calculate the (CD) value. Thus, the value of RTC is calculated as shown in equation (4.8) and subsequently the CD is derived. The corrected RCD (eqn. 4.9) is then determined as shown below;

$$RTC = TC/\sqrt{(1.452 - 1.220 \times e^{(-WE)})} \tag{4.8}$$

$$RCD = CD/WE \tag{4.9}$$

To determine the reference rock mass unit's angle of internal friction (RFRI) and cohesion (RCOH), the calculations are done according to the formulae given in SSPC (Hack, 1998). Deriving these formulae in SSPC is based on the Mohr - coulomb failure criterion optimization of intact rock strength (IRS), spacing (SPA) and condition of discontinuities (CD). Obtained are the φ'_{mass} (eqn. 4.4) and Coh'_{mass} (eqn. 4.5). Based on the above, the reference unit angle of internal friction (RFRI) in degrees and cohesion (RCOH) in Pascal are given as;

$$RFRI = RIRS \times 0.2417 + RSPA \times 5212 + RCD \times 5.779 \quad (4.10)$$

$$RCOH = RIRS \times 94.27 + RSPA \times 28629 + RCD \times 3593 \quad (4.11)$$

4.3.1.4. Determining slope rock mass parameters

The slope rock mass parameters (SRM) in SSPC system are determined by modifying the reference rock mass (RRM) parameters using the slope specific parameters (figure 10). Factors are used to assess the influence of method of excavation and future weathering on reference rock mass (RRM) parameters. Obtained are the slope rock mass intact rock strength (SIRS), slope rock mass spacing parameter (SSPA) and slope rock mass condition of discontinuities (SCD) parameters. These parameters are then used to determine the slope rock mass angle of internal friction (SFRI) and slope rock mass cohesion (SCOH) parameters. The SIRS, SFRI, and SCOH are considered important for use in assessing deterioration in strength and shear strength parameters as well as in stability assessments. The determination of the parameters as derived in SSPC system is shown:

Deriving the slope rock mass intact rock strength (SIRS) is done by assessing the influence of slope rock mass degree of weathering (SWE), on the reference rock mass intact rock strength (RIRS) (eqn. 4.6), as shown;

$$SIRS = RIRS \times SWE \quad (4.12)$$

Deriving the slope rock mass overall spacing of discontinuities (SSPA) is done by assessing the influence of SWE and slope method of excavation (SME), on the reference rock mass spacing parameter (RSPA) (eqn. 4.7), as shown;

$$SSPA = RSPA \times SWE \times SME \quad (4.13)$$

Deriving the slope rock mass overall condition of discontinuities (SCD) is done by assessing the influence SWE on the reference rock mass condition of discontinuities (RCD) (eqn. 4.9), as shown;

$$SCD = RCD \times SWE \quad (4.14)$$

Deriving the slope rock mass friction (SFRI) and cohesion (SCOH) is done by replacing the reference rock mass parameters RIRS, RSPA, and RCD in equations 4.10 and 4.11, with the slope rock mass parameters from equations 4.12, 4.13, and 4.14. The equations for SFRI and SCOH are then given as:

$$\varphi_{SRM} = SIRS \times 0.2417 + SSPA \times 5212 + SCD \times 5.779 \quad (4.15)$$

$$COH_{SRM} = SIRS \times 94.27 + SSPA \times 28629 + SCD \times 3593 \quad (4.16)$$

4.3.1.5. Weathering in time; weathering rates and deterioration in geotechnical parameters

Research has shown that weathering of rocks and rock masses is non-linear (Colman, 1981; Fookes et al., 1988; Phillips, 2005; Huisman, 2006; Tating et al., 2013). This is basically due to a stable residual layer that forms as protective cover on the exposure after a period of time (Hachinohe et al., 2000). The residual layer delays weathering agents from causing physical decay and disintegration of rock materials, there by affecting the weathering rates (Garcia-Vallès et al, 2003; Erguler, 2009). Thus, the relationship between weathering and exposure time of a rock mass is described as the change in initial property value of rock mass in a time frame (Colman, 1981; Bland and Rolls, 1988). Therefore, to determine the time related weathering and deterioration in geotechnical properties of volcanic rocks in this study, Huisman (2006) and Tating et al. (2013; 2014) equations which are modified from the empirical relation suggested by Colman (1981) for the description of weathering intensity, are used.

The degree of weathering (WE) and intact rock strength (IRS) obtained in the field, calculated values for internal friction (SFRI) and cohesion (SCOH), and the reference rock mass (RRM) parameters are used in the equations (chapter 4.3.1.3 and chapter 4.3.1.4). The intact rock strength (IRS), angle of internal friction (SFRI) and cohesion (SCOH) parameters are preferred, since they are also important in slope stability.

The empirical relation suggested by Colman (1981), to describe weathering intensity, is given as;

$$\frac{C_t}{C_0} = a + b \log(1 + t) \quad (4.17)$$

Where:
C_t = the property parameter value at time (t)
C_0 = the initial property parameter value (original value in fresh state)
a = constant (depends on initial property value)
b = constant (depends on the change in property with time)

In terms of weathering reduction values suggested by Hack (1998), the ratio C_t / C_0 stands for WE (reduction mass properties resulting from weathering). Therefore, equation 4.17 is converted to define weathering rate by replacing the ratio C_t / C_0 with the weathering quantitative value WE_t, the constant a with $WE_{initial}$ which is the WE value at time of excavation, and b with the weathering rate R_{WE} (Huisman, 2006). The weathering rate is then given as (eqn. 4.18):

$$WE_t = WE_{initial} + R_{WE} \log(1 + t)$$

$$R_{WE} = \frac{WE_{initial} - WE_{observed}}{\log\ (1 + t)} \quad (4.18)$$

Since the ratio C_t/C_0 can also be related to the geotechnical parameter change at a certain time after the rock mass is excavated with respect to the initial value of the geotechnical parameter, equation (4.17) is modified by replacing the ratio C_t/C_0 with a geotechnical parameter such as (intact rock strength) IRS_t (which is the *IRS* at time of exposure). The constant a replaced with $IRS_{initial}$, and b with the apparent rate of the change in *IRS* (R_{IRS}^{app}) (Tating et al., 2013). This gives equation (eqn. 4.19):

$$IRS_t = IRS_{initial} + R_{IRS}^{app} \log(1+t) \tag{4.19}$$

Where the apparent rate of the change in *IRS* (R_{IRS}^{app}), is given as (eqn. 4.20);

$$R_{IRS}^{app} = \frac{IRS_{initial} - IRS_{observed}}{\log\ (1+t)} \tag{4.20}$$

Similarly, analyses are conducted on the SSPC system derived parameters 'cohesion (SCOH) and angle of internal friction (SFRI).

4.3.1.6. Determining current and future stability

Most cut slopes constructed for engineering purposes are made for a certain engineering life time i.e. 50 - 100 years (Hack, 1998; Rengers et al., 2001). Therefore, determining the current and future stability for a slope requires consideration of the engineering life time for which the particular slope is designed (Huisman, 2006). In this study, both the current and future stability will be given in term of stability probability (figure 11).

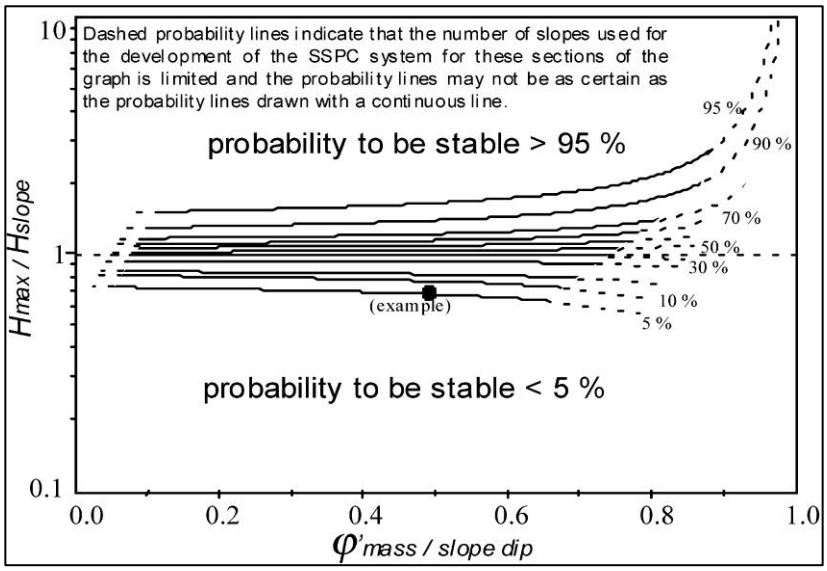

Figure 11: Stability probability as determined in SSPC system

1. Current stability

The stability of the slope as is in the field is calculated using the strength parameter values; angle of internal friction and cohesion (eqns. 4.15 and 4.16) for each geotechnical unit. The angle of internal

friction and cohesion are used in equation 4.21 to obtain the maximum height of the slope that can be sustained for a given values of shear strength parameters (Hack, 1998), given as;

$$H_{max} = \frac{1.6 \times 10 - 4 \times COH_{SRM} \times \sin(SD) \times \cos(\varphi_{SRM})}{1 - cos(SD - \varphi_{SRM})} \quad (4.21)$$

Where:

COH_{SRM} = the cohesion of slope rock mass
SD = slope dip
φ_{SRM} = angle of internal friction for slope rock mass
If the $slope_{dip}(SD) \leq \varphi_{mass}$; $maximum\ slope\ height\ (H_{max}) is\ infinite.$

The value of the maximum height the material can sustain and the slope rock mass angle of internal friction (φ_{SRM}) are subsequently used to calculate ratios (eqn. 4.22) for current stability probability classification (figure 11), as given in SSPC system;

$$\frac{\varphi_{SRM}}{SD}\ and\ \frac{H_{max}}{H_{slope}} \quad (4.22)$$

Where:

SD = slope dip
φ_{SRM} = angle of internal friction for slope rock mass
H_{max} = maximum height the material can sustain
H_{slope} = slope height and;
If the $\varphi_{SRM} > slope_{dip}\,(SD), probability\ of\ stability = 100\%,$
$else\ the\ figure\ for\ orientation\ independent\ stability\ in\ SSPC\ is\ used.$
Also; $\frac{H_{max}}{H_{slope}} = 1\,, where\ \frac{\varphi_{mass}}{slope_{dip}} \geq 1$

2. Future stability

Future stability is determined by calculating the future IRS, shear strength parameters and the maximum height such parameters can sustain using the equations (4.19), (4.20) and (4.21) for each geotechnical unit after the effect of weathering. The two parameters, maximum height and future angle of internal friction values, are then used to determine ratios (eqn. 4.23) for future stability probability classification (figure 11), as given below;

$$\frac{\varphi_{SRM(future)}}{SD_{current}}\ and\ \frac{H_{\max(future)}}{H_{slope(current)}} \quad (4.23)$$

Where:

$SD_{current}$ = observed slope dip
$\varphi_{SRM(future)}$ = future angle of internal friction for slope rock mass

$H_{\max(future)}$ = future maximum height the material can sustain
$H_{slope(current)}$ = observed slope height and;
If the $\varphi_{SRM} > slope\ dip(SD), probability\ of\ stability = 100\%$,

$$else\ the\ figure\ for\ orientation\ independent\ stability\ in\ SSPC\ is\ used.$$

4.3.2. Road embankments

Stability analysis in embankments basically involves determining the shear stress developed along the likely slip surface which depends on the soil shear strength (Terzaghi, 1943). Thus, depends mostly on six basic factors; embankment soil shear strength, soil unit weight, embankment height, embankment slope angle, soil pore pressure, and the interface between embankment soil and underlying material (Masada, 2009). The soil strength parameters are dependent on the grain size distribution, clay mineralogy and water content.

4.3.2.1. Determining the clay mineralogy and grain size distribution

Samples collected from both the embankments and borrow sources in the study area were subjected to laboratory tests to determine the presence of clay minerals and compositional variation, using the X-ray diffraction (XRD). Borrow sources in this context are referred to as quarries were fresh (unweathered) construction fill material is sourced. The X-ray diffraction (XRD) was used because of its rapid analytical technique to identify crystalline materials inclusive their unit cell dimensions, within short periods. Material preparation for analysis involves finely grinding a sample into homogenous powder crystals. An average of bulk-powdered crystals is then used to determine the mineralogical composition.

The grain size distribution analysis was done by both mechanical sieving and hydrometer procedures as outlined by Van Reeuwijk (2002) and ASTM standards. Sieve analyses were conducted by mechanical means following the ASTM D-422 standard. The resulting grain size distribution curves provide the percentages by weight of sand and fines (i.e., silt and clay). The sand fraction is classified as coarse sand (0.6 to 2 mm) medium sand (0.2 to 0.6 mm) and fine sand (0.06 to 0.2 mm) following BS5930:1999 particle size description. Hydrometer tests were carried out similar to ASTM D-421 standard but as outlined by Van Reeuwijk (2002), for fine material of less than two milimeters (<2 mm) only. This procedure involves pre-treatment of the sample to achieve complete dispersion of primary particles (fig. 12). It is done in order to facilitate a further breakdown of fine particles into silt-and-clay-sized particles (Budhu, 2011).

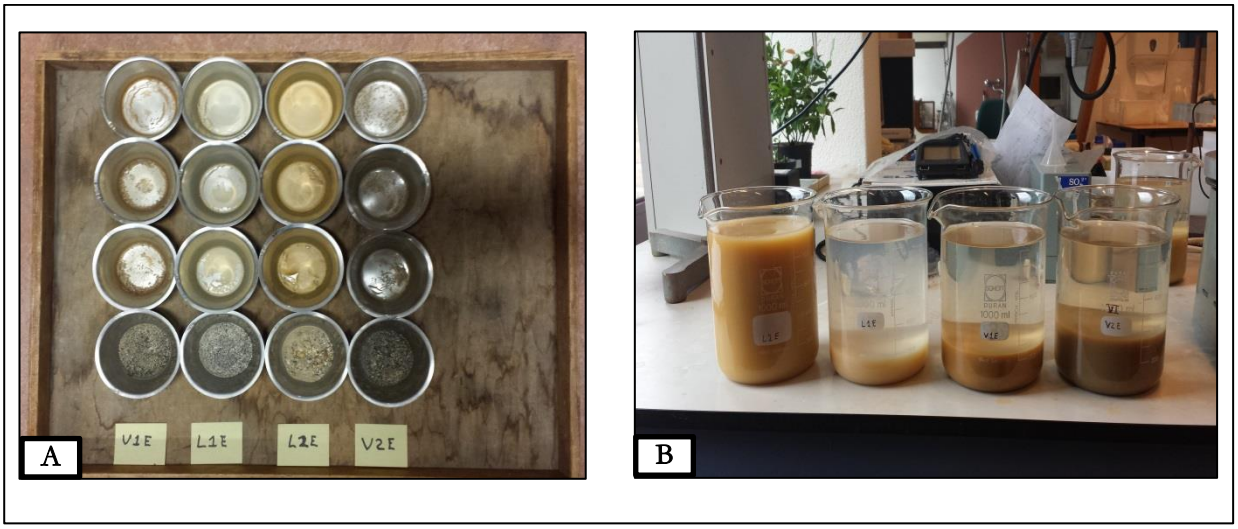

Figure 12: Laboratory particle size analysis

4.3.2.2. Determining the soil shear strength parameters and embankment stability modelling

Das (2007) defined shear strength of a soil mass as "the internal resistance per unit area that the soil mass can offer to resist failure and sliding along any plane inside it".

Shear strength is often expressed by Mohr coulomb failure envelope, as a combination of the angle of internal friction and cohesion. Cohesion is an interparticle friction bond which is very significant in clay minerals and considered zero in sand (Terzaghi, 1943; Schofield & Wroth, 1968). The angle of internal friction is the result of structural roughness between grains and is considered higher in sand than in clay. Shear strength is expressed as:

$$Shear\ strength\ (\tau) = cohesion + normal\ stress \times \tan\varphi \tag{4.24}$$

This implies that the normal stress is critical to shear strength. However, the presence of pore water pressure reduces the normal stress by carrying a part of the soil overburden load, and this is expressed interms of effective stress (Terzaghi, 1936; Skempton, 1960), given by;

$$Effective\ stress\ (\sigma') = total\ stress\ (\sigma_t) - pore\ water\ pressure\ (u) \tag{4.25}$$
$$Pore\ water\ pressure\ (u) = Height\ of\ water\ (h_w) \times\ Unit\ weight\ water\ (\gamma_w)$$

Shear strength in stability analysis is defined in terms of effective stress under unsaturated conditions, and in terms of total stress under saturated conditions (eqn.4.26):

$$Shear\ strength\ (\tau) = effective\ cohesion\ (c') + effective\ stress\ (\sigma') \times \tan\varphi'$$
$$Shear\ strength\ (\tau) = cohesion\ (c') + total\ stress\ (\sigma_t) \times \tan\varphi' \tag{4.26}$$
$$Total\ stress\ (\sigma_t) = height\ (h) \times material\ unit\ weight\ (\gamma_t)$$

However, in the field, soil materials may be dry, partially saturated, or saturated. Therefore, Bishop et al., (1960) suggested a series of equations that could be used for completely dry soil, soil at 50 percent saturation, and soil at 100 percent saturation, respectively as given below;

$$\tau = c' + (\sigma - u_a)(tan\ \varphi')$$
$$\tau = c' + (\sigma - 0.5u_a - 0.5u_w)(tan\ \varphi') \quad (4.27)$$
$$\tau = c' + (\sigma - u_w)(tan\ \varphi')$$

Where:

u_a = pore air pressure (typically <0)
u_w = pore water pressure (typically >0)

When the soil shear strength resistance is overcome by the driving force along the rupture surface, slope failure occurs (Terzaghi, 1943). For the investigated study area, which is characterized by steep valley slopes, all the embankments are constructed by cut and fill. The fill material is inhomogeneous and follows the slope profile. Assumed is a planar potential failure plane. In order to analyse the embankments with a planar failure assumption, the Culmann's 1875 method (Taylor, 1948), propounded by Murthy (2002) and (Das, 2002) among others, for analysis of a finite slope with a plane failure surface is used. The method is based on the assumption that 'the failure of a slope occurs along a plane when the average shear stress tending to cause slip is larger than the shear strength of the soil', and is suitable for applications in steep slopes were plane surfaces of sliding are widely common (University of Melbourne, 1978; Murthy, 2002). This makes it candidate for the study area of this research. An idealised embankment section is presented in figure 13 below, for the purpose of illustration.

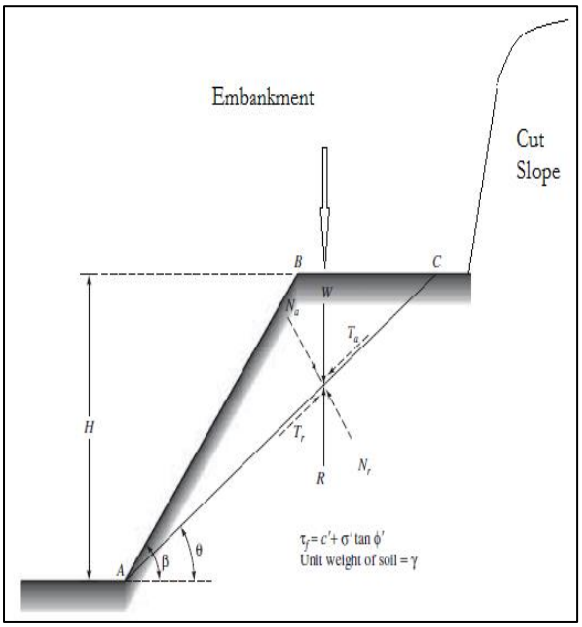

Figure 13: Typical road embankment (modified after Das, 2002).

Where: $H = Embankment\ Slope\ Height$
$\beta = Slope\ Angle$
$\theta = Slip\ Angle$
$AC = Failure\ plane$
$W = Weight\ of\ wedge\ ABC$
$N_a = Normal\ component\ of\ W$
$T_a = Tangential\ component\ of\ W$
$\gamma = Soil\ unit\ weight$

The parameters in figure 13 are used for the analysis. The weight of wedge *ABC* equal to *W*, (*ABC* = *W*) is given as;

$$W = \frac{1}{2}(H)(BC)(1)(\gamma) = \frac{1}{2}H(H\cot\theta - H\cot\beta)\gamma$$
$$= \frac{1}{2}\gamma H^2\left[\frac{\sin(\beta-\theta)}{sin\beta sin\theta}\right] \quad (4.28)$$

To calculate the normal and tangential stresses acting on the plane *AC*, N_a - normal and T_a – tangential, components of *W* (weight of *ABC*) are expressed as follows;

$$N_a = normal\ component = W\cos\theta$$
$$= \frac{1}{2}\gamma H^2\left[\frac{\sin(\beta-\theta)}{\sin\beta\sin\theta}\right]\cos\theta \quad (4.29)$$

$$T_a = tangential\ component = W\sin\theta$$
$$= \frac{1}{2}\gamma H^2\left[\frac{\sin(\beta-\theta)}{\sin\beta\sin\theta}\right]\sin\theta \quad (4.30)$$

To calculate the average stresses acting on the plane *AC*, the average effective normal and shear stresses are given by;

$$\sigma' = average\ effective\ normal\ stress$$
$$= N_a\left(\frac{\sin\theta}{H}\right) \quad (4.31)$$
$$= \frac{1}{2}\gamma H\left[\frac{\sin(\beta-\theta)}{\sin\beta\sin\theta}\right]\cos\theta\sin\theta \quad (4.32)$$

$$\tau = average\ shear\ stress$$
$$= T_a\left(\frac{\sin\theta}{H}\right)$$
$$= \frac{1}{2}\gamma H\left[\frac{\sin(\beta-\theta)}{\sin\beta\sin\theta}\right]sin^2\theta \quad (4.33)$$

The shear stress acting on the plan *AC* is given as:

$$\tau = c' + \sigma' \tan \varphi' \tag{4.34}$$

Where: $c' = effective\ chesion$

$\sigma' = effective\ normal\ stress$

$\varphi' = effective\ angle\ of\ internal\ friction$

Thus, to calculate the average resistive shearing stress developed along the plane *AC*, equation 4.32 is replaced in equation 4.34 and the new expression is given as:

$$\begin{aligned} \tau_d &= c'_d + \sigma' \tan \varphi'_d \\ &= c'_d + \frac{1}{2} \gamma H \left[\frac{\sin(\beta - \theta)}{\sin \beta \sin \theta}\right] \cos \theta \sin \theta \ tan\varphi'_d \end{aligned} \tag{4.35}$$

Where: $c'_d = effective\ cohesion\ developed\ along\ AC$

$\sigma' = average\ effective\ normal\ stress$

$\varphi'_d = effective\ angle\ of\ internal\ friction\ developed\ along\ AC$

From equations 4.33 and 4.35, the effective cohesion developed along the failure plane *AC* is given in equation 4.36:

$$\begin{aligned} \frac{1}{2} \gamma H \left[\frac{\sin(\beta - \theta)}{\sin \beta \sin \theta}\right] sin^2 \theta &= c'_d + \frac{1}{2} \gamma H \left[\frac{\sin(\beta - \theta)}{\sin \beta \sin \theta}\right] \cos \theta \sin \theta \ tan\varphi'_d \\ c'_d &= \frac{1}{2} \gamma H \left[\frac{\sin(\beta - \theta)(\sin \theta - \cos \theta \ tan\varphi'_d)}{\sin \beta}\right] \end{aligned} \tag{4.36}$$

In order to determine the critical failure plane, the principle of maxima and minima is used for a given value of effective angle of internal friction developed (φ'_d) to find an angle (θ) at which the developed cohesion becomes maximum. To achieve this, the first derivative of the effective cohesion developed (c'_d) from equation (4.36) with respect to slip angle (θ) is equated to zero.

$$\frac{\partial c'_d}{\partial \theta} = 0 \tag{4.37}$$

Since the unit weight (γ), height (H) and inclination angle (β) are constants in equation (4.36), the expression then becomes:

$$\frac{\partial}{\partial\theta}[\sin(\beta-\theta)\,(\sin\theta-\cos\theta\tan\varphi'_d)]=0 \tag{4.38}$$

Solving equation 4.38 gives the critical inclination value of theta (θ) expressed as;

$$\theta_{cr}=\frac{\beta+\varphi'_d}{2} \tag{4.39}$$

Substituting or replacing the value of $\theta=\theta_{cr}$ into equation (4.36), gives the simplified or revised equation for the effective cohesion developed (c'_d) and the maximum value of the stability number (m) for the failure plane *AC*;

$$c'_d=\frac{\gamma H}{4}\left[\frac{1-\cos(\beta-\varphi'_d)}{\sin\beta\cos\varphi'_d}\right] \tag{4.40}$$

$$m=\frac{c'_d}{\gamma H}=\frac{1-\cos(\beta-\varphi'_d)}{4\sin\beta\cos\varphi'_d} \tag{4.41}$$

To get the maximum height of the slope at which the critical equilibrium occurs, substitution of $c'_d=c'$ and $\varphi'_d=\varphi'$ into equation (4.40) gives:

$$H_{cr}=\frac{4C'}{\gamma}\left[\frac{\sin\beta\cos\varphi'}{1-\cos(\beta-\varphi')}\right] \tag{4.42}$$

In addition, the allowable slope height is then given by:

$$H_a=\frac{4c'_d}{\gamma}\left[\frac{\sin\beta\cos\varphi'_d}{1-\cos(\beta-\varphi'_d)}\right] \tag{4.43}$$

To calculate the embankment stability, the values obtained from the field and literature, slope height (H), unit weight (γ), slope inclination angles (β), slope profile (θ), and the material internal friction angle(φ) are used. Stability evaluation is done in terms of the effective cohesion developed and the maximum height at which critical equilibrium is attained on the shear plane. Note that this calculation is under unsaturated conditions. Similar procedures are followed for saturated conditions, but instead, parameters for total normal stress are considered. If the embankment slope height is greater than the critical equilibrium height (H_{cr}), the slope is not stable and failure may occur (Terzaghi, 1943; Terzaghi & Peck, 1967)

Similarly, the factors of safety with respect to effective cohesion and angle of internal friction maybe expressed as:

$$FS_{C'}=\frac{C'}{C'_d}\qquad\text{and}\qquad FS_{\Phi'}=\frac{tan\,\varphi'}{\tan\varphi'_d} \tag{4.44}$$

Further, the universally acceptable calculation for the factor of safety with respect to strength, as given below may also be used (University of Melbourne, 1978);

$$\tau = \frac{\mathrm{C}}{FS} + \frac{\sigma_n \tan\varphi}{FS} \tag{4.45}$$

By using equations (4.28), (4.29) and (4.30), where C is the cohesive force acting on plane AC, given as:

$$C = c \times length\ AC \tag{4.46}$$

Thus, using equation (4.46), the factor of safety could be expressed interms of forces as:

$$FS = \frac{\mathrm{C} + N_a \tan\varphi}{T_a} \tag{4.47}$$

5. FIELD DATA

5.1. Description of studied slopes

During fieldwork, 20 cut slopes and 2 major embankments (fig. 3 and 4) were investigated and are analysed in this thesis. However, field description of two cut slopes and two embankments are expressed in this chapter; i.e. one slope and one embankment for each respective island. The remainder eighteen cut slopes are expressed as summary in table 15 - appendix 3. The initial 'V' means a cut slope in St. Vincent and 'L' means a cut slope in St. Lucia. All slopes investigated in the study area show geological heterogeneity, which means each geological unit is of a particular rock type.

5.1.1. Cut slope V1

The cut slope V1 is located in St. Vincent along the east coast main road trending north from south, near the new international airport under construction, with coordinates Easting: 700268 and Northing 1455352. The slope length and height are approximately 60 m and 9m respectively. The slope was cut in 2006 using mechanical excavator, therefore, no physical excavation damage was observed. The accessibility was fair, although the curving nature posed danger from traffic. The slope is in the alluvial and reworked deposits formation (figure 6), with the rock mass consisting of andesitic and basaltic lava flows, tuffs and pyroclastics. The slope is divided into four geotechnical units (figure 14), with grain sizes range from fine to coarse.

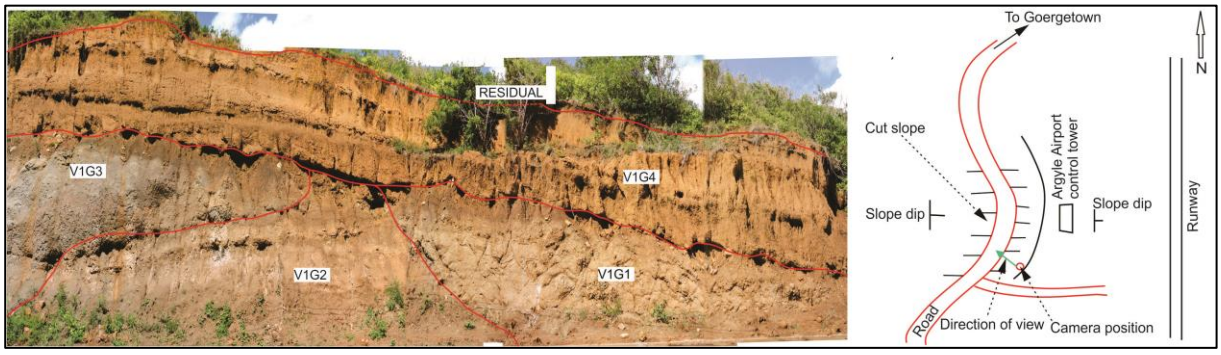

Figure 14: St Vincent, exposure V1, slope geotechnical units (photo: Mulenga, 01/10/2014, 09:30am).

GEOTECHNICAL UNIT V1G1 – The unit is basaltic lava flow of approximate length of 20m and mapped height of 3m; moderately weathered. The colour is greyish- brownish, with massive structure exhibiting spheroidal weathering. The existing slope SDD/SD is $094^0/70^0$; the discontinuity orientations SDD_{disc} and SD_{disc} are $308^0/30^0$, $050^0/60^0$ and $038^0/75^0$ (figure 38 - appendix 3): the persistence along strike and along dip > 1m. Condition of discontinuities: Roughness large scale (Rl) - slightly curved, small scale (Rs) - rough undulating; Infill material (Im)- soft sheared material fine and medium; Karst (Ka)- none.

GEOTECHNICAL UNIT V1G2 – The unit is a highly weathered pyroclastic deposit of approximate length of 15m and height of 2.5m. The colour is greyish darkish brownish, and thick bedded. The existing slope SDD/SD is $094^0/70^0$; the discontinuity orientations SDD_{disc} and SD_{disc} are $286^0/39^0$, $050^0/60^0$ and $174^0/85^0$; the persistence along strike and along dip > 0.15m. Condition of discontinuities: Roughness large scale (Rl) - slightly curved; Roughness small scale (Rs) – rough and polished undulating, and rough planar; Infill material (Im) - soft sheared material fine and no fill-surface staining; Karst (Ka) - none.

GEOTECHNICAL UNIT V1G3 – The unit is a highly weathered basaltic lava flow of approximate length of 15m and height of 3m. The colour is yellowish darkish brownish, and thick bedded. The existing slope SDD/SD is $160^0/75^0$; the discontinuity orientations SDD_{disc} and SD_{disc} are $286^0/39^0$, $050^0/60^0$, $174^0/85^0$, $126^0/80^0$ and $204^0/80^0$; the persistence along strike and along dip > 0.15m. Condition of discontinuities: Roughness large scale (Rl) - slightly curved, small scale (Rs) – rough and polished undulating, and rough planar; Infill material (Im)- soft sheared material fine and no fill-surface staining; Karst (Ka)- none.

GEOTECHNICAL UNIT V1G4 – The unit is a highly weathered tuff deposit of approximate length of 35m and mapped height of 3m. The colour is yellowish darkish brownish and thick weathering horizon. The existing slope SDD/SD is $094^0/70^0$; the discontinuity orientations SDD_{disc} and SD_{disc} are $314^0/25^0$, $233^0/80^0$ and $296^0/90^0$; spacing (SPA) 0.72; the persistence along strike and along dip > 1m. Condition of discontinuities: Roughness large scale (Rl) - slightly curved and straight, small scale (Rs) – rough undulating and planar; Infill material (Im) - soft sheared material fine, no fill-surface staining and flowing material; Karst (Ka) – none.

5.1.2. Belmont Embankment-St. Vincent

The Belmont embankment was constructed in 1970 and it collapsed in September 2013. It was constructed with a height of approximately 25 meters, and embankment inclination angle of about 77 degrees. The natural slope profile angle of 65 degrees was measured from the existing slope. The dry unit weight of the material 14 kN/m^3 was obtained from literature (Belén and Leonardo, 2006; Anon, 2014). The geology along this part of the road embankment is typical of the area, consisting of the alluvial and reworked deposits formation. The embankment was constructed by cut and fill method. Material in the embankment was observed to be typical of the material on the adjacent cut slope. This material consists of slightly humid, brownish red, clayey sandy materials with a few highly weathered corestones. Samples for mineralogy and grain size distribution analyses were collected from both the embankment slope material as well as the cut slope. Drainage pipes daylight on the embankment slope face. A channel was dug and buried on top of the remaining road embankment mass structure for a domestic water pipe. Part of the material from this channel has clogged the drainage channel and culverts. This has led to a further recharge of water into the remaining embankment mass. The remaining segment of the road embankment

showed a slight tilt towards the slope face. Progressively, this might result into another slide or slip (fig 15).

Figure 15: St Vincent, Belmont embankment, viewed from west, north-east and top (photos: Mulenga, 24/09/2014, 14:17pm)

5.1.3. Cut slope L3

The cut slope L3 is located in the east coast of Dennery village, St. Lucia. It is at the Mandele viewpoint along the main road Castries to Vieux Fort (Easting: 728077; Northing 1538164). The slope length and height are approximately 100m and 5m respectively. The slope was cut in the year 1972 by mechanical excavator. The accessibility was fair though with a lot of vegetation along the scree slope. The slope falls in the Andesite agglomerate formation (Central series – figure 7). The rock mass consists of fine to coarse grained matrix and clasts of pebbles to cobbles, with rock units of agglomerate deposits, tuff, alluvial deposits of agglomerate nature, and well graded ash and lapilli pyroclastics. Four geotechnical units of were mapped on this slope face.

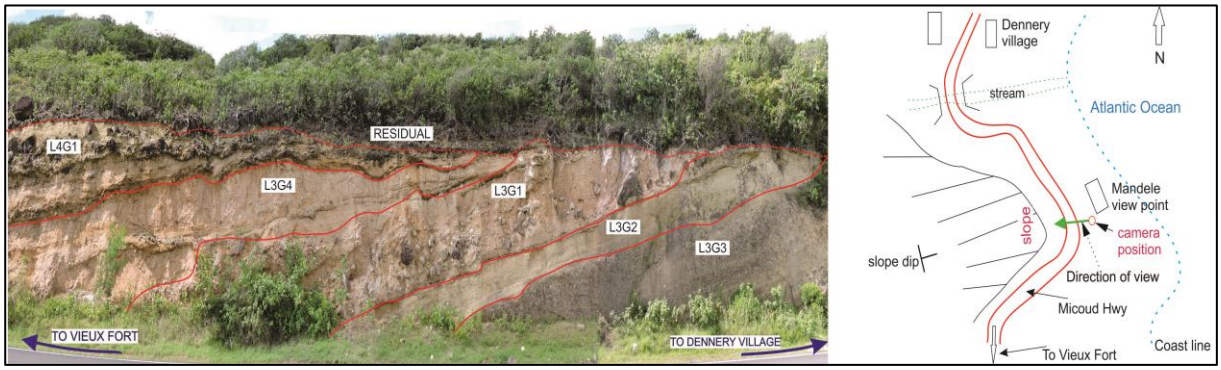

Figure 16: St Lucia, exposure L3, slope geotechnical units (photo: Mulenga, 13/10/2014, 09:15am)

GEOTECHNICAL UNIT L3G1 – The unit is an agglomerate of approximate length of 20m and mapped height of 3m; highly weathered. The colour is greyish yellowish brownish, with thick bedded, matrix supported, poorly sorted andesitic clasts. The existing slope SDD/SD is $040^0/65^0$; the discontinuity orientations SDD_{disc} and SD_{disc} are $012^0/15^0$, $292^0/70^0$, $256^0/85^0$, $358^0/78^0$ and $008^0/75^0$; the spacing (SPA) 0.53; persistence along strike and along dip > 0.2m. Condition of discontinuities: Roughness large scale (Rl) - slightly wavy and curved, and straight; Roughness small scale (Rs) - rough and smooth undulating; Infill material (Im)- no infill –surface staining, and fine non softening and soft sheared material; Karst (Ka)- none. The unit face is eroded, exposing fresh corestones.

GEOTECHNICAL UNIT L3G2 – The unit is a highly weathered pyroclastic ash deposit of approximate length of 20m and height of 1m. The colour is yellowish greyish darkish, and thin bedded fine matrix and well sorted clasts. The existing slope SDD/SD is $040^0/65^0$; the discontinuity orientations SDD_{disc} and SD_{disc} are $144^0/21^0$, $354^0/70^0$, $232^0/75^0$, $298^0/40^0$ and $160^0/65^0$; the spacing (SPA) 0.27; persistence along strike and along dip > 0.07m. Condition of discontinuities: Roughness large scale (Rl) - wavy, curved, slightly curved and straight; Roughness small scale (Rs) – smooth stepped, rough and smooth undulating; Infill material (Im)- fine soft sheared material and no infill-surface staining; Karst (Ka)- none.

GEOTECHNICAL UNIT L3G3 – The unit is a moderately weathered pyroclastic lapilli deposit of approximate length of 50m and height of 4m. The colour is darkish greyish, and thick bedded well-sorted clasts, and clasts supported. The existing slope SDD/SD is $028^0/80^0$; the discontinuity orientations SDD_{disc} and SD_{disc} are $138^0/32^0$, $126^0/20^0$, $354^0/70^0$, $028^0/75^0$ and $024^0/55^0$; the spacing (SPA) 0.34; the persistence along strike and along dip > 0.2m. Condition of discontinuities: Roughness large scale (Rl) - slightly curved, small scale (Rs) – rough and polished undulating, and rough planar; Infill material (Im)- soft sheared material fine and no fill-surface staining; Karst (Ka)- none. The interface between the matrix and clasts is sharp, making discontinuities to be rarely visible.

GEOTECHNICAL UNIT L3G4 – The unit is a highly weathered tuff deposit of approximate length of 16m and mapped height of 2m. The colour is yellowish brownish and thick bedded weathering horizon, with few andesitic corestones. The existing slope SDD/SD is $038^0/67^0$; the discontinuity orientations SDD_{disc} and SD_{disc} are $126^0/20^0$, $160^0/22^0$, $018^0/65^0$, $309^0/27^0$ and $040^0/35^0$; spacing (SPA) 0.29; persistence along strike and along dip > 0.2m. Condition of discontinuities, the roughness large scale (Rl) – wavy, curved, and slightly curved, and the roughness small scale (Rs) – rough stepped and undulating; Infill material (Im) – fine non softening and soft sheared material; Karst (Ka) – none. The unit shows some layer of iron oxidation (iron oxide), evident of chemical weathering.

5.1.4. Barre de l'sle embankment – St. Lucia

The Barre de I'sle embankments were constructed in 1972, at the same time as the Castries to Vieux fort road via Dennery. These embankments collapsed in October 2010, during the hurricane Tomas in which many lives were lost and property damaged. These embankments are located along a ridge characterised by steep to near vertical slopes in residual volcanic soil and rock profiles of the central series (figure 7). Three embankments had collapsed in this location and formation. At the time of fieldwork, all three were under rehabilitation. Rehabilitation works are done by building gabion retaining walls on top of old material and use of geotextiles for drain purposes and retention of fine materials. Representative samples of materials from both borrow source material used in rehabilitation as well as old embankment materials

were collected. From field observation, initial construction of these embankments was done by cut and fill methods, and hence, there mode of failure was similar. Cut slopes in the area are covered by thick vegetation canopies resulting into poor accessibility. Vegetation canopies along the slopes are likely to trap water, necessitate ingress into the embankments mass. No intact materials were observed in the embankments, despite the initial method of construction being non-selective. The likelihood is that the material has undergone weathering and has led to the breakdown and decay of materials with time.

Figure 17: St Lucia, Barre de I'sle embankment under rehabilitation (photo: Mulenga, 10/10/2014, 07:20 am).

6. ANALYSIS AND INTERPRETATION

6.1. Cut slopes

The analyses of cut slopes are carried out in accordance with the method outlined in chapter 4.3.1.

6.1.1. Influence of weathering on geotechnical properties

Geotechnical parameters used for analyses are obtained following methods in chapter 4.3.1.1 to chapter 4.3.2.3. The influence of weathering action on geotechnical properties important for slope stability is determined by observing the change in properties with degree of weathering. The result for correlative plots between average values for intact rock strength (IRS) (field estimates), and the SSPC system calculated angle of internal friction (SFRI), cohesion (SCOH) and spacing parameter (SPA), against field observed degree of weathering for all geotechnical units are shown in figure 18. A geotechnical unit may be defined as a portion of rock mass exhibiting uniform mechanical characteristics and properties of intact material and discontinuities (Robert Hack, 2006). Different degrees of weathering in the field are established by observation and using the scale of weathering grades classification for uniform materials (Chapter 4.2.3.1). The result for the SSPC system calculated slope rock mass intact rock strength (SIRS), internal friction angle (SFRI) and cohesion (SCOH); plotted against degree of weathering reduction values (WE) are shown in figure 19. Figure 19 is also meant to show clearly how the dispersion of points seen in figure 18 would appear in space without the visualisation dashed guidelines. The result for correlative plotting between changes in geotechnical parameters (i.e. ΔSFRI) with changes in degree of weathering reduction values (ΔWE) are given in figure 29 (appendix 1).

Figures 18 and 19 both show the intact rock strength (SIRS) generally decreasing with increase in the degree of weathering for all units. The linear deterioration in intact rock strength observed in tuff is comparable to the linear result obtained by (Esaki & Jiang, 2000) (figure 20A). Similarly, the observed decrease in intact rock strength with increase in degree of weathering for pyroclastics is comparable to the result obtained by Yokota and Iwamatsu (2000), in their study of weathering distribution in pyroclastics in Japan (Figure 20B). The shear strength parameters (cohesion – SCOH and internal friction - SFRI) show a general reduction trend for four units (agglomerates, tuff, andesite, and basalt) with increase in degree of weathering (figure 18). An exception are the pyroclastics which show an increasing trend in cohesion and angle of internal friction, with increase in field observed degree of weathering. The block size (SPA) show an increasing trend in all units of vesicular nature (agglomerates, tuffs, basalts and pyroclastics), as the degree of weathering increases (fig. 18). A decreasing trend is shown in andesite, which is non-vesicular. The susceptibility to weathering of rock units that are vesicular in nature on exposure is generally high due to availability of enough surface area for weathering action (chapter 2.1.3). Andesite is less susceptible to weathering due to its non-vesicular nature.

The correlation between changes (Δ) in geotechnical parameters and increase in degree of weathering (WE) is seen to exist (fig.19). The difference in change for geotechnical parameters increases linearly with the degree of weathering (increase in values for change in weathering) figure 29 (appendix 1).

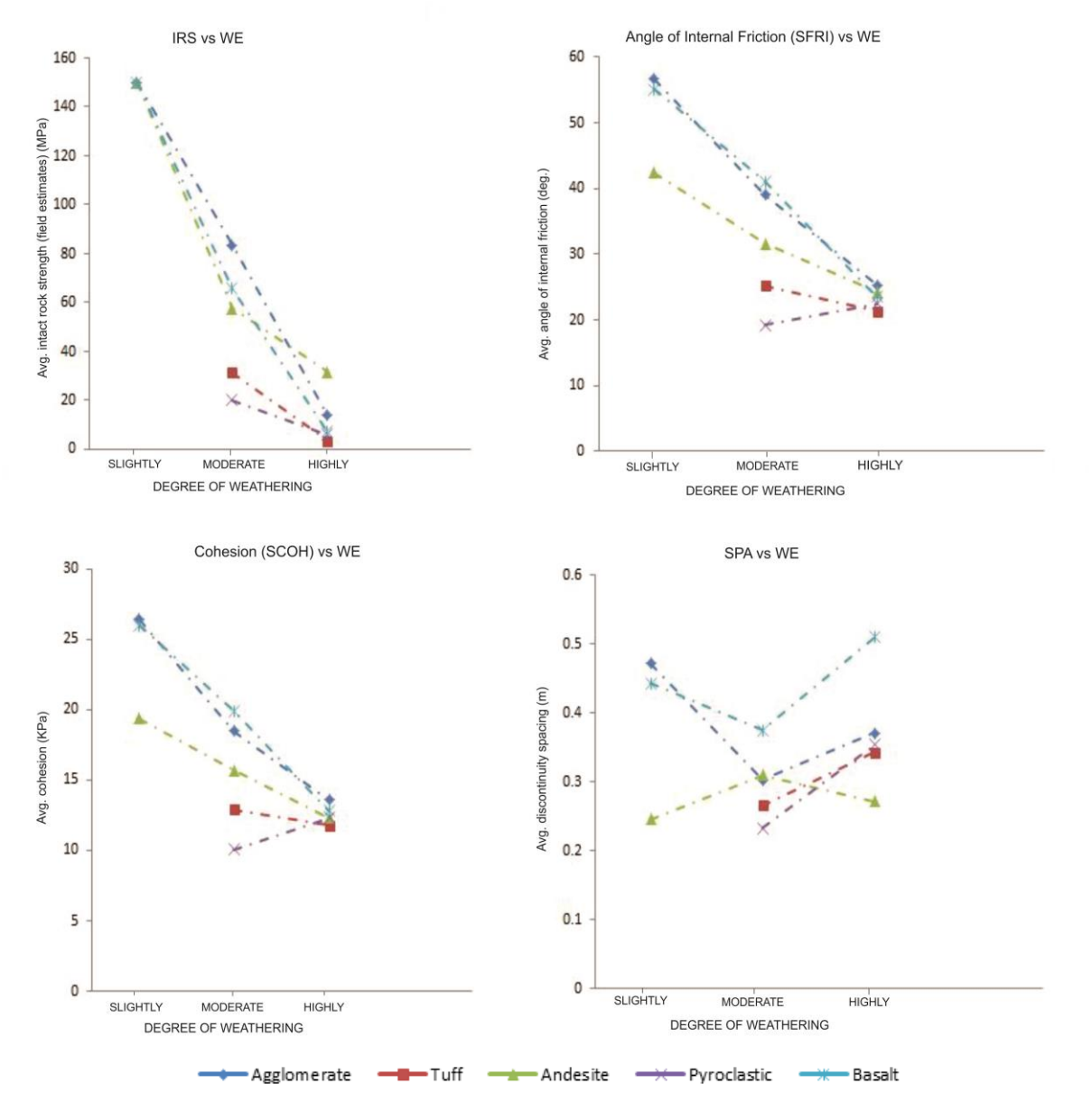

Figure 18: Graphs for average values of geotechnical properties against observed degree of weathering for St. Vincent and St. Lucia (the dashed lines between the makers have no meaning and are only for identification).

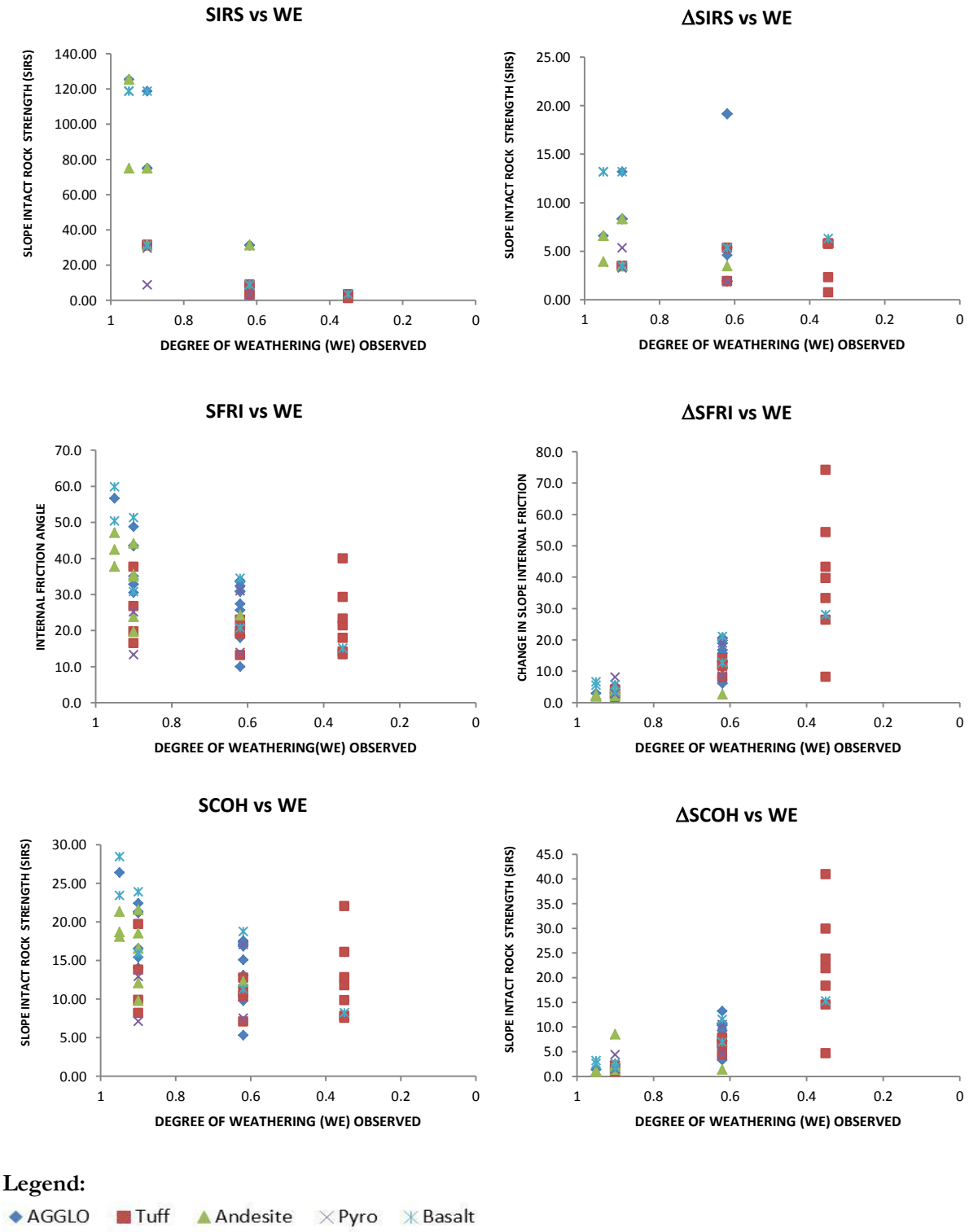

Figure 19: Geotechnical parameters important for slope stability plotted against degree of weathering reduction values (WE).

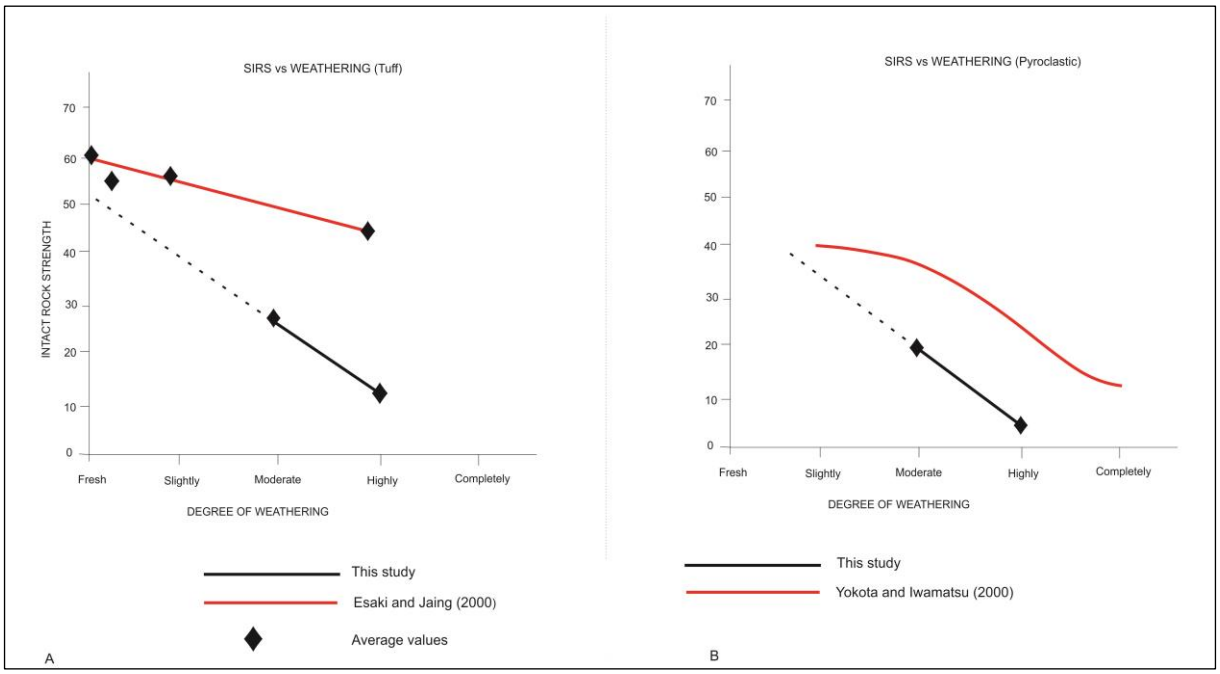

Figure 20: Comparison linear graphs for SIRS vs. weathering; (A) Black shows the result of this study and red shows the result from Esaki & Jiang (2000); (B) Black shows result obtained in this study and red shows the result from Yokota and Iwamatsu (2000). (The dashed lines have no meaning and are only for identification of what would be expected trend)

6.1.2. Weathering in time; weathering rates

The analyses for weathering in time and weathering rates are done according to the methods given in chapter 4.3.1.4. The results for the time related weathering and change in weathering (ΔWE) are shown in figure 21. The graphs for the effect of exposure time (t), logarithmic scale of exposure time (Log (1+1) in years) with change in geotechnical properties for each geotechnical unit, per geological formation are shown in figure 30 and 31 appendix 1. The results for the average weathering rates using equations (4.13) to (4.15) for geotechnical units in each lithological unit are presented in table 7 and table 16 appendixes 1.

The degree of weathering (WE) in all rock units shows an increasing trend (fig. 21). On the other hand, the change in degree of weathering (ΔWE) also shows an increasing trend in all rock units with exposure time (fig. 21). The change (Δ) in geotechnical parameters (i.e. SIRS, SCOH and SFRI) shows a general reduction trend plotted against increasing logarithmic scale of time (log (1 + t)), figure 30 (appendix 1).
Table 7 shows that the average values for weathering (WE), angle of internal friction (SFRI) and cohesion (SCOH) deterioration rates are highest in the weaker rock unit (tuff) and are about 6 times lower in the stronger unit (andesite). Intact rock strength (SIRS) deterioration rate show highest in basalts and lowest in the pyroclastics.

Table 7: Summary of average weathering and geotechnical properties deterioration rates in each lithological unit

UNIT	WE	IRS	SFRI	SCOH
TUFF	0.413	4.601	20.862	11.435
BASALT	0.288	17.552	16.431	8.440
PYRO	0.237	3.787	9.510	5.166
AGGLOMERATE	0.199	6.395	8.087	4.477
ANDESITE	0.098	5.077	2.820	2.194

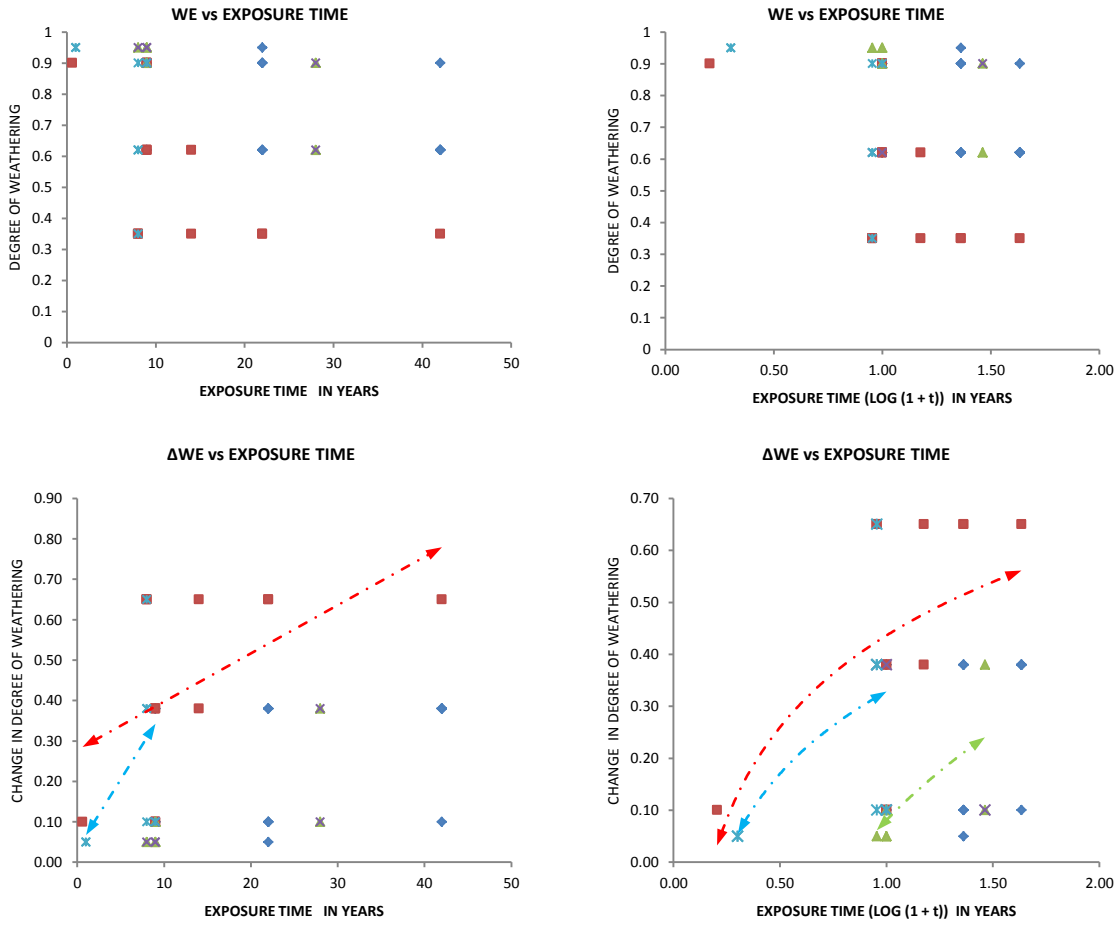

Legend:

Figure 21: Plots for time related weathering and change in weathering (ΔWE). (Blue and green dashed lines show basalt and andesite curving towards constant rates and the red dashed line shows trend, these makers have no meaning and are only for identification).

6.1.3. Current and future stability

The current and future stability are calculated based on the method given in chapter 4.3.1.5. The results are presented as a summary in table 8, and categorically as current and future stability in tables 11 and 12 (appendix 1) respectively for each unit. Currently, all the slopes show a probability of being stable (table 8). However, the future stability probability of the slopes at the end of the engineering life time (50 years), calculated using varying heights, and assuming a uniform height and slope angle, show drastic deterioration in stability probability for most units, except for andesite which maintains a high stability probability (table 8).

Table 8: Current and future stability probability classification

STABILITY PROBABILITIES			
UNIT	CURRENT STABILITY PROBABILITY (%)	FUTURE STABILITY PROBABILITY (%) (Log (1+t) @ t =50 years)	
		Taking maximum values of height and slope angle	Uniform height (7m) and Slope angle (81) for all slopes
AGGLO	95	<5	7.5
TUFF	95	<5	<5
ANDESITE	100	50	80
PYRO	65	<5	6.5
BASALT	85	<5	25

6.2. Embankments

6.2.1. Mineralogy and grain size distribution

The analyses of the mineralogy and grain size distributions in the embankment materials are done as described in chapter 4.3.2.1.

6.2.1.1. Clay mineralogy

The results of laboratory clay mineralogy tests conducted on the embankments fill and borrow materials using X-ray diffraction (XRD) show sharp peaks at 6^0 , 12^0 , and 21^0 (2 theta), suggesting the presence of kaolinite, chlorites and montmorilonite (smectite) clay minerals, and quartz (Figures 22 and 23, and Figures 33 and 34 in appendix 2).

Figure 22 and 33 (appendix 2), show that material from both borrow sources contain quartz and kaolinite. Borrow sources are defined in chapter 4.3.2.1 as quarries where fresh (unweathered) or slightly weathered construction fill material is available. Quartz is expected as it is abundant in igneous rocks and is least susceptible to weathering on exposure to the surface (table 1, chapter 2.1.3). Kaolinite is a product of chemical weathering (equation 2.1 through 2.3, chapter 2.1.2), therefore, its presence in the borrow material indicates that the material has already been subject to weathering.

Figure 23 of embankment fill material show the presence of kaolinite and chlorite, while figure 35 (appendix 2) shows the presence of kaolinite and montmorilonite (smectite) clay minerals. Chlorite clay mineral is a weathering product of basalt and ultrabasic rocks (Tong, 2000; Velde & Meunier, 2008). It is considered as a pore-filling clay mineral, and occurs as individual plates of cabbage head like morphotypes(Ahmed, 2008). Montmorilonite is an alteration product of volcanic tuffs and ash. All of these clay minerals are products of weathering (table 2, chapter 2.1.3), and their presence indicates that the material has undergone weathering. These clay minerals as products of weathering have an effect on the embankment stability in terms of changes caused in fill material permeability and porosity (chapter 2.1.5).

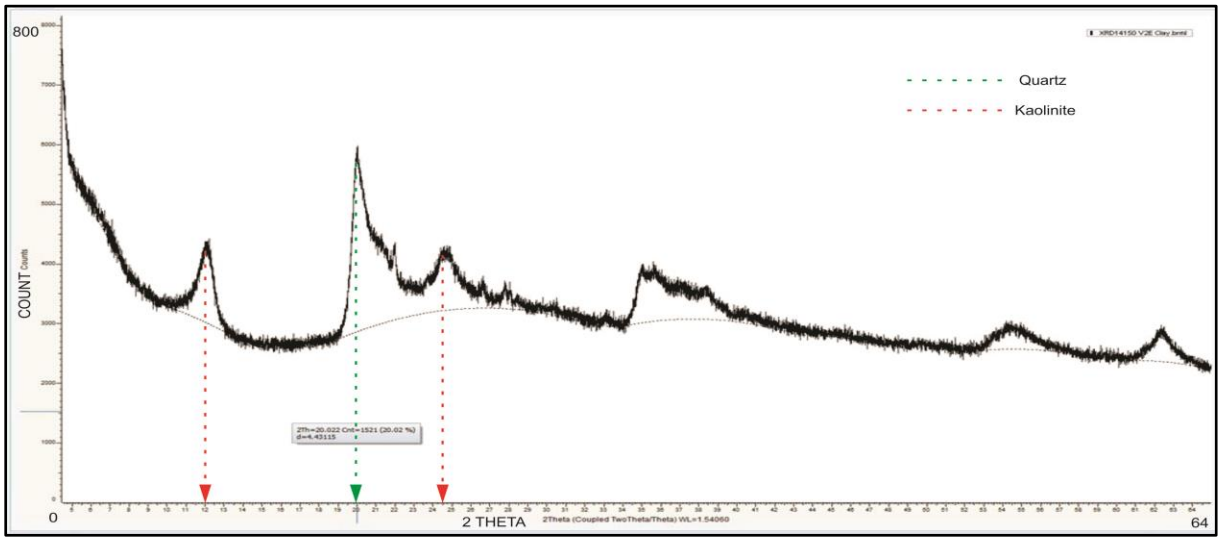

Figure 22: X-ray diffractogram (XRD) for borrow material, Belmont embankment (St Vincent) (the dashed lines on the peaks have no meaning and are only for identification, red for kaolinite peak and green for a quartz peak).

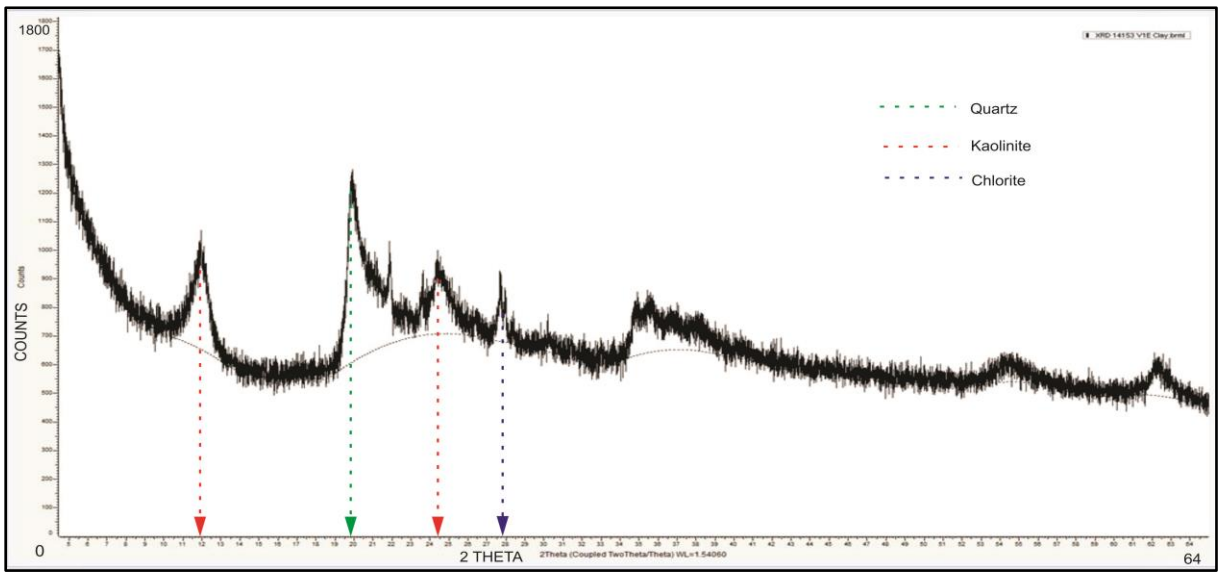

Figure 23: X-ray diffractogram (XRD) for embankment fill material, Belmont embankment (St Vincent) (the dashed lines on the peaks have no meaning and are only for identification, red for kaolinite peak, green for quartz peak, and purple for chlorite peak).

6.2.1.2. Grain size distribution

The weathering degree in fill materials depends significantly on available surface area of grains determined by grain size distribution (chapter 2.1.5). The method for grain size distribution analyses on embankment materials is given in chapter 4.3.2.1. The results from mechanical sieving and hydrometer tests show the presence of sand and fines of varying percentages by weight. The grading curves are shown in figure 24 and figure 36 - appendix 2.

Figure 24 shows a non-uniform, well-graded soil having particle sizes ranging from fines (<0.056 mm) to coarse sand. Using the particle size classification of BS 10-5930 (1999), the embankment material consists of 7% coarse sand, 50.5% medium sand, 30.5% fine sand, and 12% fines. Based on these, the Belmont embankment material can be described as clay-silty-sand, dominantly medium grained. Generally, well-graded soils are very good foundation materials for embankments and backfill (Samtani and Nowatzki, 2006). However, the presence of fine materials, regardless of their plasticity, may have a significant effect on stability of an embankment constructed in steep slopes, due to their effect in the permeability, compaction, and susceptibility to weathering (Holtz & Kovacs, 1981; Budhu, 2011) (chapter 2.1.5). Well-graded soils on densification cause smaller particles to move into the voids in between the larger particles, reducing the porosity. On the other hand, as the voids in soil are reduced, strength and density also increase (Samtani and Nowatzki, 2006). However, in steep valleys, regardless of the compactive effort on the fill material, the angle of repose created by the material may be a source of instability.

Soil strength is determined by its ability to support the load of a structure or keeping it in stability. Its ability to withstand shear stress is dependent on the grain size distribution, clay mineralogy and water content (Craig and Knappett, 2012). In the Mohr-coulomb equation, shear strength of rock or soil is related to cohesion, pore pressure, normal stress, and angle of internal friction (chapter 4.3.2.2). The shear strength in the Mohr-Coulomb theory of failure has two components; which may represent inherent strength due to bonds between particles if they are bonded, and the friction resistance to shearing movement between particles. For cohesive soils, such as the embankment material in Belmont which is shown to be clayey-silty-sand (Figure 24), both strength and friction components are considered. Thus literature estimate values of angle of internal friction (27° – 35°) (USCS) and cohesion 37 kPa (Anon, 2014) for this type of soils are used in the analysis.

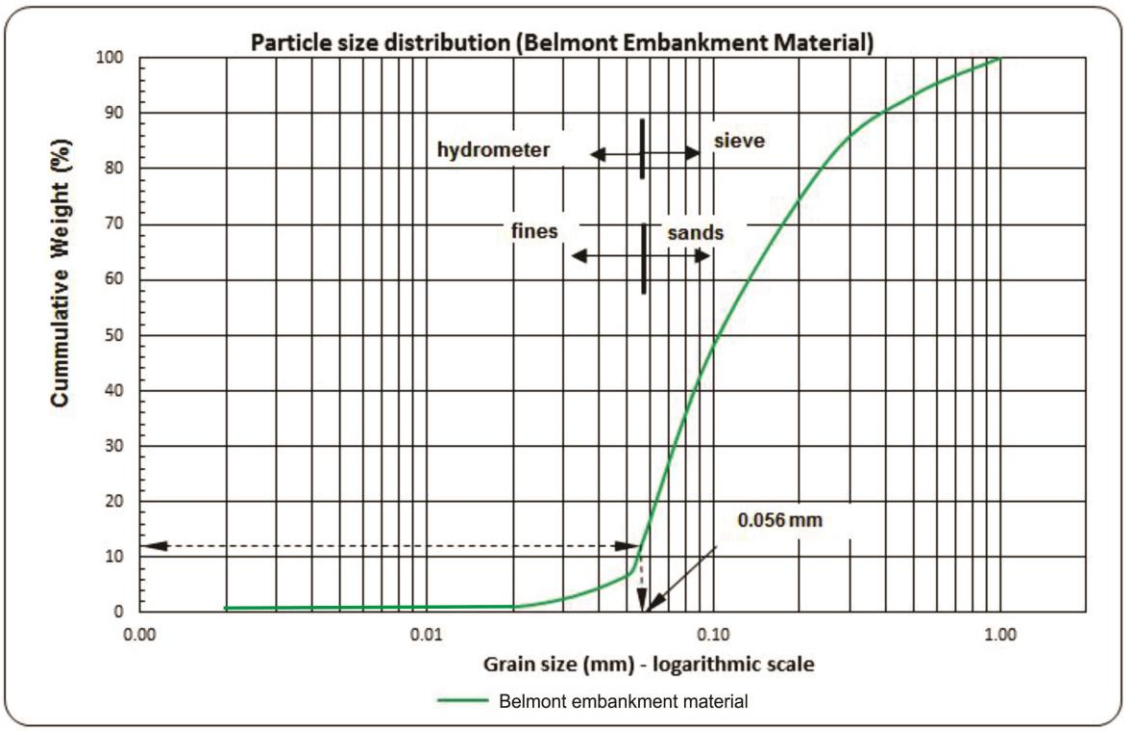

Figure 24: Particle size distribution grading curve of Belmont embankment material

6.2.2. Structural and stability modelling

6.2.2.1. Structural

The road embankments in the study area are constructed along steep valleys by cut and fill methods. This is where a road has been constructed by cutting into the slope and dumping the material below as backfill on the slope profile as road embankment (figure 25A). This mode of construction has a consequence on the stability of both the road embankment and the slope above it. The cause of instability in the cut slope is due to loss of toe support causing stress regime changes, and this result into stress relief. Stress relief causes opening of discontinuities, which may result into rock falls, or possible failure of a slope (chapter 2.1.1). During precipitation events, the discontinuities created in the cut slope may act as rain water recharge vents into the whole mass (slope and embankment) and, this may cause rise in pore water pressure in the material. The continuous loading on the material, due to the embankment structure and traffic, will cause the pore water to move into lower pressure regions, of which in this case is the embankment slope face. The material in the embankment slope is not fully consolidated, but rather stabilises due to the angle of repose created. When pore water is pushed into this region of unconsolidated material, the material is likely to lose its shear strength. Failure may start from the material slope profile bottom were the stress is concentrated, causing the embankment to tilt towards its slope face. Tilt on the road embankment was observed during fieldwork (Chapter 5.1.2). A continuous flow of the pore water causes further loss in material strength and may finally lead to failure of the road embankment. Alternatively, the ingress of water through the discontinuities may widen fissures on the interface between

fill material and the bedrock, creating a slip surface. This may also be referred to as piping, common in poorly compacted and well-graded soils, similar to the dominant soils in figure 24.

Normally, when road embankments are constructed in steep or non-steep slopes, the slope profile maybe benched with varying widths and depths (figure 25B) in order to optimize compaction and consolidation of the fill material to enhance stability (Schweizer and Wright, 1974; Keller and Sherar, 2003). The slope profile may also be cleaned (removal of highly weathered material and organic matter) to facilitate sharp interface between slope profile material and fill material to enhance shear resistance (Hearn et al., 1997; Sachpazis, 2013). For the study site, because of the method of construction, fill material was placed on top of the steep slope profile surface (figure 25A) consisting of highly weathered materials and organic matter. Organic material decomposition is most likely to create a slip surface plane on the interface between the fill material and slope profile surface (Keller and Sherar, 2003).

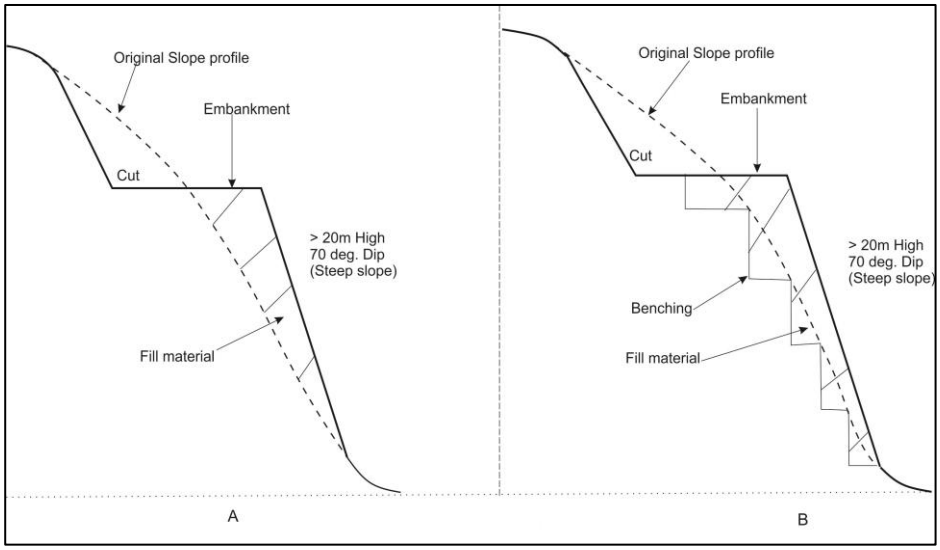

Figure 25: (A) Embankment typical of sites in study area; (B) Embankment when constructed with benched slope profile (after Hearn et al., 1997).

6.2.2.2. Stability modelling

Slope stability analysis is conducted in accordance with chapter 4.3.2.2. From chapter 6.2.1.2 and 6.2.2.1, shear strength of the material is seen to be important in stability. Terzaghi & Peck (1967) attributed failure of most slopes to shear strength. It is considered as an important factor in embankment fill material failure (Waltham, 2009). Thus, the factor of safety with respect to strength of materials will be considered paramount in stability modelling. The stability modelling of the embankment is done in terms of the effective cohesion and effective internal friction developed on the shear plane and the maximum height at which critical equilibrium is attained for a stable constructed slope using equation (4.40), (4.42), and (4.43). However, the role of groundwater is considered critical, and its mechanism theoretically and briefly is given in chapter 6.2.2.1. Groundwater affects the effective stress of a material through the pore water by

carrying part of the soil overburden load (eqn. 4.25 and 4.26, chapter 4.3.2.2). It may enter the road embankment through cracks or surface defects on the embankment road surface or through infiltration from the cuts and fills. Moisture may also be drawn by capillary action from the water table causing the saturation and weakening of the road base (Akin et al., 2012). Therefore, evaluating an embankment in saturated conditions requires consideration of precipitation pattern of the area, ground water level, and recharge conditions, knowledge of pore water pressure in the material, and human activity. Although some of these parameters may be estimated, it is rather an iterative procedure and may be beyond the resources of this thesis. Thus, the embankment stability is evaluated under unsaturated conditions, and effective stress is considered.

In this analysis, a value of one is considered as the factor of safety of a slope at impending failure state, and a factor of safety of 1.5 as an acceptable value for design of a stable slope with respect to strength (Das, 2007). These values are considered in calculating the critical and allowable heights (eqn. 4.42 and 4.43) at which the modelled embankment in figure 26 is expected to be stable or to be failed. The parameters used are estimate values from chapter 6.2.1.2. The embankment height, slope angle, and slope profile angle are obtained from field measurements (chapter 5.1.2).

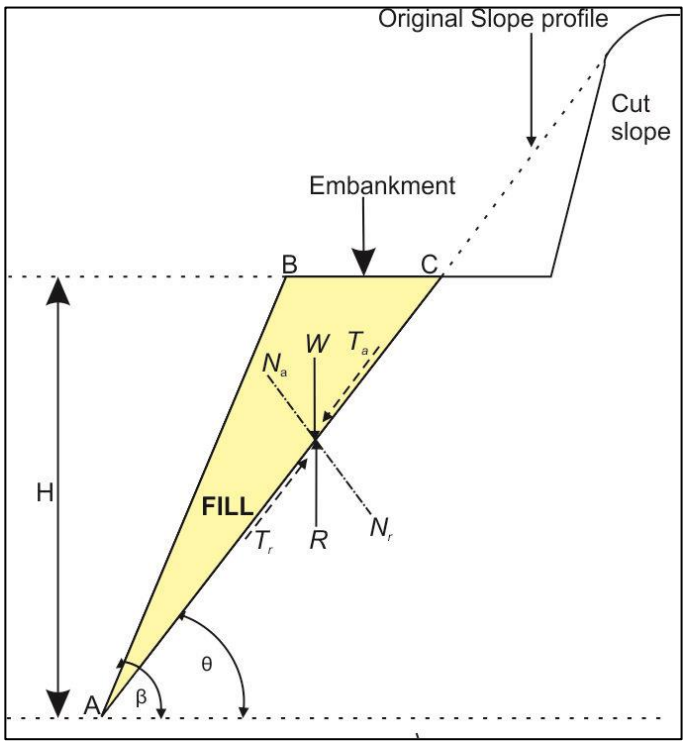

Figure 26: Typical cross section of Belmont embankment (St. Vincent)

Where: $H = Embankment\ Slope\ Height$
$\beta = Slope\ Angle$
$\theta = Slip\ Angle$
$AC = Failure\ plane$
$W = Weight\ of\ wedge\ ABC$
$R = Resisitive\ force$
$N_a = Normal\ component\ of\ W$
$N_r = Resistive\ normal\ component\ of\ W$
$T_a = Tangential\ component\ of\ W$
$T_r = Resistive\ tangential\ component\ of\ W$

Based on the literature estimates of cohesion and angle of internal friction from grain size distribution analyses (chapter 6.2.1.2), and using equations (4.40), (4.42), and (4.43), the stability of the embankment is evaluated for factors of safety of 0.9, 1.5 and 2.0, as shown in tables 12, 13 and 14 (appendix 2), and the summary given in table 9 below;

Table 9: Stability analyses summary for factors of safety 0.9, 1.5, and 2.0

Design factor of safety (FS)	Cohesion (kN/m^2)	Friction angle $(deg.)$	Cohesion developed on failure plane (C'_d) $kN/m2$	Friction angle developed on failure plane $(tan\ \Phi'_d)$ Degrees	Current embankment height (m)	Critical embankment height – H_{CR} (m)	Allowable embankment height - H_a (m)
0.9	37	32	25.47	35.5	25	22.8	23
1.5	37	32	24.67	21.3	25	22.8	18.8
2.0	37	32	18.5	16	25	22.8	9.3

Table 9 shows that the value for calculated cohesion developed along the shear plane at factor of safety 0.9 is lower than the estimated value. The angle of internal friction is rather higher. At this factor of safety, the embankment assumes a height of 23, same as the critical value. The rest of the shear strength parameters are seen to be lower than the estimated values and so are their allowable heights to critical values.

6.3. Discussion on cut slopes

The lithological heterogeneity in the study area has given rise to complex weathering profiles, affirming the Geological Society of London (1995), statement that 'different lithologies weather in different ways in the same climatic regime'. Some materials at time of deposition are already weathered (chapter 2.1.3), and therefore, this has led to differential form of weathering in some slopes (figure 33, appendix 1). In this study, the weathering profile was not defined due to the limited time and resources available during fieldwork. However, geotechnical parameters required to examine the influence of weathering on

deterioration of rock mass properties were defined using the BS 10-5930:1999 (1999), 'simple means' and the Slope Stability Probability Classification System (Hack, 1998) (Chapter 4.2.1).

6.3.1. Deterioration in geotechnical parameters with degree of weathering

For all geotechnical parameters analysed, the effect of weathering is shown by a general trend of increasing deterioration in geotechnical properties of volcanic rock materials as the degree of weathering increases. The intact rock strength (SIRS) of all the rock units plotted against the degree of weathering show a general decreasing trend which suggest that the strength of intact blocks in exposed volcanic rock masses generally deteriorates as the degree of weathering increases (fig. 18). For the tuff and pyroclastics, this is affirmed by the graphs (figure 20, A and B) which show results obtained in this study, and that of Esaki and Jiang (2000), and Yokota and Iwamatsu (2000). All the results show that deterioration in intact rock strength increases as the degree of weathering increases. The results from Esaki and Jiang, and Yokota and Iwamatsu were obtained from Japan, which has a humid temperate climatic, governed by both tropical and polar winds. Aside, both Japan, and the study area are volcanic in origin. Therefore, similar results are expected. The shear strength parameters, cohesion, and angle of internal friction show a gradual decreasing trend in agglomerate, tuff, andesite, and basalt rock units; in pyroclastic, a gradual rise in trend is seen (fig. 18).

The increasing trend in shear strength parameters for pyroclastic could be attributed to the effect of material mode of weathering. The weathering processes occur by alteration and itching of plagioclase and volcanic glass which results in differences in shapes of material grains (Hay, 1959b; Yokota & Iwamatsu, 2000; Oyama & Chigira, 2000) (chapter 2.1.3). These variations in grain surface roughness (texture), likely enhance internal friction angles. Much of the study area is overlain by pyroclastic ash and tuff deposits, and as such, the weathering product halloysite clay mineral is reported to be abundant in the study area (Hay, 1959). Halloysite is also evident in samples obtained from St. Vincent and analysed by analytical spectral device (ASD) (figure 32 - appendix 1). Halloysite is reported to form firm and sharp contact bonds with itched minerals (Hay, 1959b). The strong bond it creates with itched minerals is likely the reason for enhanced cohesion exhibited in the pyroclastic. Aside, pyroclastics ash deposits tend to weld on deposition if they did not completely cool in flight on expulsion from volcanic eruption. This may also enhance cohesion.

The discontinuity spacing (SPA) for basalt, pyroclastic, tuff and agglomerate, shows a general increasing trend with increase in the degree of weathering (fig.18). The high susceptibility to weathering of these vesicular rock units leads to production of various clay minerals as weathering products (Bates, 1960), among them halloysite which acts as vermicular or cavity filling, thereby sealing off some discontinuities

(chapter 2.1.3). This is likely the cause for the general increase in trend for discontinuity spacing with increase in degree of weathering for the vesicular rock units. Non-vesicular rock units are less affected by alteration, as such, the surface area for weathering susceptibility is narrow (Bates, 1960). In addition, the production of weathering clay mineral products is minimal; hence, this could be the reason for the normal decrease in block size and discontinuity spacing with increase in degree of weathering for andesite (fig 18). The decrease in block size with increased degree of weathering is also observed in sandstones by Tating et al., (2014), although in a different environment. The form of weathering and alteration exhibited in vesicular rock units result in blocks appearing solid and unweathered when mapped or observed (figure 41 – appendix 1), a similar observation made by Hay (1960).

6.3.2. Weathering in time; Weathering rates

The weathering time related analyses done on geotechnical units of different lithologies show higher deterioration rate in intact rock strength (SIRS) exhibited in basalt. This is attributed to higher susceptibility to weathering of basalt resulting from availability of surface area for weathering action due to cooling joints. The lower deterioration rate in intact rock strength (SIRS) seen in pyroclastic, is asserted to emanate from cyclic weathering on rock mass (figure 27). This is where the weathered matrix material is washed down (i.e., by slope surface erosion), and fresh (formerly buried) intact blocks are exposed. These blocks at time of investigation may give higher field estimate values for intact rock strength (IRS). Consequently, this may lead to lower calculated values for SIRS deterioration rates in pyroclastic.

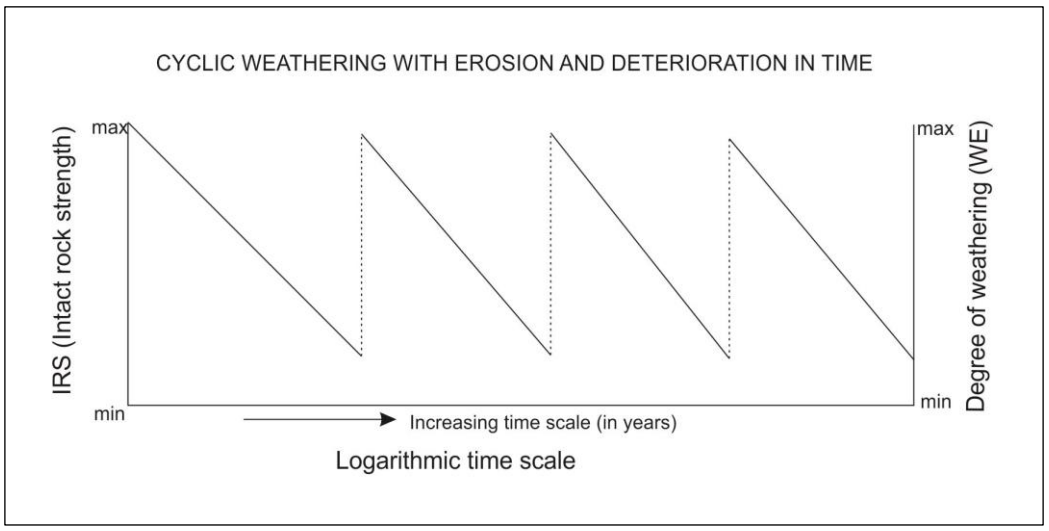

Figure 27: Cyclic weathering with erosion and deterioration in intact rock strength (IRS)

The influence of weathering time related is rather clearly seen in the shear strength parameters (cohesion and angle of internal friction) of rock mass. As the weathering rate decreases in each unit, deterioration

rates for cohesion and internal friction are also seen to decrease. In general, the rate of weathering may be related directly to deterioration rates in shear strength properties of rock mass (table 7).

The degree of weathering (WE) in all units is seen to increase with exposure time and logarithmic scale of time. On the other hand, the change in degree of weathering (ΔWE) increases in all units with both exposure time and logarithmic scale of time, and this can be seen as such on a decreasing rate of a linear or logarithmic scale (fig. 21). The increase shows an approximate linear plot against the logarithmic time scale. The result in pyroclastic is comparable to that of Huisman (2006) in the sandstones; as generally, pyroclastics have similar engineering properties with sandstones (Franklin and Dusseault, 1989).

All the five units show non-linearity in weathering rates (figure 21, table 16 - appendix 3). The result for basalt and andesite agrees with the suggestion of non-linearity by (Colman, 1981). Colman postulated that as the degree of weathering increases with time, the residue thickness also increases, and so the weathering rate begins to approach a constant as an equilibrium thickness of residue is approached (or reached). The plots showing curving towards constant weathering rates for basalt and andesite are shown by the blue and green dashed lines (figure 21). Tuff shows an average weathering rate (0.4mm/year) higher than the other units do (table 7). This average is calculated from values of weathering rates ranging from 0.1 to 0.68 mm/year (table 16- appendix 1); generally, in steep cut slopes (> 70 degrees). The result is comparable to the weathering rates (0.03-0.59 mm/year) obtained by Erguler (2009) from a field investigation of tuff in Ankara, Turkey which are reported to be low, attributing to steep slopes of greater than 70 degrees, despite the difference in climatic conditions. Climatic conditions have an important effect on weathering rates and processes. Humid climates such as the study area are expected to give higher weathering rates. However, Ankara, Turkey from which the measurements are taken has a very harsh climate, hot summers temperatures ranging 36 to 40 degrees Celsius, cold (ice/snow) winters, annual precipitation (>300 mm), and this is coupled with large changes in day and night temperatures. Hence, such climatic conditions are likely to give weathering rate values similar to that of humid climates like the study area.

6.3.3. Slope stability and weathering

From the analyses, it is shown that weathering exhibits a profound influence on the deterioration of intact rock strength and shear strength properties of volcanic rocks in the study area. In general, deterioration in geotechnical properties (intact rock strength, cohesion, and internal friction angle) of volcanic rock masses in the slope exposures is seen to increase with increase in degree of weathering and exposure time. The assessed deterioration in properties due to weathering and exposure time has culminated into lower assessed stability probabilities in engineering lifetime of slopes (table 8). Andesite shows probability of being stable in engineering lifetime of 50 years. This is mainly due to the lower susceptibility to weathering it exhibits because of its non-vesicular nature, which also give rise to lower deterioration rates in shear strength parameters (table 7). The low stability probabilities seen in the other rock units, coupled with

other environmental factors (i.e., rise in pore water pressure), result into slope failures. Thus, it is postulated that deterioration in geotechnical properties of rock materials due to weathering seen in chapter 6.1, is likely the main cause for most slope failures that occur in the study area. However, due to uncertainties in the data, firm conclusions cannot be drawn.

6.4. Discussion on embankments

The results suggest that borrow source materials in their in-situ state have already been weathered, and include weathering product kaolinite. Kaolinite clay minerals poses an engineering challenge in embankments water flow (permeability) which is an important component on effective stress and subsequent shear strength in embankment stability (chapter 4.3.2.2). Kaolinite clay mineral has a low affinity for water; therefore, its presence also indicates that the soil is likely to have low plasticity. The presence of chlorite clay mineral in the embankment material, which is a product of basalt and ultrabasic rocks, indicates that the material has been subject to weathering. It is a pore-filling clay mineral, and is likely to influence the permeability of the material. Volcanic tuffs and ash overlay much of the study area, and their alteration product is montmorilonite (fig.35, Barre de I'sle embankment St. Lucia – appendix 2). Montmorilonite (smectite) clay on weathering also forms kaolinite clay minerals. Hence, the few peaks of montmorilonite (smectite) and more peaks of kaolinite clay minerals observed in the embankment material (fig. 35 – appendix 2), may be likely due to montmorilonite further weathering with time into kaolinite (table 2, chapter 2.1.3); especially that conditions for chemical weathering are highly favourable in the region. It is also likely that montmorilonite is present in the Belmont embankment in St Vincent. This is because geological conditions in which the embankments are constructed are similar. However, its omission may have been due to the limited number of samples collected for analysis, mainly due to the limited accessibility to slope face posed by steep terrain. Montmorilonite is expansive clay, and its swelling potential causes heaving and shrinkage of materials. This is likely to induce cracks on the top of the road embankment facilitating water ingress.

Water is supplied into the embankments by infiltration of rainfall, the rise in ground water level, and at times because of human action. These may be associated with relative decrease of suction towards the zero value. The processes in opposition are the removal of water from the ground by evapo-transpiration, and depression of ground water level (O'Connell & Gourley, 1993). Thus, water sources and its availability must be investigated before stability assessments are performed on road embankments. If the sources of water are not identified correctly, accounting for the likely changes in moisture conditions in the road embankment material may be impossible. In tropical environments like the study area, notable changes in suction in the soil material may occur only seasonally. Therefore, the effective values for shear strength

parameters used in modelling the embankment in figure 26 may be valid only in dry conditions and not in rainfall seasons during which the moisture content and ground water phreatic level is expected to be high.

Fill material weathering involves both physical and chemical weathering. These two modes of weathering are responsible for the breakdown of coarse grained particles into fine grains and formation of clay minerals by alteration and oxidation processes. Reduced particle size affects the roughness and circumference of fill material grains, with further weathering in time causing them to become smoother, and resulting into reduced internal friction angles. Particle size reductions also causes decrease in permeability and subsequently increase in pore water pressures, resulting into reduced cohesion and tensile strength (chapter 2.1.5). This action by weathering leads to deterioration of fill material geotechnical properties (soil shear strength parameters). This is likely to have occurred in the embankment fill materials, and consequently may have led to the failure. The presence of liesegang rings in some lithological units (figure 37 - appendix 2) suggest chemical weathering (Vysinka et al., 2011).

From table 9, chapter 6.2.2.2, it can be seen that increasing the factor of safety from 0.9 to 1.5 and then 2.0 leads to a decline in cohesion and friction angle developed along the shear plane, and the allowable height. The critical height, which is the maximum height at which the critical equilibrium occurs in the embankment slope, is 29.8 meters, and it is calculated based on the effective cohesion and internal friction angle. A factor of safety 0.9 for the embankment is assumed to have failed, since the calculated allowable height is above the critical height. At this height, the calculated cohesion is less than the estimate value, while the angle of internal friction is slightly higher than the estimate value. This scenario results into a definite failure since the allowable value of height is also higher than the critical value. The acceptable design factor of safety 1.5 gives the maximum allowable height of 18.8 meters. At this height, the slope is expected to be stable. The factor of safety 2 at which the embankment slope would be very stable gives the lowest allowable height of 9.3 meters. The embankment was constructed at a height of aboout 25 meters well above the calculated maximum critical and allowable height of failure. The material was probably held in place by the artisanal retaining wall built on the fill material repose slope surface (Figure 28). This assertion is evident from the wall's remains still hanging on the embankment slope face, and the nearby intact embankment roads.

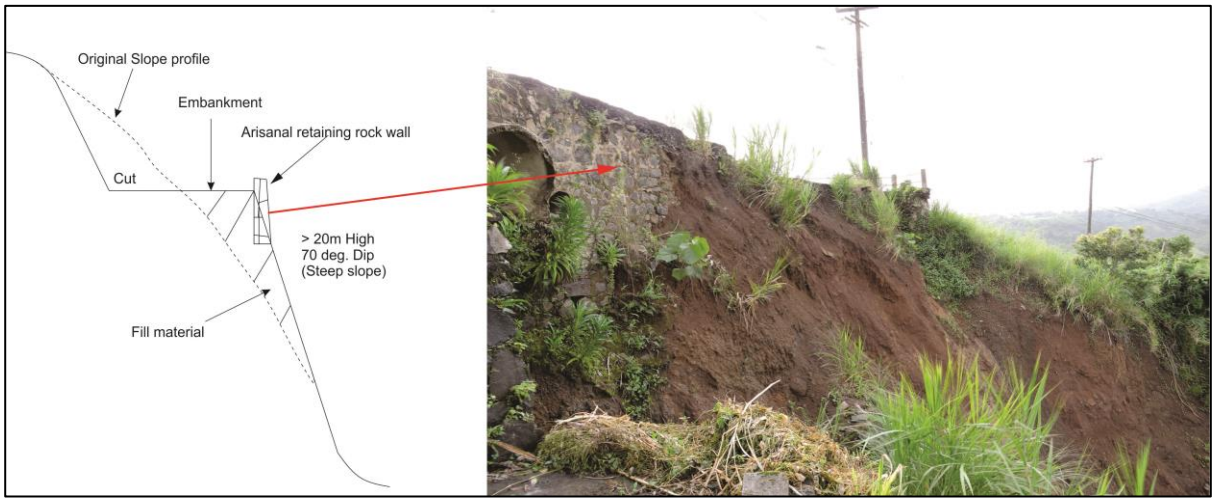

Figure 28: Belmont embankment showing the retaining rock wall (St Vincent).

The analyses establish some factors that could have led to failure of the road embankments. These factors are given as follows;

a. The weathering of materials led to deterioration on geotechnical parameters causing the loss of shear strength of materials;

b. Ground water recharge from precipitation, led to daylighting on slope face causing loss of material shear strength;

c. The method of construction (design) and height of the embankment, caused material consolidation failure resulting into the stability being controlled by the angle of repose created, or;

d. The combination of a, b, and c.

7. CONCLUSION AND RECOMMENDATION

7.1. Conclusion

Cut slopes

In this region, it is common to find volcanic rock formations interbedded in an exposure, following sequences of volcanic deposition, alluvial and reworked deposition, or intrusion. This heterogeneous nature of the geological formations demands understanding the response of each lithological rock unit to weathering and stress relief. For instance, if a rock mass is interbedded by tuffs which have higher weathering rates than other lithologies examined in this research, such a slope may undergo undercutting due to preferential weathering (i.e. figure 40 – appendix 3). This implies that such a slope may not stand to its engineering lifetime and may lead to untimely failure. Therefore, in such cases, remedial measures that take into consideration the action of weathering and deterioration on rock mass should be considered immediately after excavation.

Embankments

Figure 17 (chapter 5), shows the use of geotextiles on gabion retaining structures in the rehabilitaion of the collapsed Barre de I'sle embankment, St. Lucia. From the discusion (chapter 6.3.2) on fill material weathering and chapter 2.1.5, it is the authors opinion that the use of geotextiles on gabion retaining walls in this geological formation could be inappropriate. From the XRD analysis and grain size distibution done on samples obtained from the study area, it can be seen that kaolinite, chlorite and montemorilinite (smectite) clay minerals, and fines of varying properties and character are products of fill material weathering in this formation. These clay minerals and fines are likely to clog the geotextile material, limiting the amount of water discharged from the embankment fill material. Resulting is pore water pressure rise during heavy rains. Rise in pore water may lead to reduction in fill material shear strength (Davis, 1995). The weight of the embankment material, with reduced shear strength will have to be supported by the gabion retaining structure, which is also founded on weathered embankment material on steep slopes. The authors speculation is that the embankments are still not safe, and therefore, recommends that weathering and weathering susceptibilty of materials be considered as guide in planning and construction of such vital and costly infrastructure to prevent recurrence of failures.

7.2. Recommendation

The study shows that it is possible to determine the influence of weathering on deterioration of geotechnical properties of volcanic rocks and soil masses in both cut slopes and road embankments in the tropical environment of St. Vincent and St. Lucia, using the BS standards, SSPC system, and Colman's formula based methods. However, in order to improve this study results, the following recommendations are made:

- It is important to take a time series of measurements from the study area to determine the physical changes of properties (i.e., IRS) of known exposures with time, in order to validate the methods and data used in this study, for easy determination of weathering and future weathering (chapters 4.3.1.5).
- Since tropical and humid environments are conducive for chemical weathering, other methods for determining the change in properties important for geotechnical parameters in embankments materials, i.e., elemental or oxide analysis, may be valuable (chapters 2.1.3).

LIST OF REFERENCES

14689-1: ISO. (2003). Geotechnical investigation and testing -- Identification and classification of rock -- Part 1: Identification and description. *European Committee for Standardization*, (015), pp 24.

Admassu, Y., Shakoor, A., & Wells, N. a. (2012). Evaluating selected factors affecting the depth of undercutting in rocks subject to differential weathering. *Engineering Geology*, *124*, 1–11. doi:10.1016/j.enggeo.2011.09.007

Ahmed, W. (2008). Contrast in clay mineralogy and their effect on reservoir. *Bulletin of Chemical Society of Ethtiopia*, *22*(1), 41–65. doi:ISSN 1011-3924

Aires-Barros, L. (1978). Comparative study between rates of experimental laboratory weathering of rocks and their natural environmental weathering decay. *Bulletin of the International Association of Engineering Geology*, *18*(1), pp 169–174. doi:10.1007/BF02635366

Akin, M., Fay, L., and Shi, X. (2012). *SYNTHESIS 430 Cost-Effective and Sustainable Road Slope Stabilization and Erosion Control* (p. 82). National Academy of Sciences. ISBN: 978-0-309-22362-1.

Anderson, M. G. (1982). Predicting pore-water pressures in road cut slopes in the West Indies. *Applied Geography*, *2*(1), 55–68. doi:10.1016/0143-6228(82)90017-0

Anderson, M. G. (1983). Road-cut slope topography and stability relationships in St Lucia, West Indies. *Applied Geography*, *3*(2), 105–114. doi:10.1016/0143-6228(83)90033-4

Anderson, M. G., Holcombe, E., Blake, J. R., Ghesquire, F., Holm-Nielsen, N., & Fisseha, T. (2011). Reducing landslide risk in communities: Evidence from the Eastern Caribbean. *Applied Geography*, *31*(2), 590–599. doi:10.1016/j.apgeog.2010.11.001

Anderson, M. G., Holcombe, L., & Renaud, J.-P. (2007). Assessing slope stability in unplanned settlements in developing countries. *Journal of Environmental Management*, *85*(1), 101–11. doi:10.1016/j.jenvman.2006.08.005

Anderson, M. G., & Kneale, P. E. (1980). An examination of the relationship between strom precipitation and pore water conditions in road cut slopes, St. Lucia, West Indies. *Singapore Journal of Tropical Geography*, *1*(1), 1–8. doi:10.1111/j.1467-9493.1980.tb00096.x

Anderson, M. G., & Kneale, P. E. (1985). Empirical approaches to the improvement of road cut slope design, with special reference to St. Lucia, West Indies. *Singapore Journal of Tropical Geography*, *6*(2), 91–100. doi:10.1111/j.1467-9493.1985.tb00163.x

Anderson, M., & Holcombe, E. (2013). *Community based landslide risk reduction: Managing Disasters in Small Steps*. (p. 447). World Bank Publications 2013, Washington, DC 20433, USA. ISBN: 978-0-8213-9491-5.

Anon. (1961). Soil conservation service (US Department of Agriculture). In *SCS National Engineering Handbook: Section 8 Engineering Geology* (p. 192).

Anon. (2014). Goelogical and geotechnical investigation conducted for the government of St. Vincent. *Government of St. Vincent, Ministry of Transport, Unpublished Report*.

Arıkan, F., Ulusay, R., & Aydın, N. (2007). Characterization of weathered acidic volcanic rocks and a weathering classification based on a rating system. *Bulletin of Engineering Geology and the Environment*, *66*(4), 415–430. doi:10.1007/s10064-007-0087-0

Aryal, K. (2006). *Slope stability evaluations by limit equilibrium and finite element methods. (pp146)*. Norwegian University of Science and Technology. ISBN: 82-471-7881-8.

Augustine, S., Lindsay, J., David, J., Shepherd, J., & Ephraim, J. (2002). Volcanic Hazard Assessment for Saint Lucia , Lesser Antilles. *Unpublished Report Presented to the Government of St. Lucia, August 2002.*, pp 46.

Barton, N. R., Lien, R., Lunde, J. (1974). Engineering classification of rock masses for the design of tunnel support. *Rock Mechanics and Rock Engineering*, *vol. 6*(4), pp 189–236. doi:10.1007/BF01239496

Bates, T. F. (1960). Halloysite and gibbsite formation Hawaii clays. *Clay and Clay Minerals*, *vol. 9*(1), p 315 – 328. doi:10.1346/CCMN.1960.0090119

Belén, L. A., and Leonardo, P. P. (2006). Technical report on the soil investigation for the argyle international airport project, Saint Vincent. Retrieved from http://www.embsvg.com/IADC/PDF/

Bell, F. G. (1992). Influence of weathering and discontinuities on the behaviour of rock masses. *Engineering in Rock Masses*, 27–53 (580). doi:10.1016/B978-0-7506-1965-3.50006-6

Bishop, A. W., and Bjerrum, L. (1960). "The Relevance of the Triaxial Test to the Solution of Stability Problems," Proceedings, American Society of Civil Engineers, Research Conference on Shear Strength of Cohesive Soils, Boulder, Colorado, (pp. 437–501).

Bland, W. and Rolls, D. (1998). *Weathering – An introduction to the scientific principles*. (1st ed., p. 288). Arnold Pubishers, London. ISBN: 0340677449.

Borrelli, L., Greco, R., & Gullà, G. (2007). Weathering grade of rock masses as a predisposing factor to slope instabilities: Reconnaissance and control procedures. *Geomorphology*, *87*(3), 158–175. doi:10.1016/j.geomorph.2006.03.031

Bouysse, P. (1984). The lesser antilles island-arc-structure and geodynamic evolution. In Biju-Duval et al., (eds), Initial Reports of the Deep Sea Drilling Project; Washington, DC., US Government Printing Office., *vol. 78a*, p 83–103.

BS 10-5930:1999. (1999). *Code of practice for site investigations, British standard. British Standards Institution, London 152*. (p. 207). ISBN: 0 580 33059 1.

Budhu, M. (2011). *Soil mechanics and foundations* (3 rd., p. 781). John Wiley & Sons, Inc. ISBN: 9780470556849.

Calcaterra, D., and Parise, M., (Eds). (2010). *Weathering as a Predisposing Factor to Slope Movements. Engineering Geology Special Publications: Geological Society of London; 23; 77–103*. (p. 248). ISBN-10: 1862392978.

Colman, S. M. (1981). Rock-weathering rates as functions of time. *Quaternary Research*, *15*(3), 250–264. doi:10.1016/0033-5894(81)90029-6

Craig, J. A. and Knappett, R. F. (2012). *Craig ' s Soil Mechanics* (Eighth edi., p. 580). Spon Press, London. ISBN: 9780415561259.

Das, B. (2002). *Principles of geotechnical engineering* (Firth edit., p. 607). wadsworth group, USA. ISBN: 053438742X.

Das, B. (2007). *Fundamentals of geotechnical engineering* (Third Edit., p. 622). Cengage Learning, USA. ISBN: 9780495295723.

Davis, R. O. (1995). Pore pressure effects on interface behavior. *Studies in Applied Mechanics*, *vol. 42*, 449–461. doi:10.1016/S0922-5382(06)80021-8

De Mulder, E., Hack, H., & Ree, C. Van. (2012). *Sustainable development and management of the shallow subsurface*. Geological Society of London. ISBN: 1-86239-343-5.

Dearman W.R. (1976). Weathering classification in the characterisation of rock. A revision . *Bulletin of the International Association of Engineering Geology,*, *13*(1), 123–127. doi:10.1007/BF02634744

Del Potro, R., & Hürlimann, M. (2008). Geotechnical classification and characterisation of materials for stability analyses of large volcanic slopes. *Engineering Geology*, *98*(1-2), 1–17. doi:10.1016/j.enggeo.2007.11.007

Del Potro, R., & Hürlimann, M. (2009). The decrease in the shear strength of volcanic materials with argillic hydrothermal alteration, insights from the summit region of Teide stratovolcano, Tenerife. *Engineering Geology*, *104*(1-2), 135–143. doi:10.1016/j.enggeo.2008.09.005

Duzgoren-Aydin, N. ., Aydin, A., & Malpas, J. (2002). Distribution of clay minerals along a weathered pyroclastic profile, Hong Kong. *CATENA*, *50*(1), 17–41. doi:10.1016/S0341-8162(02)00066-8

Ebuke, J., Hencher, S.R., and Lumsden, A. C. (1993). The influence of structure on the shearing mechanisms of weakly bonded soils. *The Engineering Geology of Weak Rock, Cripps et Al., (Eds)*, (Balkema, Rotterdam, pp 207-215. ISBN: 90 61911672).

Erguler, Z. A. (2009). Field-based experimental determination of the weathering rates of the Cappadocian tuffs. *Engineering Geology*, *105*(3-4), 186–199. doi:10.1016/j.enggeo.2009.02.003

Esaki, T., & Jiang, K. (2000). Comprehensive study of the weathered condition of welded tuff from a historic stone bridge in Kagoshima , Japan. *Developments in Geotechnical Engineering*, *84*, 341–350. doi:10.1016/S0165-1250(00)80028-0

Fell, R., MacGregor, P., Stapledon, D., & Bell, G. (2005). *Geotechnical engineering of dams* (p. 912). Balkema, Leiden. ISBN: 04 1536 440 x.

Fookes, P.G., Gourley, C.S., & Ohikere, C. (1988). Rock weathering in engineering time. *Quarterly Journal of Engineering Geology*, *21*, pp 33–57. doi:10.1144/GSL.QJEG.1988.021.01.03

Franklin, J. A., and Dusseault, M. B. (1989). *Rock Engineering*. (p. 600). McGraw-Hill, New York. ISBN: 0070218889.

Gabler, E. R., Peterson, J. F., Trapasso, L. M., and Sack, D. (2009). *Physical geography* (9th ed., p. 557). Belmont, CA 94002-3098, USA. ISBN:13:978-495-55506-3.

Gabrieli, F., Lambert, P., Cola, S., & Calvetti, F. (2012). Micromechanical modelling of erosion due to evaporation in a partially wet granular slope, (April 2011), 918–943. doi:10.1002/nag

Garcia-Vallès, M., Topal, T., & Vendrell-Saz, M. (2003). Lichenic growth as a factor in the physical deterioration or protection of Cappadocian monuments. *Environmental Geology*, 776–781. doi:10.1007/s00254-002-0692-y

Goldich, S. (1938). A study in rock-weathering. *The Journal of Geology*, *vol. 46*(1), 17–58. doi:10.1086/624619

Gupta, A. S., & Rao, S. K. (2001). Weathering indices and their applicability for crystalline rocks. *Bulletin of Engineering Geology and the Environment*, *60*(3), 201–221. doi:10.1007/s100640100113

Hachinohe, S., Hiraki, N., & Suzuki, T. (2000). Rates of weathering and temporal changes in strength of bedrock of marine terraces in Boso Peninsula, Japan. *Engineering Geology*, *55*(1-2), 29–43. doi:10.1016/S0013-7952(99)00104-0

Hack, H., & Price, D. (1997). Quantification of weathering. *In Marinos, Kouikis, Tsiambaos, Stournaras (eds) Proceedings of the Engineering Geology and the Environment. A.A. Balkema, Rotterdam*, pp 145–150.

Hack, R. (1998). *Slope Stability Probability Classification (SSPC). 2nd Edition* (p. 258). ITC Publication no. 43, Enschede, The Netherlands. ISBN: 90 6164 154 3.

Hack, R. (2006). Discontinuous Rock Mechanics:lecture note, 5.0 ed. ITC lecture note. ITC, Enschede., pp 334.

Hack, R. (2008). Weathering deteriorating and slope stability classification for the future,. *Namur, Belgium.*, (12, June 2008), 59.

Hack, R., & Huisman, M. (2002). Estimating the intact rock strength of a rock mass by simple means. *Engineering Geology for Developing Countries - Proceedings of 9th Congress of the International Association for Engineering Geology and the Environment. Durban, South Africa, 16 - 20 September 2002.*, (0), 16–20. ISBN: 0–620–28559–1.

Hack, R., Price, D., & Rengers, N. (2003). A new approach to rock slope stability–a probability classification (SSPC). *Bulletin of Engineering Geology and the Environment,Springer Berlin / Heidelberg, 62 (2)*, pp 167–184. doi:10.1007/s10064-002-0155-4

Hay, R. (1959a). Formation of the crystal-rich glowing avalanche deposits of St. Vincent, BWI. *The Journal of Geology*, *vol.67*(5), pp 540–562. doi:10.1086/626606

Hay, R. (1959b). Origin and weathering of late Pleistocene ash deposits on St. Vincent, BWI. *The Journal of Geology*, *vol. 67*(1), 65–87. doi:10.1086/626558

Hay, R. (1960). Rate of clay formation and mineral alteration in a 4000-year-old volcanic ash soil on Saint Vincent, BWI. *American Journal of Science*, *vol. 258*(5), pp 354–368. doi:10.2475/ajs.258.5.354

Hearn, G .J., Lawrance, C. J., & Weekes, R. M. (1997). *Overseas road note 16 principles of low cost road engineering in mountainous regions , with special reference to the nepal himalaya.* (p. 166). ISBN:0951-8797.

Hodder, A. P. W. (1984). Thermodynamic interpretation of weathering indices and its application to engineering properties of rocks. *Engineering Geology*, *20*(3), 241–251. doi:10.1016/0013-7952(84)90004-8

Hoek, E., Read, J., Karzulovic, A., & Chen, Z. Y. (2000). Rock slopes in Civil and Mining Engineering. *In Proceedings of the International Conference on Geotechnical and Geological Engineering, GeoEng2000, 19-24 November, 2000, Melbourne.*

Holtz, R., & Kovacs, W. (1981). *An introduction to geotechnical engineering* (p. 746). Prentice hall, Englewood Cliffs, New Jersey 07632. ISBN: 0134843940.

Homand F. and Souley M. (1996). Stability of Jointed Rock Masses Evaluated by UDEC with an Extended Saeb-Amadei Constitutive Law, *33*(3), 233–244. doi:10.1016/0148-9062(95)00063-1

Huisman, M. (2006). *Assessment of rock mass decay in artificial slopes*. PhD thesis. Technical University Delft (ITC dissertation number 137). pp 299. ISBN: 90-6164-246-9.

Irfan,T. Y. (1996). Mineralogy, fabric properties and classification of weatbered granites in Hong Kong. *Quarterly Journal of Engineering Geology*, *29(1)*, pp 5–35.

Kainthola, A., Singh, P. K., & Singh, T. N. (2014). Stability investigation of road cut slope in basaltic rockmass, Mahabaleshwar, India. *Geoscience Frontiers*, 1–9. doi:10.1016/j.gsf.2014.03.002

Karpuz, C., & Pa¸ amehmetog˘lu, A. G. (1997). Field characterisation of weathered Ankara andesites. *Engineering Geology*, *46*(1), 1–17. doi:10.1016/S0013-7952(96)00002-6

Keller, G., & Sherar, J. (2003). Low-volume roads engineering: Best management practices field guide book. *Produced for US Agency for International Development (USAID)*, pp 147. Retrieved from http://www.blm.gov/bmp/field guide.htm

Laubscher, D. H. (1990). A geomechanics classification system for rating of rock mass in mine design. *Journal of the South African Institute of Mining and Metallurgy, 90 (10)*, pp 257–273. doi:10.1016/0148-9062(91)90830-F

Lee, C. H., Lee, M. S., Suh, M., & Choi, S.-W. (2004). Weathering and deterioration of rock properties of the Dabotap pagoda (World Cultural Heritage), Republic of Korea. *Environmental Geology*, *47*(4), 547–557. doi:10.1007/s00254-004-1177-y

Lindsay, J., David, J., Shepherd, J. and Ephraim, J. (2002). Volcanic Hazard Assessment for St. Lucia, Lesser Antilles. *Unpublished Report Presented to the Government of St. Lucia,August 2002*.

Lindsay, J., Robertson, R., Shepherd, J. and Ali, S. (2005). *Volcanic Hazard Atlas of the Lesser Antilles. Seismic Research Unit, University of the West Indies, St. Augustine.* (1st ed., p. 279). ISBN-10: 9769514209.

Marinos, P., & Hoek, E. (2001). Estimating the geotechnical properties of heterogeneous rock masses such as flysch. *Bulletin of Engineering Geology and the Environment*, *60*(2), 85–92. doi:10.1007/s100640000090

Masada, T. (2009). Shear Strength of Clay and Silt Embankments. *U.S. Department of Transportation, Federal Highway Administration. State Job Number 134319 (0), September 2009*.

Matula, M. (1981). Rock and soil description and classification for engineering geological mapping. *Bulletin of International Association of Engineering Geology*, *24*(1), 235–274. doi:10.1007/BF02595273

MDoT. (2008). Roadway Slopes and Embankments. *Montana Department of Transport Geotechnical Manual*, (July).

Miščević, P., & Vlastelica, G. (2014). Impact of weathering on slope stability in soft rock mass. *Journal of Rock Mechanics and Geotechnical Engineering*, *6*(3), 240–250. doi:10.1016/j.jrmge.2014.03.006

Moon, V., & Jayawardane, J. (2004). Geomechanical and geochemical changes during early stages of weathering of Karamu Basalt, New Zealand. *Engineering Geology*, *74*(1-2), 57–72. doi:10.1016/j.enggeo.2004.02.002

Moses, C., Robinson, D., & Barlow, J. (2014). Methods for measuring rock surface weathering and erosion: A critical review. *Earth-Science Reviews*, *135*, 141–161. doi:10.1016/j.earscirev.2014.04.006

Murthy, V. (2002). *Geotechnical engineering: principles and practices of soil mechanics and foundation engineering* (1st ed., p. 1050).

Newman, W. R. (1965). A Report on General and Economic Geological Studies St. Lucia, West Indies., United Nations report prepared for the Government of St. Lucia. *Unpublished*.

Nicholson, D. T. (2000). *Deterioration of excavated rockslopes: mechanisms , morphology and assessment*. PhD Thesis. University of Leeds, School of Earth Sciences. Retrieved from http://etheses.whiterose.ac.uk/334/1/uk_bl_ethos_416598.pdf

Nicholson, D. T. (2003). Breakdown mechanisms and morphology for man-made rockslopes in North West England, *vol. 3*(1).

Nishiyama, K., & Matsukura, Y. (2006). Weathering rates and mechanisms causing changes in rock properties of sandstone. *10th Congress International Association of Engineering Geology*, (278), 1–6. Retrieved from http://www.iaeg.info/iaeg2006/PAPERS/IAEG_278.PDF

Nuric, A., Nuric, S., Kricak, L., & Husagic, R. (2013). Numerical Methods in Analysis of Slope Stability. *International Journal of Science and Engineering Investigations*, *vol. 2*(14), pp 41–48. doi:2251-8843

O'Connell, M., & Gourley, C. (1993). Expansive clay road embankments in arid areas: moisture-suction conditions. *Proceedings of the First International Symposium on Engineering Characteristics of Arid Soils, City University, London, 5-8 July 1993*.

Onedera, T.F., Yoshinaka, R. Oda, M. (1974). Weathering and its relation to mechanical properties of Granite. *Proc. 3rd Cong. Int. Soc. Rock Mech., Denver, 2A: 71-78*.

Orhan, M., Işık, N. S., Topal, T., & Özer, M. (2006). Effect of weathering on the geomechanical properties of andesite, Ankara – Turkey. *Environmental Geology*, *50*(1), 85–100. doi:10.1007/s00254-006-0189-1

Oyama, T., & Chigira, M. (2000). Weathering rate of mudstone and tuff on old unlined tunnel walls. *Engineering Geology*, *55*(1-2), 15–27. doi:10.1016/S0013-7952(99)00103-9

Pacheco, F. a. L., & Alencoão, A. M. P. (2006). Role of fractures in weathering of solid rocks: narrowing the gap between laboratory and field weathering rates. *Journal of Hydrology*, *316*(1-4), 248–265. doi:10.1016/j.jhydrol.2005.05.003

Pantelidis, L. (2009). Rock slope stability assessment through rock mass classification systems. *International Journal of Rock Mechanics and Mining Sciences*, *46*(2), 315–325. doi:10.1016/j.ijrmms.2008.06.003

Patino, L. C., Velbel, M. a, Price, J. R., & Wade, J. a. (2003). Trace element mobility during spheroidal weathering of basalts and andesites in Hawaii and Guatemala. *Chemical Geology*, *202*(3-4), 343–364. doi:10.1016/j.chemgeo.2003.01.002

Phillips, J. D. (2005). Weathering instability and landscape evolution. *Geomorphology*, *67*, 255–272. doi:10.1016/j.geomorph.2004.06.012

Piteau, D. R. (1975). Geological factors significant to the stability of slopes cut in rock. *In: Proceedings Symposium on Planning Open Pit Mines Johannesburg, Pp. 33-53*.

Pola, A., Crosta, G. B., Fusi, N., & Castellanza, R. (2014). General characterization of the mechanical behaviour of different volcanic rocks with respect to alteration. *Engineering Geology*, *169*, 1–13. doi:10.1016/j.enggeo.2013.11.011

Pola, A., Crosta, G., Fusi, N., Barberini, V., & Norini, G. (2012). Influence of alteration on physical properties of volcanic rocks. *Tectonophysics*, *566-567*, 67–86. doi:10.1016/j.tecto.2012.07.017

Pourkhosravani, A., & Kalantari, B. (2011). A Review of current methods for slope stability evaluation. *Electronic Journal of Geotechnical Engineering*, *v 16*, pp 1245 – 1254.

Price, DG., De Frietas, M.H., Hack, H.R.G.K., Higginbottom, I.E., Knill, J.K., & Maurnenbrecher, M. (2009). *Engineering geology: principles and practice*. (M. H. De Freitas, Ed.) (p. 450). Springer - Publishers, Berlin, Heidelberg.

Ramana, Y. V., & Gogte, B. S. (1982). Quantitative studies of weathering in saprolitized charnockites associated with a landslip zone at the porthimund dam, India. *Engineering Geology*, *19*(1), 29–46. doi:10.1016/0013-7952(82)90004-7

Rao, S. (1996). Role of apparent cohesion in the stability of Dominician allophane soil slopes. *Engineering Geology*, *43*(4), pp 265–279. doi:10.1016/S0013-7952(96)00036-1

Rengers, N., Huisman, M., Hack, R., & Rupke, J. (2001). Quantification of Engineering Geological Parameters. *In: Felsbau, 19 (2001)1*, pp. 102–107.

Rijkers, R., & Hack, R. (2000). Geomechanical analysis of volcanic rock on the island of Saba (Netherlands Antilles). Conference Proceeding GeoEng2000, IAEG, ISSFME, ISRM, Melbourne, Australia, pp 1–6.

Robertson, R. (2014). Making Use of Geology-the Relevance of Geology and Geological Information to the Development Process in St Vincent and the Grenadines. *Conference Paper*, 1–9. Retrieved from http://www.open.uwi.edu/sites/default/files/bnccde/svg/conference/papers/robertson.html

Ruxton, B. P., and Berry, L. (1957). Weathering of granite and associated erosional features in Hong Kong. *Bulletin of Geological Society of America 68,1263-1292*.

Sachpazis, C. (2013). Detailed Slope Stability Analysis and Assessment of the Original Carsington Earth Embankment Dam Failure in the UK. *The Electronic Journal of Geotechnical Engineering*, *18*, 6021–6060.

Saito, T. (1981). Variation of physical properties of igneous rocks in weathering. *Proc. of the Int. Symp. on Weak Rock, Tokyo, I: 191-196*.

Samtani, N. C., and Nowatzki, E. A. (2006). Soils and Foundations: Reference Manual. *U.S. Department of Transportation Federal Highway Administration Publication, Publication No. FHWA NHI-06-088*, *I*(132012).

Saunders, M. K., and Fookes, P. G. (1970). A review of the relationship of rock weathering and climate and its significance to foundation engineering. *Engineering Geology*, *vol. 4*(4), pp 289–293. doi:10.1016/0013-7952(70)90021-9

Savanick, G. a., & Johnson, D. I. (1974). Measurements of the strength of grain boundaries in rock. *International Journal of Rock Mechanics and Mining Sciences & Geomechanics Abstracts*, *11*(5), 173–180. doi:10.1016/0148-9062(74)90884-5

Schmid, R. (1981). Descriptive nomenclature and classification of pyroclastic deposits and fragments: Recommendations of the IUGS Subcommission on the Systematics of Ignous Rocks. *International Journal of Earth Sciences*, *vol. 70*(2), pp 794 – 799. doi:10.1007/BF01822152

Schofield, A., & Wroth, P. (1968). *Critical state soil mechanics* (p. 310). McGraw-Hill Inc., US. ISBN: 0070940487.

Schweizer, R., & Wright, S. (1974). A survey and evaluation of remedial measures for earth slope stabilization. *Stability of Earth Slopes Research Project 3-8-71-161. Conducted for the Texas Highway Department. Center for Highway Researrch The University of Texas at Austin.*, *vol. 7*(2), pp 138.

Selby, M. J. (1993). *Hillslope Materials and Processes* (2 nd Editi., p. 480). Oxford: Oxford University Press. ISBN: 0198741839.

Serrano, A., Olalla, C., & Hernandez-Gutierrez, L. E. (2007). *Strength and deformability of low density pyroclasts. In Volcanic Rocks-Malheiro & Nunes (Eds)*. (pp. 35–44). Taylor & Francis Group, London. ISBN: 978-0-415-45140-6.

Skempton, A. W. (1960). The Pore-Pressure Coefficient in Saturated Soils. *Geotechnique*, *vol. 4*(4), pp 186–187. doi:10.1680/geot.1960.10.4.186

Tating, F., Hack, R., & Jetten, V. (2013a). Engineering aspects and time effects of rapid deterioration of sandstone in the tropical environment of Sabah, Malaysia. *Engineering Geology*, *159*, 20–30. doi:10.1016/j.enggeo.2013.03.009

Tating, F., Hack, R., & Jetten, V. (2013b). Engineering aspects and time effects of rapid deterioration of sandstone in the tropical environment of Sabah, Malaysia. *Engineering Geology*, *159*, 20–30. doi:10.1016/j.enggeo.2013.03.009

Tating, F., Hack, R., & Jetten, V. (2014). Quantification of rock mass deterioration process for cut slope design in humid tropical areas–case study Northern Kota Kinabalu, Sabah Malaysia. *In Conference: National Geoscience Conference 2013 of the Geological Society of Malaysia*, 2–4.

Tating, F., Hack, R., & Jetten, V. (2014). Weathering effects on discontinuity properties in sandstone in a tropical environment: case study at Kota Kinabalu, Sabah Malaysia. *Bulletin of Engineering Geology and the Environment*. doi:10.1007/s10064-014-0625-5

Taylor, D. W. (1948). *Fundamentals of Soil Mechanics* (p. 712). John Wiley & Sons, Inc. ISBN: 1258768925.

Taylor, G., & Eggleton, R. (1992). Cool climate lateritic and bauxitic weathering. *The Journal of Geology*, *vol. 100*(6), pp 669 – 677. doi:10.1086/629620

Taylor, H. W. (1980). A geomechanics classification applied to mining problems in the Shabanie and King Chrysotile asbestos mines, Rhodesia. M.Phil thesis. Institute of Mining Research, University of Rhodesia, Harare, Zimbabwe. p. 312.

Terzaghi, K. (1936). Relation between soil mechanics and foundation engineering;Presidential address. In *International Conference on Soil Mechanics and Foundation Engineering, 1. Cambridge, Mass. Proceedings, Vol. 3,* (pp. 13 –18).

Terzaghi, K. (1943). *Theoretical soil mechanics* (p. 528). New York N.Y.: John Wiley & Sons, Inc. ISBN: 0471853054 .

Terzaghi, K. (1996). *Soil mechanics in engineering practice* (3rd editio., p. 534). John Wiley & Sons, Inc. ISBN: 047108658-4.

Terzaghi, K. & Peck, R. B. (1967). *Soil mechanics in engineering practice.* (2nd Editio., p. 729). John Wiley & Sons. ISBN: 0471852732.

Terzaghi, K., Peck, B. R., Gholamreza, M. (1996). *Soil Mechanics in Engineering Practice* (3rd editio., p. 534). New York N.Y.: John wiley and Sons, inc. ISBN: 0471086584.

The Geological Society of London. (1995). The description and classification of weathered rocks for engineering purposes. *Quarterly Journal of Engineering Geology and Hydrogeology*, *28*, 207–242. doi:10.1144/GSL.QJEGH.1995.028.P3.02

Thomas, M. F. (1994). *Geomorphology in the Tropics.* Wiley, Chichester. ISBN-10: 0471930350.

Thomas, M., Clarke, J.D.A., Pain, C. F. (2005). Weathering, erosion and landscape processes on Mars identified from recent rover imagery, and possible Earth analogues. *Aust. J. Earth Sci. 52, 365–378*.

Thomson, B. J., Hurowitz, J. A., Baker, L. L., Bridges, N. T., Lennon, A. M., Paulsen, G., & Zacny, K. (2014). The effects of weathering on the strength and chemistry of Columbia River Basalts and their implications for Mars Exploration Rover Rock Abrasion Tool (RAT) results. *Earth and Planetary Science Letters*, *400*, 130–144. doi:10.1016/j.epsl.2014.05.012

Tong, W. K. (2000). Introduction to Clay Minerals & Soils. *Earth Science*. Retrieved from http://www.oakton.edu/user/4/billtong/eas100/clays.htm

Tuğrul, A., & Gürpinar, O. (1997). A proposed weathering classification for basalts and their engineering properties (Turkey). *Bulletin of the International Association of Engineering Geology*, *55*(1), 139–149. doi:10.1007/BF02635416

Tugrul, E. A. and A. (2001). Weathering and its relation to geomechanical properties of Cavusbasi granitic rocks in northwestern Turkey. *Bulletin of Engineering Geology and the Environment*, *60*(2), 123–133. doi:10.1007/s100640000091

University of Melbourne. (1978). Chapter 11 . The Stability of Slopes, 1–20. Retrieved from http://people.eng.unimelb.edu.au/stsy/geomechanics_text/Ch11_Slope.pdf

US Army Corps. (2003). Engineering and Design, Slope Stability, Engineer Manual. *US Army Corps of Engineers*, EM 1110–2–1902.

US Army Corps. (2010). SCDOT Geotechnical design manual. Chapter 17 -Embankments. *US Army Corps of Engineers*, *Chapter 17*(June).

Vallejo, L., Hijazo, T., Ferrer, M., & Seisdedos, J. (2007). Geomechanical characterization of volcanic materials in Tenerife. *Internationl Workshop on Volcanic Rocks. Proceedings of ISRM Workshop W2, Ponta Delgada, Azores, Portugal, 14-15 July, 2007*, pp 20–28. doi:10.1201/NOE0415451406.ch3

Van Reeuwijk, L. P. (2002). *Procedures for soil analysis* (6th editio., p. 120). Wageningen: ISRIC, FAO. ISBN: 90-6672-044-1.

Velde, B., & Meunier, A. (2008). *The Origin of Clay Minerals in Soils and Weathered Rocks* (p. 406). Berlin, Heidelberg: Springer Berlin Heidelberg. ISBN-10: 3540756337.

Vysinka, M., Mizusawa, M., and Sakurai, K. (2011). Growth and Characteristics of Liesegang Rings in Cu – Cr System : Optical and XRF Study. *WDS'11 Proceedings of Contributed Papers, Part III*, 147–154, ISBN 978–80–7378–186–6.

Waltham, T. (1993). *Foundations of Engineering Geology* (2 nd Editi., p. 96). CRC Press, Taylor & Francis Group, London. ISBN: 9780419248705.

Waltham, T. (2009). *Foundations of Engineering Geology* (3 rd Editi., p. 105). Spon Press, London. ISBN-10: 0415469600.

White, A. F., & Brantley, S. L. (2003). The effect of time on the weathering of silicate minerals: why do weathering rates differ in the laboratory and field? *Chemical Geology*, *202*(3-4), 479–506. doi:10.1016/j.chemgeo.2003.03.001

Wyllie, D.C., & Mah, C. W. (2004). *Rock slope engineering: Civil and mining "Based on Rock Slope Engineering (third edition, 1981) by Hoek, E. and Bray, J."* (Fourth Edi., p. 456). Spon Press: London. ISBN: 0-203-57083-9.

Yokota, S., & Iwamatsu, A. (2000). Weathering distribution in a steep slope of soft pyroclastic rocks as an indicator of slope instability. *Engineering Geology*, *55*(1-2), 57–68. doi:10.1016/S0013-7952(99)00106-4

APPENDICES

APPENDIX 1 - Cut slopes

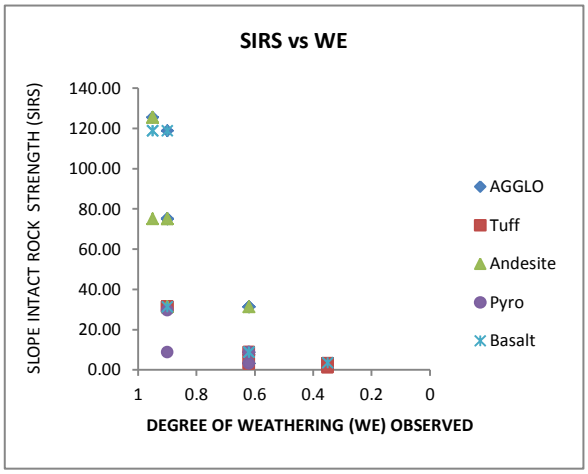

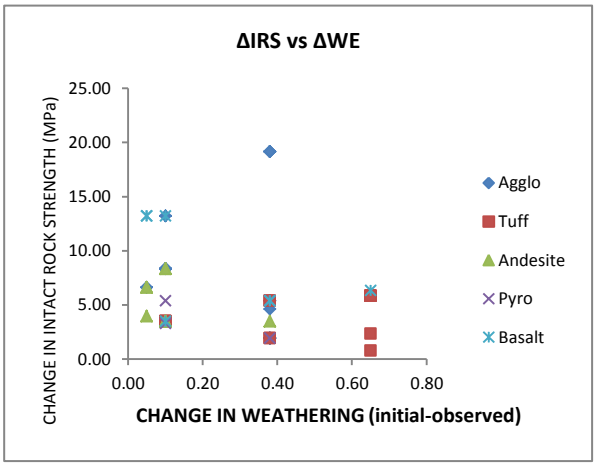

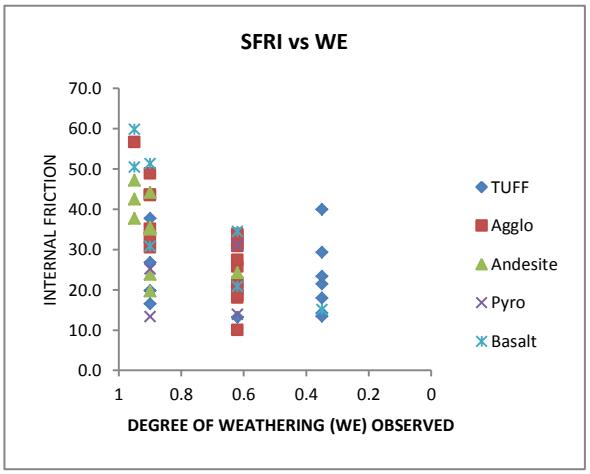

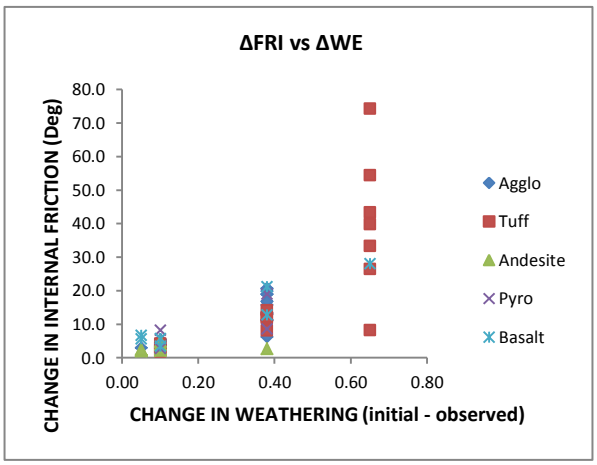

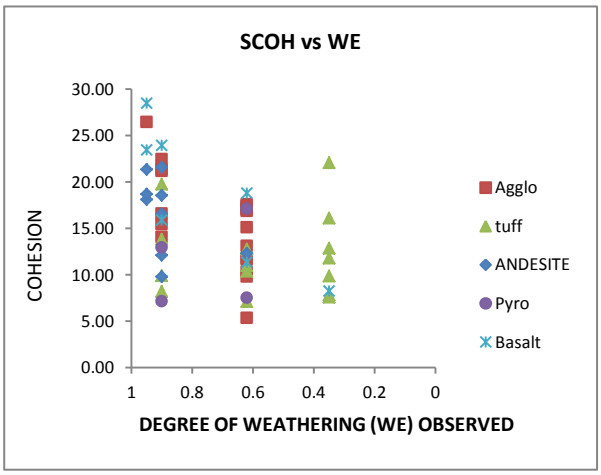

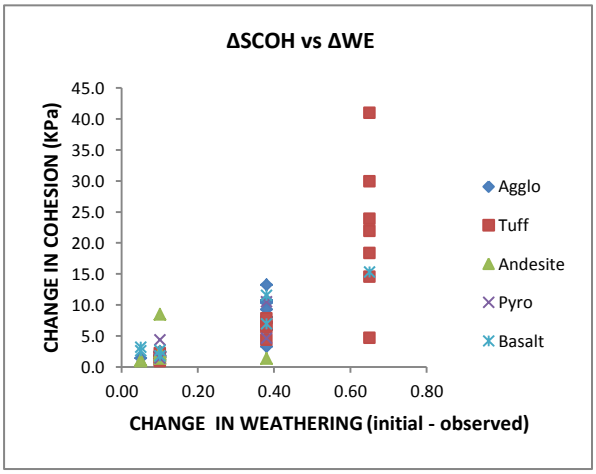

Figure 29: Graphs for geotechnical parameters important for slope stability plotted against degree of weathering reduction values (WE) (left). Graphs for correlative plots, change in geotechnical parameter with change in weathering (Right)

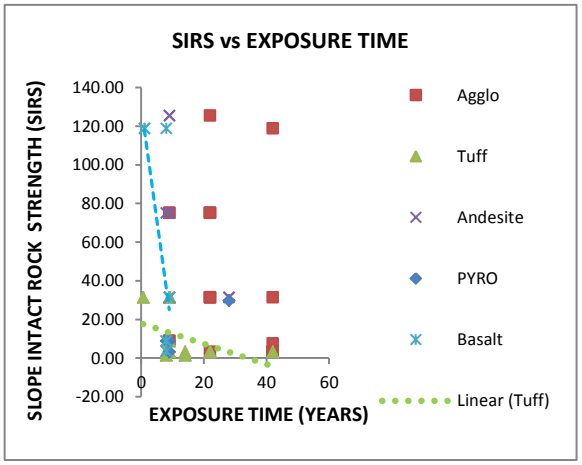

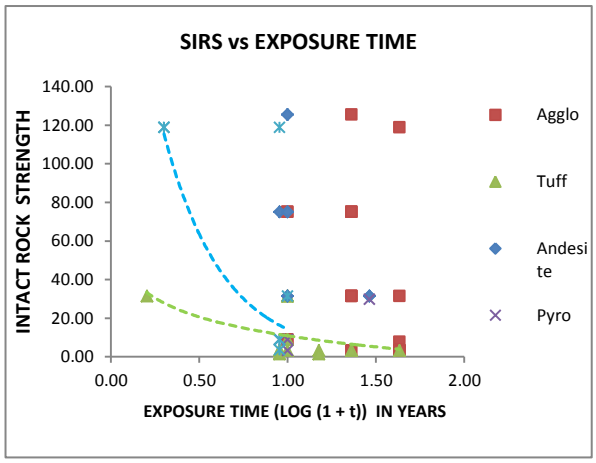

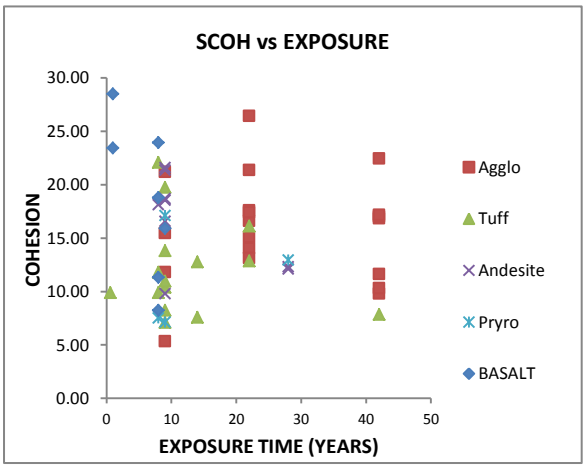

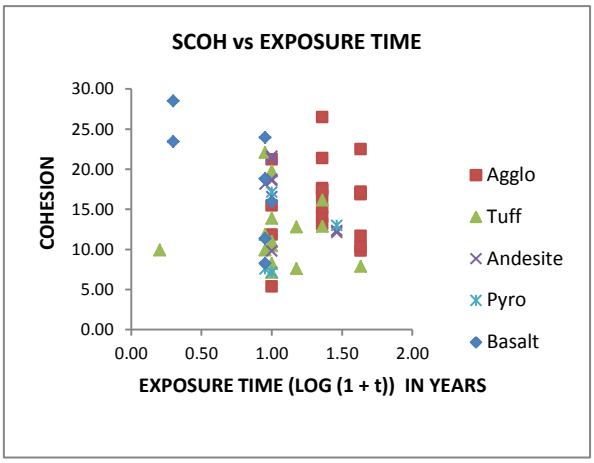

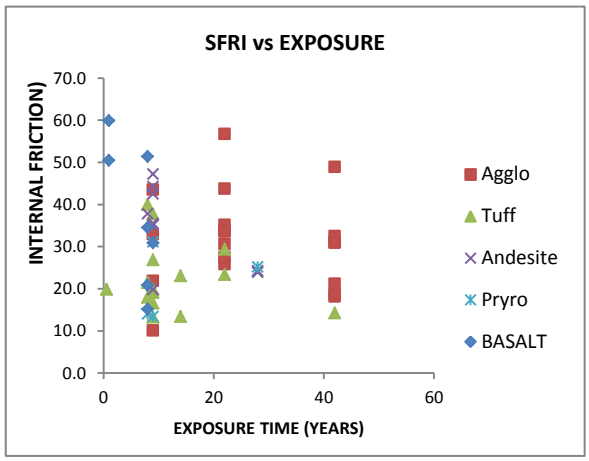

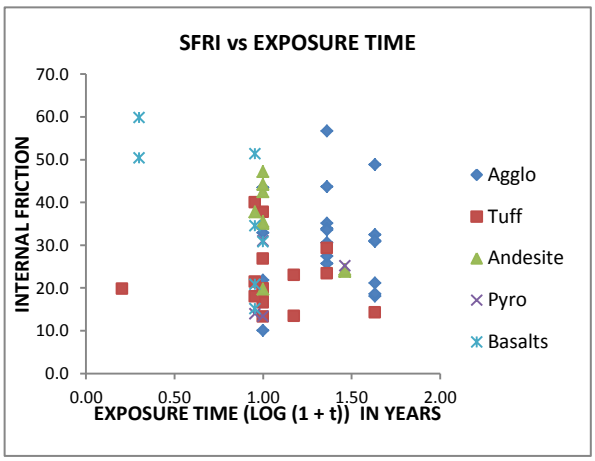

Figure 30: The effect of exposure time (in years) and logarithmic scale of exposure time on geotechnical properties of geological formations (the dashed lines between the makers have no meaning and are only for identification).

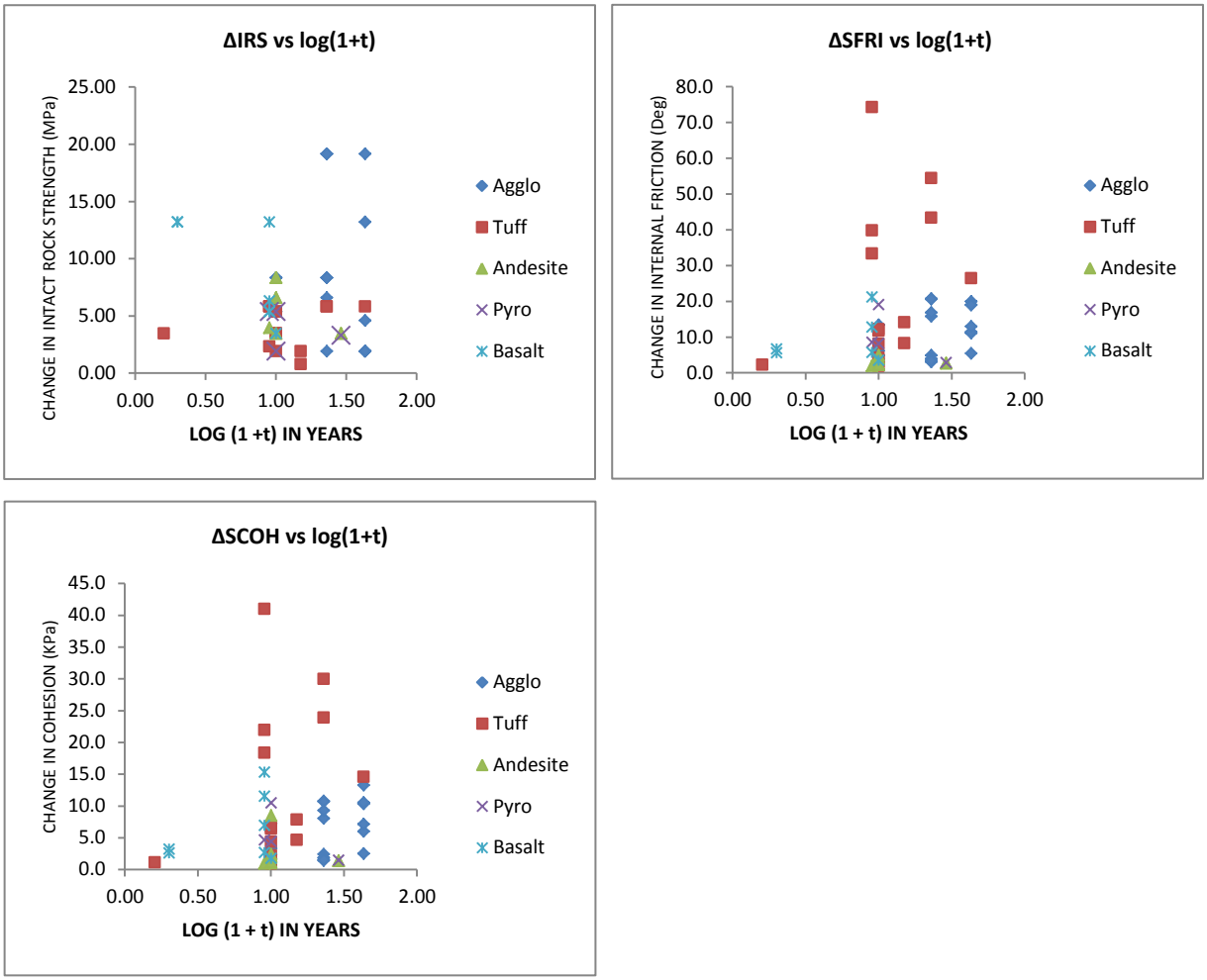

Figure 31: The influence of logarithmic scale of exposure time as a function of change in geotechnical parameter

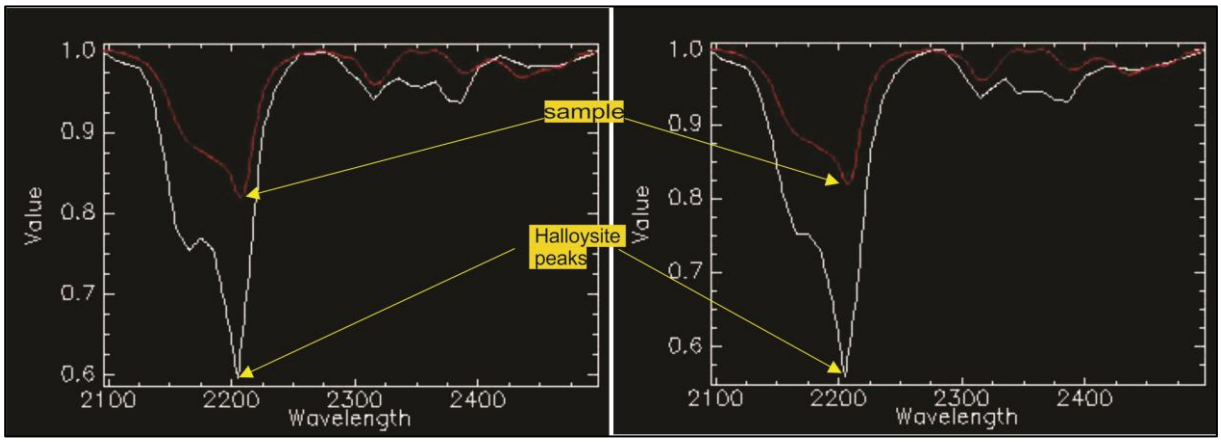

Figure 32: Analytical spectral analysis of rock sample for halloysite

Figure 33: St Vincent, slope showing differential weathering due to lithological heterogeneity, east coast (Direction of view 035 degrees).

Table 10: Current stability using maximum minimum and average heights

AGLO	***Height***	φ/S_{dip}	H_{max}/H_s	***Stability probability***
Max	10	0.495725	0.866075	40
Min	2.7	0.334393	1.871392	95
Avge	5.96	0.39568	1.372082	90
ANDESITE	***Height***	φ/S_{dip}	H_{max}/H_s	***Stability probability***
Max	15	0.524163	0.666971	7.5
Min	3	0.434082	2.197536	100
Avge	8.22	0.457392	1.835119	100
BASALT	***Height***	φ/S_{dip}	H_{max}/H_s	***Stability probability***
Max	40	0.720173	0.969569	50
Min	9	0.492971	1.391567	85
Avge	18.9	0.632737	0.792222	20
TUFF	***Height***	φ/S_{dip}	H_{max}/H_s	***Stability probability***
Max	15	0.24457	0.209639	<5
Min	2.7	0.284461	1.441311	95
Avge	7.9	0.280697	0.765871	20
PYRO	***Height***	φ/S_{dip}	H_{max}/H_s	***Stability probability***
Max	15	0.164459	0.117999	<5
Min	4	0.314573	1.087922	65
Avge	9.3	0.266464	0.557068	<5

Table 11: Future stability on field observed maximum slope dip (SD) and height (Hs) for slopes exposed for a period of 9 years

FUTURE STABILITY								
Log(1+ t) =1.70757			Time (t) = 50yrs					
UNIT	**SFRI**	**SCOH**	**SD**	H_{max}	H_S	$\varphi/_{SD}$	H_{max}/H_S	**Stability probability**
AGGLO	22.1	17068.2	88	4.3	9	0.25	0.47	<5%
TUFF	17.4	15374.7	89	3.4	14	0.20	0.24	<5%
ANDESITE	35.0	20562.2	85	7.5	7	0.41	1.07	50%
PYRO	12.6	19527.9	81	4.8	15	0.16	0.32	<5%
BASALT	28.4	17668.5	81	6.3	15	0.35	0.42	<5%

Future stability for slopes exposed for a period of 9 years, assuming same slope dip (SD) and height (H)

FUTURE STABILITY								
Log(1+ t) = 1.70757			t=50yrs					
UNIT	**SFRI**	**SCOH**	**SD**	H_{max}	H_S	$\varphi/_{SD}$	H_{max}/H_S	**stability probability**
AGGLO	22.1	17068.2	75	6.2	7	0.29	0.88	25%
TUFF	17.4	15374.7	75	4.9	7	0.23	0.70	5%
ANDESITE	35.0	20562.2	75	11.1	7	0.47	1.59	95%
PYRO	12.6	19527.9	75	5.5	7	0.17	0.78	10%
BASALT	28.4	17668.5	75	7.7	7	0.38	1.10	55%

APPENDIX 2 - Embankments

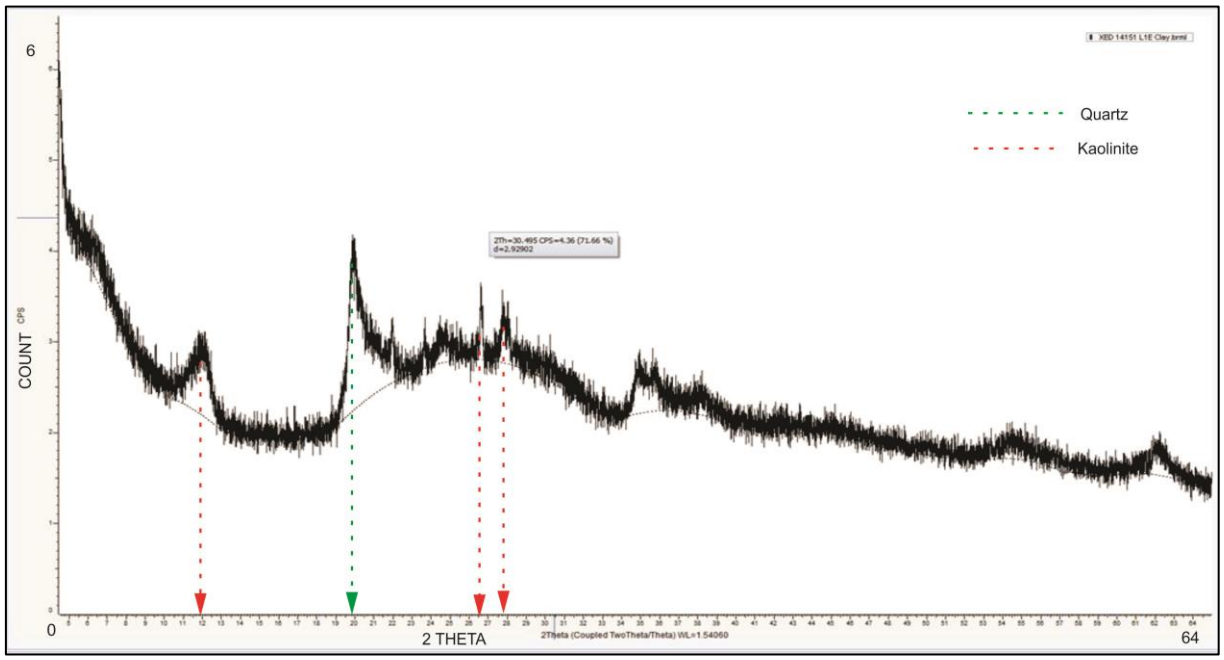

Figure 34: X-ray Diffractogram (XRD), Barre de I'sle embankment borrow material

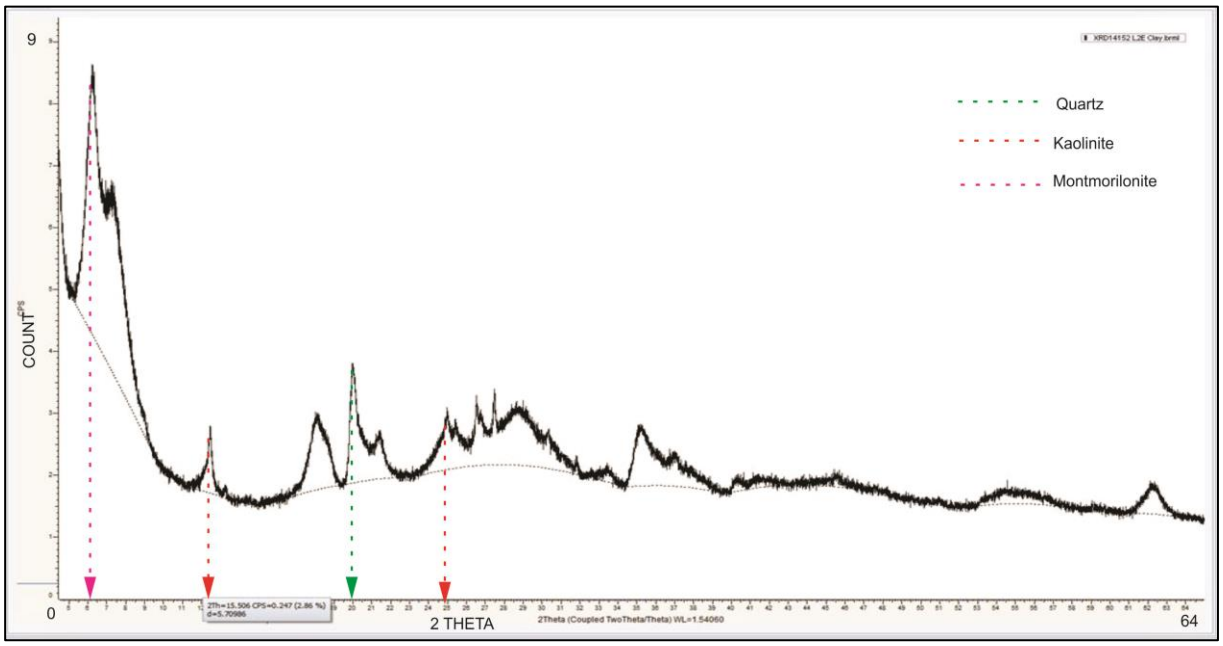

Figure 35: X-ray Diffractogram (XRD), Barre de I'sle embankment material

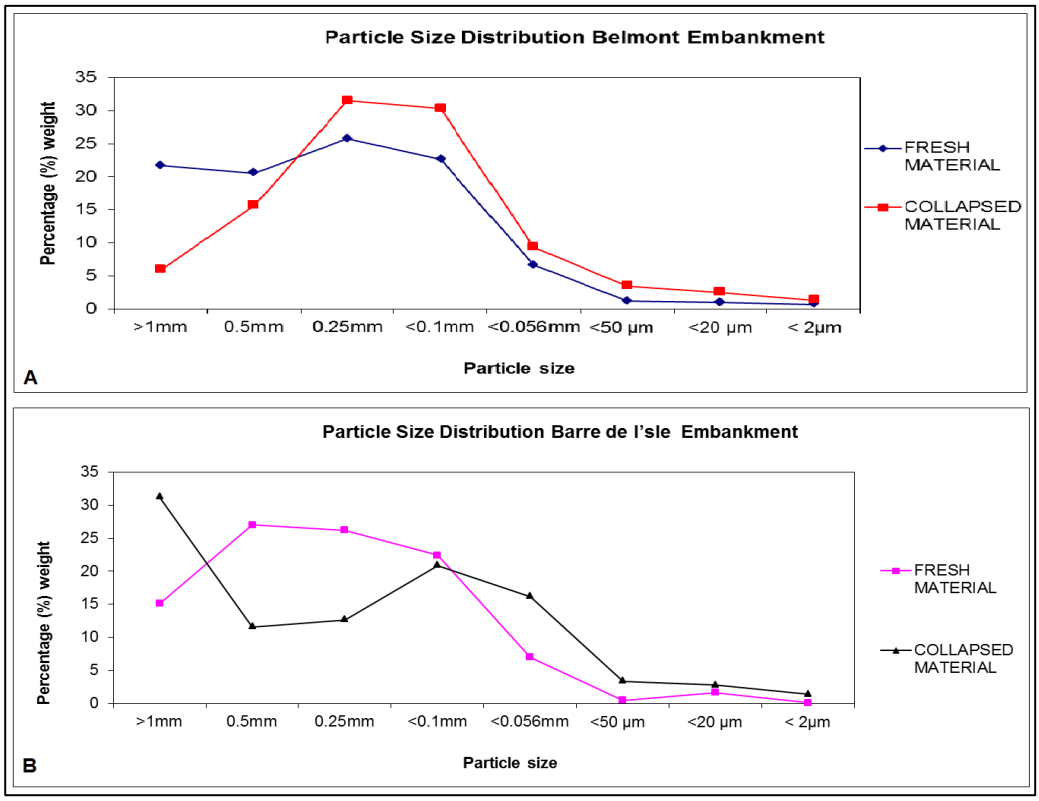

Figure 36: Particle size distribution grading curves

Table 12: Stability analysis at factor of safety 0.9

Embankment critical height (eqn. 4.42)

Cohesion (kN/m²)	Internal friction angle (degree)	Slope angle (degree)	Unit weight (kN/m²)	Current height (m)	Critical height – H_{CR} (m)
37	32	77	14	25	22.8

Cohesion (C_d') and friction angle (Φ_d') developed at factor of safety equivalent to failure (eqn. 4.40)

Design factor of safety (FS)	Cohesion (kN/m²)	Friction angle (deg)	Friction angle developed $(tan\ \Phi_d' in\ deg)$	Cohesion developed (C_d' - kN/m²)
0.9	37	32	35.5	25.47

Allowable height (H_a) at factor of safety equivalent to failure (eqn. 4.43)

Design factor of safety (FS)	Slope angle (degree)	Unit weight (kN/m²)	Cohesion developed $(C_d' - kN/m2)$	Friction angle developed $(tan\ \Phi_d'\ in\ deg)$	Allowable height – H_a (m)	Current height (m)
0.9	77	14	25.47	35.5	23	25

Table 13: Stability analysis at factor of safety 1.5

Embankment critical height (eqn. 4.42)

Cohesion (kN/m²)	Internal friction angle (degree)	Slope angle (degree)	Unit weight (kN/m²)	Current height (m)	Critical height – H_{CR} (m)
37	32	77	14	25	22.8

Cohesion (C_d') and friction angle (Φ_d') developed at acceptable design factor of safety (eqn. 4.40)

Design factor of safety (FS)	Cohesion (kN/m²)	Friction angle (deg)	Friction angle developed $(tan\ \Phi_d' in\ deg)$	Cohesion developed (C_d' - kN/m²)
1.5	37	32	21.3	24.67

Allowable height (H_a) at design factor of safety (eqn. 4.43)

Design factor of safety (FS)	Slope angle (degree)	Unit weight (kN/m²)	Cohesion developed $(C_d' - kN/m2)$	Friction angle developed $(tan\ \Phi_d'\ in\ deg)$	Allowable height – H_a (m)	Current height (m)
1.5	77	14	24.67	21.3	18.8	25

Table 14: Stability analysis at factor of safety 2.0

Embankment critical height (eqn. 4.42)

Cohesion (kN/m²)	Internal friction angle (degree)	Slope angle (degree)	Unit weight (kN/m²)	Current height (m)	Critical height – H_{CR} (m)
37	32	77	14	25	22.8

Cohesion (C_d') and friction angle (Φ_d') developed at acceptable design factor of safety (eqn. 4.40)

Design factor of safety (FS)	Cohesion (kN/m²)	Friction angle (deg)	Friction angle developed $(tan\ \Phi_d' in\ deg)$	Cohesion developed (C_d' - kN/m²)
2.0	37	32	16	18.5

Allowable height (H_a) at design factor of safety (eqn. 4.43)

Design factor of safety (FS)	Slope angle (degree)	Unit weight (kN/m²)	Cohesion developed $(C_d' - kN/m2)$	Friction angle developed $(tan\ \Phi_d'\ in\ deg)$	Allowable height – H_a (m)	Current height (m)
2.0	77	14	18.5	16	9.3	25

Figure 37: St Lucia, liesegang rings suggesting chemical weathering

APPENDIX 3 - Field Data and photographs of slopes

Table 15: Field data summary

SLOPE NAME	GENERAL INFORMATION	MATERIAL CHARACTERISTICS	MASS CHARACTERISTICS
V1	*Location*: 700268E, 1455352N *Date & method of excavation*: 2006, Excavator *Geological formation*: Alluvial and reworked deposits *Accessibility*: Good *Geotechnical Units*: 04	The Intact rock strength (IRS) ranges from 8.75 to <1.25, with texture & structure of thick, massive, blocky, poorly sorted, matrix supported, and thick weathering horizons. Colours are of brown, greyish-brownish, and greyish-darkish. Rock names include tuff, basalt and pyroclastic.	Moderately weathered; 9 m high; 60 m length; Dip 70 degrees, Dip direction 094 degrees; Discontinuity sets, 39/286, 60/050, 85/174; Spacing between 0.02 to 2m
V2	*Location*: 701475E, 1458474N *Date & method of excavation*: 2000, Excavator. *Geological formation*: Alluvial and reworked deposits *Accessibility*: Good *Geotechnical units*: 05	The Intact rock strength (IRS) ranges from 150 to 3.125, with texture & structure of thick, massive, blocky, poorly sorted, matrix supported, and thick weathering horizons. Colours are of brown, greyish-brownish, and brownish-dark. Rock names include tuff, andesites and pyroclastic.	Slightly to highly weathered; 15m high; 100m length; Dip 81 degrees, Dip direction 170 degrees; variable discontinuity orientation, with spacing varying from 0.03m to 2m. persistence along strike from >1m to >10m and along dip >1m to >8m
V3	*Location*: 687450E, 1462569N *Date & method of excavation*: 2000, Excavator. *Geological formation*: Pyroclastic deposits of pre-soufriere volcanic centres *Accessibility*: Good *Geotechnical units*: 02	Intact rock strength (IRS) of 150 and 1.25 respectively; texture & structure of thick, massive, poorly sorted, matrix supported, and thick weathering horizons. Colours are of yellowish - brownish. Tuff	Highly weathered; 7m high; 56m length; Dip 85 degrees, Dip direction 302 degrees; variable discontinuity orientation, with spacing varying from 0.14m to 2.5m. persistence along strike from >1m to >20m and along dip >1m to >5m
V4	*Location*: 687372E, 1462615N *Date & method of excavation*: 1986, Conventional blasting (fractured intact rock). *Geological formation*: Pyroclastic deposits of pre-soufriere volcanic centres. *Accessibility*: Good *Geotechnical units*: 04	Intact rock strength (IRS) ranges from 75 to 3.125, with texture & structure of thick, massive, blocky, poorly sorted, matrix supported, and thick weathering horizons. Colours are of brown, greyish-brownish, and brownish-dark. Rock names include tuff, andesites and pyroclastic.	Slightly and highly weathered units; 6m high; 100m length; Dip 80 degrees, Dip direction 232 degrees; variable discontinuity orientation, with spacing varying from 0.1m to 1m. persistence along strike from >0.5m to >5m and along dip >1m to >5m
V5	*Location*: 701757E, 1458825N *Date & method of excavation*: 2005, Excavator *Geological formation*: Pyroclastic deposits of pre-soufriere volcanic centres *Accessibility*: Good	Intact rock strength (IRS) of 8.75 and 3.125, bedded deposit, and thick weathering horizons. Colours are of brown, greyish-brownish, and brownish-dark. Rock names include tuff and pyroclastic.	Slightly weathered; 15m high; 100m length; Dip 81 degrees, Dip direction 170 degrees; variable discontinuity orientation, with spacing varying from 0.012m to 1.5m. persistence along strike from >0.2m to >2m and along

	Geotechnical units: 02		dip >1m to >5m
V6	*Location*: 690466E, 1457238N *Date & method of excavation*: 2014, Excavator *Geological formation*: Yellow Tephra underlain by volcaniclastic *Accessibility*: Good *Geotechnical units*: 01	Intact rock strength (IRS) 31.25, tuffaceous matrix with lapilli poorly sorted clasts. Yellowish - brownish colour. Rock names include tuff, andesites and pyroclastic.	Slightly weathered; 3m high; 100m length; Dip 65 degrees, Dip direction 306 degrees; variable discontinuity orientation, with spacing varying from 0.123m to 1.5m. persistence along strike from >0.05m to >2m and along dip >0.5m to >3m
V7	*Location*: 700592E, 1453659N *Date & method of excavation*: 2013, Excavator *Geological formation*: Alluvial and reworked deposits *Accessibility*: Good *Geotechnical units*: 02	Intact rock strength (IRS) of 150, fine- coarse grained, massive and poorly sorted clasts, basaltic lava flow. Yellowish - brown colour. Rock name: Basalt.	Slightly weathered; 15m high; 60m length; SDD/SD: 130/ 70, $130^0/50^0$; Discontinuity orientation SDD/SD: 314/85, 134/41, 258/70,122/52, 015/45, 054/80, 280/25; spacing 0.13m to 1m; persistence along strike >0.2m and along dip >0.4m; Roughness large scale: slightly wavy and curved; Roughness small scale: rough stepped, rough and smooth undulating; Infill material: no fill- surface staining; Karst: none.
V8	*Location*: 691408E, 1455812N *Date & method of excavation*: 2006, Excavator *Geological formation*: Pyroclastic deposits of pre-soufriere volcanic centres *Accessibility*: Good *Geotechnical units*: 01	Intact rock strength (IRS) 100 MPa, fine-coarse grained, massive, poorly sorted clasts. Greenish – brownish colour, Basaltic.	Moderately weathered; 10m high; 60m length; Dip 45 degrees, Dip direction 128 degrees; variable discontinuity orientation 55/128, 85/100, 70/130; spacing 0.23m to 1m. persistence along strike from >0.2m, along dip >1m
L1	*Location*: 714355E, 1547603N *Date & method of excavation*: 2005, Excavator *Geological formation*: Altered Andesite Porphyritic, Tuff (Central series) *Accessibility*: Good *Geotechnical units*: 03	Intact rock strength (IRS) 8.75MPa, Coarse grained, thick weathering horizon, poorly sorted, matrix supported. Greyish-brownish colour. Sediment layer mixer of tuff.	Slightly to highly weathered; 6m high; 50m length; Dip 71,70 degrees, Dip direction 94,105 degrees; variable discontinuity orientation, with spacing varying from 0.1m to 1.2m. persistence along strike from >0.1m to >5m and along dip >0.2m to >4m
L2	*Location*: 714355E, 1547603N *Date & method of excavation*: 2005, Excavator *Geological formation*: Altered Andesite Porphyritic(Central series) *Accessibility*: Good *Geotechnical units*: 07	Intact rock strength (IRS) ranges from 100 to 31.25, fine- coarse, frothy and porphyritic with vesicles, thick, massive, blocky, poorly sorted, matrix supported, and thick weathering horizons. Colours are of yellowish-brownish and dark stained. Rock	Moderately weathered; 14,9,6m high; 120m length; Dip 88 degrees, Dip direction 292 degrees; variable discontinuity orientation, with spacing varying from 0.03m to 2m. persistence along strike from >0.2m to >10m and along dip >0.1m to >8m

		names include tuff, andesites and agglomerates.	
L3	*Location*: 728077E, 1538164N *Date & method of excavation*: 1972, Excavator *Geological formation*: Andesite Agglomerate, Mu(Central series) *Accessibility*: Good *Geotechnical units*: 04	Intact rock strength (IRS) ranges from 75 to 3.125; Pebble-cobble clasts, fine matrix, Thick bedded, Poorly sorted andesitic clasts matrix supported, Yellowish-brownish colour; Agglomerates.	Moderate and highly weathered; 5m high; 100m length; Dip/Dip direction: 65/40, 80/28, 67/38 degrees; variable discontinuity orientation, spacing varying from 0.07m to 3m. persistence along strike from >0.2m to >10m and along dip >1m to >3m
L4	*Location*: 728077E, 1538164N *Date & method of excavation*: 1972, Excavator *Geological formation*: Andesite Agglomerate, Mu(Central series) *Accessibility*: Good *Geotechnical units*: 03	Intact rock strength (IRS) 75 and 3.125 MPa, Pebble-cobble clasts, medium matrix, Thick bedded, fine matrix supported with Poorly sorted corestones, Yellowish-brownish colour; Agglomerates.	highly weathered; 10m high; 100m length; Dip 88 degrees, Dip direction 54 degrees; variable discontinuity orientation, with spacing varying from 0.1m to 3m. persistence along strike from >0.1m to 50m and along dip >0.2m to >3m
L5	*Location*: 727727E, 1539591N *Date & method of excavation*: 1972, Excavator *Geological formation*: Agglomerates tuffs, tuffs(Central series) *Accessibility*: Good *Geotechnical units*: 02	Intact rock strength (IRS) 75MPa, fine grained, thick bedded weathering horizon, matrix supported with weathered corestones; Greyish-brownish colour; Tuff	Highly and completely weathered; 4m high; 100m length; Dip 80 degrees, Dip direction 75 degrees; variable discontinuity orientation, with spacing varying from 0.04m to 5m. persistence along strike from >0.1m to 20m and along dip >0.2m to >2.5m
L6	*Location*: 716375E, 1547592N *Date & method of excavation*: 2006, Excavator *Geological formation*: Altered Andesite Porphyritic (Central series) *Accessibility*: Good *Geotechnical units*: 02	Intact rock strength (IRS) 3.125MPa, fine-coarse grained, thick weathering horizons, poorly sorted clasts, Yellowish-brownish colour; Tuff.	Completely weathered; 7m high; 22m length; Dip/Dip direction 85/146,75/217 degrees; variable discontinuity orientation, with spacing varying from 0.1m to 1.5m. persistence along strike from >0.6m to >4m and along dip >0.2m to >4m
L7	*Location*: 710870E, 1534060N *Date & method of excavation*: 1992, Excavator *Geological formation*: Andesitic Agglomerates, Cal (southern series) *Accessibility*: Good *Geotechnical units*: 01	Intact rock strength (IRS) 150MPa, thick clastic, poorly sorted, matrix supported, and thick weathering horizons. Greyish –dark colour. Agglomerates	Slightly weathered; 9m high; 100m length; Dip 83 degrees, Dip direction 34 degrees; variable discontinuity orientation, with spacing varying from 0.3m to 1.5m. persistence along strike from >0.1m to >1m and along dip >0.2m to >3m
L8	*Location*: 709161E, 1537437N *Date & method of excavation*: 1992, Excavator	Intact rock strength (IRS) 75, coarse grained, massive clastic, poorly sorted, clasts supported,	Moderately weathered; 6m high; 100m length; Dip /Dip direction: 75/74, 75/100 degrees; variable

	Geological formation: Andesitic Agglomerates, Cal (southern series) *Accessibility*: Good *Geotechnical units*: 02	Greyish –dark colour. Agglomerates	discontinuity orientation; spacing varying from 0.02m to 1m. persistence along strike from >0.2m to >0.4m and along dip >0.1m to >0.6m
L9	*Location*: 708905E, 1537619N *Date & method of excavation*: 1992, Excavator *Geological formation*: Agglomerates Tuff, Tuff (southern series) *Accessibility*: Good *Geotechnical units*: 02	Intact rock strength (IRS) ranges from 31.25 and 3.125 MPa, coarse grained, massive clastic, poorly sorted, clasts supported, Greyish –dark colour. Agglomerates	Highly and completely weathered; 3.5m high; 20m length; Dip 85 degrees, Dip direction 50 degrees; variable discontinuity orientation, with spacing varying from 0.2m to 1.9m. persistence along strike from >0.1m to >10m and along dip >1m to >1.5m
L10	*Location*: 708905E, 1537619N *Date & method of excavation*: 1992, Excavator *Geological formation*: Agglomerate tuffs, tuffs (southern series) *Accessibility*: Good *Geotechnical units*: 02	Intact rock strength (IRS) 3.125MPa; coarse grained, bedded and clastic, poorly sorted, clasts supported, Greyish –dark, brownish colours. Agglomerates, Tuff	Highly and completely weathered; 2.7m high; 30m length; Dip 82 degrees, Dip direction 37 degrees; variable discontinuity orientation, with spacing varying from 0.2m to 1.5m. persistence along strike from >0.1m to >10m and along dip >0.4m to >1m
L11	*Location*: 712362E, 1543261N *Date & method of excavation*: 1972, Excavator *Geological formation*: Andesite Ash altered Andesite (Central series) *Accessibility*: Good *Geotechnical units*: 01	Intact rock strength (IRS) 150MPa; fine grained, bedded, poorly sorted, matrix supported, brownish-dark colour. Tuff	Slightly weathered; 3m high; 100m length; Dip 87 degrees, Dip direction 80 degrees; variable discontinuity orientation, with spacing varying from 0.14m to 1m. persistence along strike from >0.2m to >1m and along dip >0.2m to >2m
L12	*Location*: 710594E, 1533993N *Date & method of excavation*: 1992, Excavator *Geological formation*: Andesite Agglomerates (Central series) *Accessibility*: Good *Geotechnical units*: 02	Intact rock strength (IRS) 31.25MPa, coarse grained, massive clastic, poorly sorted, clasts supported, Greyish –dark colour. Agglomerates	Highly weathered; 5m high; 100m length; Dip /Dip direction: 81/233, 75/49 degrees; variable discontinuity orientation, with spacing varying from 0.1m to 1.2m. persistence along strike from >1m to >4m and along dip >0.2m to >3m

Figure 38: Geotechnical unit V1G1

Figure 39: Cut slope V2

Figure 40: Cut slope V3

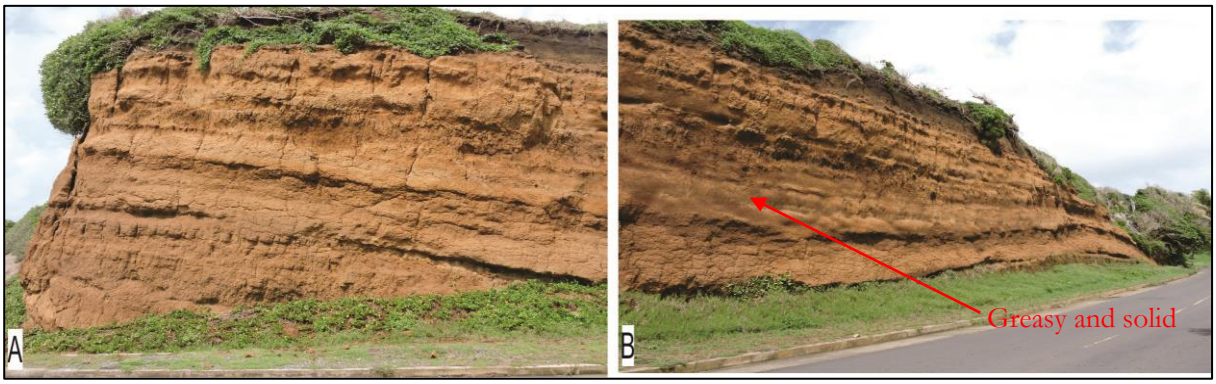

Figure 41: Cut slope V5 east coast (Direction of view 045-060 degrees)


Figure 42: Cut slope L1 west coast (direction of view 090 degrees)

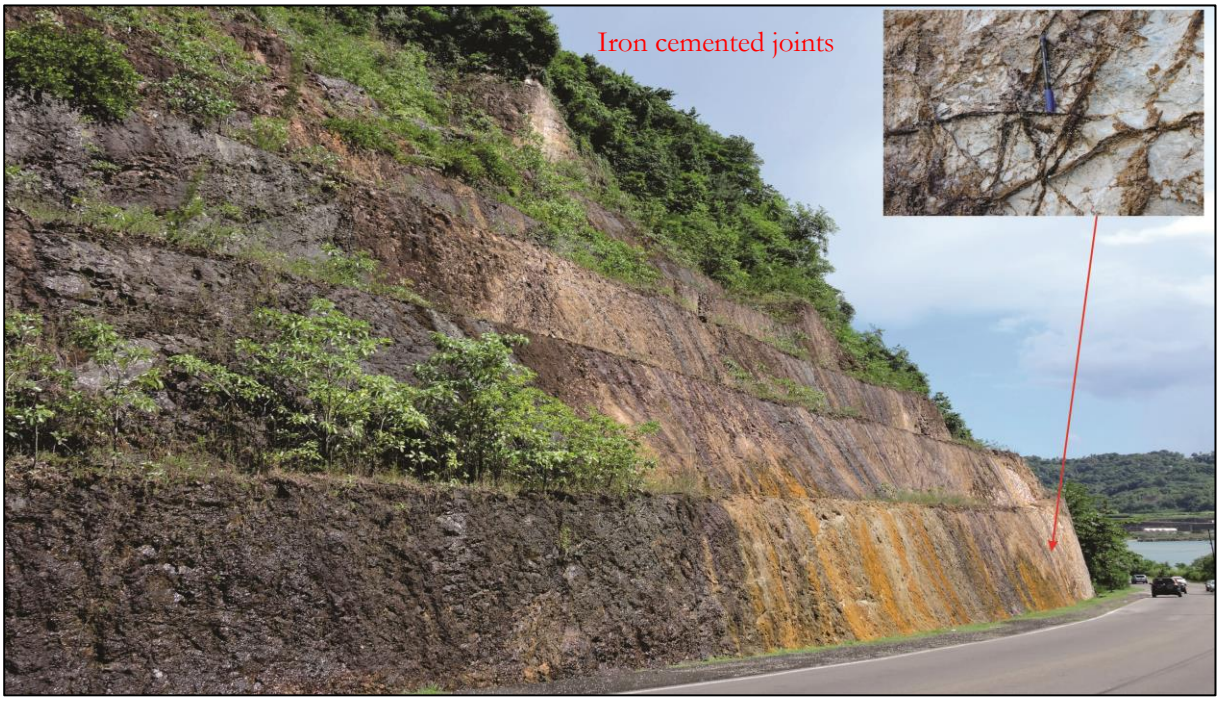

Figure 43: Cut slope L2 west coast (Direction of view 150 degrees)

Figure 44: Cut slope L4

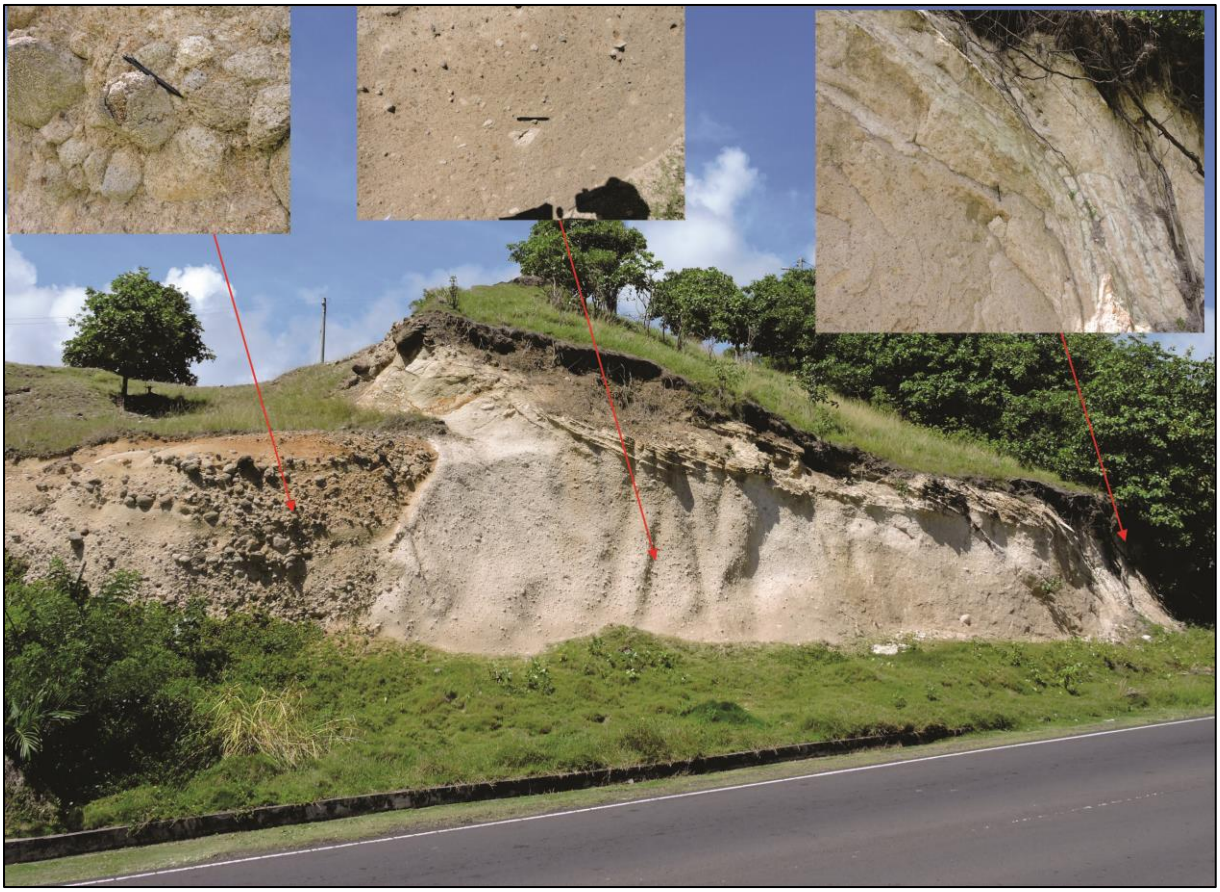

Figure 45: Cut slope L5

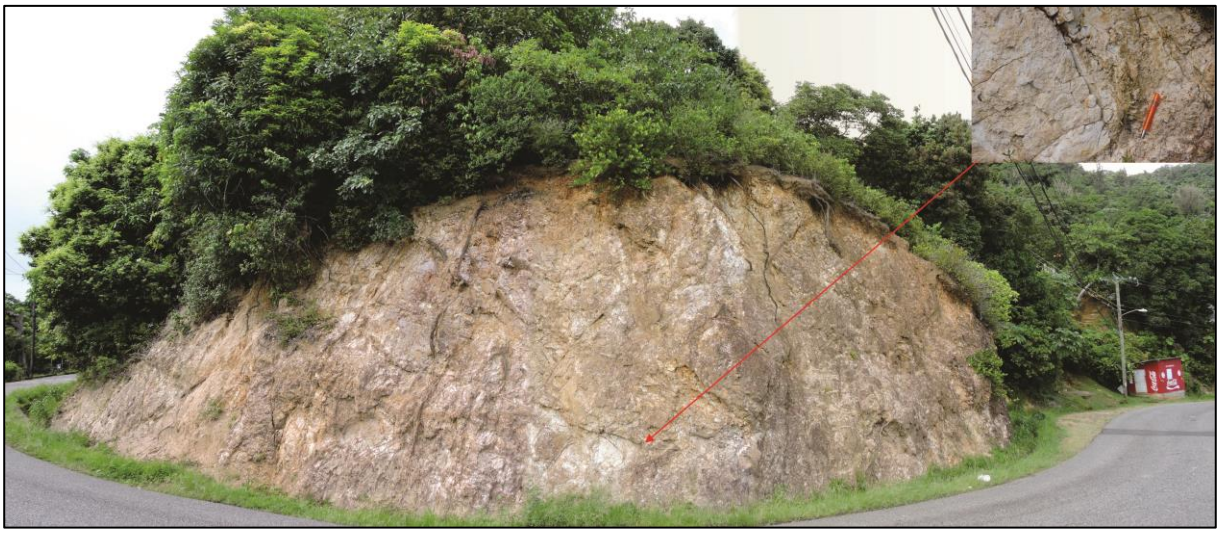

Figure 46: Cut slope L6 (direction of view 045 degrees)

Figure 47: Cut slope L7

Figure 48: Cut slope L8

Figure 49: Cut slope L9

Figure 50: Cut slope L10

Figure 51: Cut slope L11

Figure 52: Cut slope L12

Table 16: Geotechnical data and parameters

	ID	E	N	SDD	SD	H	Exp. Yrs	SIRS	RIRS	WE(in)	FRI(in)	SCOH(in)	SPA(in)	IRS	WE	SFRI (Deg)	SCOH (Pa)	(KPa)	SPA
AGGLOMERATES																			
SLIGHTLY	L7	710870	1534061	34	83	9	22	125.40	132	1	59.6	27815.0	0.5	150	0.95	56.7	26424.206	26.42	0.5
	L3G3	728077	1538164	28	80	5	42	118.80	132	1	54.3	24924.8	0.4	75	0.9	48.8	22432.278	22.43	0.3
MODERATE	L2G4	714355	1547603	292	88	9	9	75.00	83	1	36.5	17151.8	0.2	100	0.9	32.9	15436.622	15.44	0.2
	L2G5	714355	1547603	291	85	6	9	75.00	83	1	48.3	23519.4	0.5	100	0.9	43.4	21167.424	21.17	0.4
	L4G2	728077	1538164	54	88	10	22	75.00	83	1	48.5	23713.4	0.5	75	0.9	43.6	21342.024	21.34	0.4
	L8	709161	1537437	74	75	6	22	75.00	83	1	39.0	18438.0	0.3	75	0.9	35.1	16594.171	16.59	0.3
	L8B	709161	1537437	100	75	6	22	75.00	83	1	33.9	15607.7	0.2	75	0.9	30.5	14046.941	14.05	0.1
HIGHLY	L1G1	714355	1547603	94	71	3.5	9	8.75	14	1	16.2	8604.1	0.2	8.75	0.62	10.0	5334.5558	5.33	0.1
	L1G1b	714355	1547603	94	71	3.5	9	8.75	14	1	35.1	19022.3	0.5	8.75	0.62	21.8	11793.84	11.79	0.3
	L3G2	728077	1538164	40	65	5	42	7.50	12	1	29.1	15779.6	0.4	8.75	0.62	18.1	9783.3242	9.78	0.3
	L4G1	728077	1538164	54	88	10	42	31.25	50	1	52.3	27162.7	0.7	31.25	0.62	32.4	16840.878	16.84	0.4
	L9G1	708905	1537619	50	85	3.5	22	31.25	50	1	54.6	28346.2	0.7	31.25	0.62	33.8	17574.616	17.57	0.4
	L12G1	710594	1533993	233	81	5	22	31.25	50	1	41.5	21142.3	0.5	31.25	0.62	25.7	13108.218	13.11	0.3
	L12G2	710014	1539312	49	75	5	22	31.25	50	1	54.0	28042.9	0.7	31.25	0.62	33.5	17386.577	17.39	0.4
	L3G1	728077	1538164	40	65	5	42	3.13	5	1	49.8	27421.4	0.9	3.125	0.62	30.9	17001.273	17.00	0.5
	L3G4	728077	1538164	38	67	5	42	3.13	5	1	30.0	23519.4	0.5	3.125	0.62	18.6	10290.898	10.29	0.3
	L4G3	728077	1538164	54	88	10	42	3.13	5	1	34.0	18758.7	0.6	3.125	0.62	21.1	11630.39	11.63	0.3
	L5G2	727727	1539591	75	80	4	42	3.13	5	1	49.9	27658.6	0.8	3.125	0.62	31.0	17148.349	17.15	0.5
	L10G1	708905	1537619	37	82	2.7	22	3.13	5	1	44.2	24362.2	0.8	3.125	0.62	27.4	15104.547	15.10	0.5
TUFF																			
MODERATELY	L2G1	714355	1547603	282	89	14	9	31.25	35	1	41.9	21928.2	0.6	31.25	0.9	37.7	19735.414	19.74	0.5
	L2G1B	714355	1547603	282	89	14	9	31.25	35	1	29.8	15350.5	0.3	31.25	0.9	26.8	13815.419	13.82	0.3
	L2G1C	714355	1547603	282	89	14	9	31.25	35	1	18.4	9133.5	0.1	31.25	0.9	16.5	8220.1114	8.22	0.1
	V6REF	690466	1457238	306	65	3	0.6	31.25	35	1	22.0	10987.1	0.2	31.25	0.9	19.8	9888.3507	9.89	0.2
HIGHLY	L1G2	714355	1547603	105	70	6	9	8.75	14	1	30.8	16754.0	0.4	8.75	0.62	19.1	10387.466	10.39	0.3
	V2G1	701475	1458474	170	81	15	9	3.13	5	1	32.0	17673.9	0.5	3.125	0.62	19.8	10957.801	10.96	0.3
	V4G1	687372	1462615	232	80	3	14	3.13	5	1	37.1	20598.3	0.6	3.125	0.62	23.0	12770.974	12.77	0.4
	L5G1	727727	1539591	75	80	4	42	3.13	9	1	40.6	22383.0	0.6	3.125	0.35	14.2	7834.0556	7.83	0.2
	L6G1	716375	1547592	146	85	7	8	3.13	9	1	61.2	33684.4	1.0	3.125	0.35	21.4	11789.553	11.79	0.4
	L6G2	716375	1547592	217	75	7	8	3.13	9	1	51.2	28200.1	0.8	3.125	0.35	17.9	9870.0219	9.87	0.3
	L9G2	708905	1537619	50	85	3.5	22	3.13	9	1	83.6	46026.0	1.5	3.125	0.35	29.3	16109.096	16.11	0.5
	L10G2	708905	1537619	37	82	2.7	22	3.13	9	1	66.6	36689.3	1.1	3.125	0.35	23.3	12841.268	12.84	0.4
	V1G4	700268	1455352	94	70	9	8	1.25	4	1	114.2	63013.8	2.1	1.25	0.35	40.0	22054.823	22.05	0.7
	V3G1	687450	1462569	302	85	7	14	1.25	2	1	21.6	12212.2	0.3	1.25	0.35	13.4	7571.5464	7.57	0.2
	V5G1	701757	1458825	112	80	9	9	8.75	14	1	21.3	11445.6	0.3	3.125	0.62	13.2	7096.28	7.10	0.2
ANDESITE																			
SLIGHTLY	L11	712362	1543261	80	87	3	8	75.00	79	1	39.8	19066.5	0.3	150	0.95	37.8	18113.207	18.11	0.3
	V2G3	701475	1458474	170	81	15	9	125.40	132	1	44.7	19677.9	0.2	150	0.95	42.5	18693.98	18.69	0.2
	V3G2	687450	1462569	302	85	7	9	125.40	132	1	49.6	22472.0	0.3	150	0.95	47.1	21348.391	21.35	0.2
MODERATELY	L2G2	714355	1547603	154	70	6	9	31.25	35	1	39.4	20608.5	0.5	31.25	0.9	35.5	18547.664	18.55	0.5
	L2G3	714355	1547603	282	80	9	9	75.00	83	1	49.1	23980.8	0.5	75	0.9	44.2	21582.675	21.58	0.4
	V2G2	701475	1458474	170	81	15	9	31.25	35	1	21.9	18271.8	0.5	31.25	0.9	19.7	9779.8437	9.78	0.2
	V2G5	701475	1458474	88	50	7	9	75.00	83	1	38.9	18391.3	0.3	75	0.9	35.0	16552.206	16.55	0.3
	V4G3B	687372	1462615	232	80	6	28	31.25	35	1	26.5	13437.3	0.3	31.25	0.9	23.8	12093.582	12.09	0.2
HIGHLY	V4G3	687372	1462615	232	80	6	28	31.25	35	1	26.9	13664.4	0.3	31.25	0.62	24.2	12297.963	12.30	0.3
PYRO																			
MOERATELY	V4G2	687372	1462615	232	80	4	28	29.61	33	1	28.0	14377.3	0.3	31.25	0.9	25.2	12939.611	12.94	0.3
	V2G1B	701475	1458474	170	81	15	9	8.75	14	1	21.5	11513.8	0.5	8.75	0.9	13.3	7138.5279	7.14	0.2
HIGHLY	V1G2	700268	1455352	94	70	9	8	8.75	14	1	22.5	12133.7	0.3	3.125	0.62	13.9	7522.9186	7.52	0.2
	V5G2	701757	1458825	112	80	9	9	3.13	5	1	50.0	27567.4	0.9	8.75	0.62	31.0	17091.814	17.09	0.5
BASALTS																			
SLIGHTLY	V7G1	700952	1453659	130	70	40	1	118.80	132	1	56.0	26027.9	0.4	150	0.95	50.4	23425.067	23.43	0.3
	V7G2	700952	1453659	130	50	40	1	118.80	132	1	66.5	31630.5	0.6	150	0.95	59.8	28467.481	28.47	0.6
MODERATELY	V2G4	701475	1458474	170	81	15	9	31.25	35	1	34.2	17671.5	0.4	31.25	0.9	30.8	15904.321	15.90	0.4
	V8	691408	1455812	128	45	10	8	118.80	132	1	57.0	26571.5	0.4	100	0.9	51.3	23914.353	23.91	0.4
HIGHLY	V1G1	700268	1455352	94	70	9	8	8.75	14	1	55.7	30293.6	0.9	8.75	0.62	34.5	18782.031	18.78	0.6
	V1G3	700268	1455352	94	70	9	8	8.75	14	1	33.6	18271.8	0.5	8.75	0.62	20.8	11328.541	11.33	0.3
	V1G5	700268	1455352	160	75	9	8	3.40	10	1	43.2	23538.5	0.7	3.125	0.35	15.1	8238.4685	8.24	0.7

	ID	Log(1-t)	ΔIRS	Δ WE	ΔFRI	ΔSCOH	ΔSPA	D.Rate (IRS)	Rate (WE)	D.Rate (FRI)	D.Rate (SCOH)	D.Rate (SPA)
AGGLOMERATES												
SLIGHTLY	L7	1.36	6.60	0.05	3.0	1.4	0.025	4.847	0.037	2.190	1.021	0.018
	L3G3	1.63	13.20	0.10	5.4	2.5	0.038	8.081	0.061	3.322	1.526	0.023
MODERAT	L2G4	1.00	8.33	0.10	3.7	1.7	0.023	8.333	0.100	3.652	1.715	0.023
	L2G5	1.00	8.33	0.10	4.8	2.4	0.048	8.333	0.100	4.827	2.352	0.048
	L4G2	1.36	8.33	0.10	4.8	2.4	0.047	6.120	0.073	3.560	1.741	0.034
	L8	1.36	8.33	0.10	3.9	1.8	0.030	6.120	0.073	2.862	1.354	0.022
	L8B	1.36	8.33	0.10	3.4	1.6	0.069	6.120	0.073	2.490	1.146	0.051
HIGHLY	L1G1	1.00	5.36	0.38	6.2	3.3	0.067	5.363	0.380	6.151	3.270	0.067
	L1G1b	1.00	5.36	0.38	13.4	7.2	0.205	5.363	0.380	13.354	7.228	0.205
	L3G2	1.63	4.60	0.38	11.1	6.0	0.166	2.814	0.233	6.776	3.671	0.102
	L4G1	1.63	19.15	0.38	19.9	10.3	0.257	11.725	0.233	12.173	6.319	0.157
	L9G1	1.36	19.15	0.38	20.7	10.8	0.309	14.065	0.279	15.223	7.910	0.227
	L12G1	1.36	19.15	0.38	15.8	8.0	0.182	14.065	0.279	11.568	5.900	0.134
	L12G2	1.36	19.15	0.38	20.5	10.7	0.275	14.065	0.279	15.082	7.826	0.202
	L3G1	1.63	1.92	0.38	18.9	10.4	0.326	1.173	0.233	11.576	6.379	0.199
	L3G4	1.63	1.92	0.38	11.4	13.2	0.177	1.173	0.233	6.976	8.098	0.109
	L4G3	1.63	1.92	0.38	12.9	7.1	0.213	1.173	0.233	7.917	4.364	0.130
	L5G2	1.63	1.92	0.38	19.0	10.5	0.312	1.173	0.233	11.616	6.434	0.191
	L10G1	1.36	1.92	0.38	16.8	9.3	0.287	1.407	0.279	12.342	6.798	0.211
TUFF												
MODERAT	L2G1	1.00	3.47	0.10	4.2	2.2	0.057	3.472	0.100	4.188	2.193	0.057
	L2G1B	1.00	3.47	0.10	3.0	1.5	0.032	3.472	0.100	2.975	1.535	0.032
	L2G1C	1.00	3.47	0.10	1.8	0.9	0.009	3.472	0.100	1.836	0.913	0.009
	V6REF	0.20	3.47	0.10	2.2	1.1	0.020	17.011	0.490	10.779	5.383	0.097
HIGHLY	L1G2	1.00	5.36	0.38	11.7	6.4	0.160	5.363	0.380	11.695	6.367	0.160
	V2G1	1.00	1.92	0.38	12.1	6.7	0.192	1.915	0.380	12.142	6.716	0.192
	V4G1	1.18	1.92	0.38	14.1	7.8	0.219	1.629	0.323	11.980	6.655	0.186
	L5G1	1.63	5.80	0.65	26.4	14.5	0.406	3.553	0.398	16.156	8.907	0.249
	L6G1	0.95	5.80	0.65	39.8	21.9	0.663	6.082	0.681	41.670	22.945	0.695
	L6G2	0.95	5.80	0.65	33.3	18.3	0.545	6.082	0.681	34.909	19.209	0.571
	L9G2	1.36	5.80	0.65	54.4	29.9	0.943	4.262	0.477	39.926	21.970	0.692
	L10G2	1.36	5.80	0.65	43.3	23.8	0.731	4.262	0.477	31.812	17.513	0.537
	V1G4	0.95	2.32	0.65	74.2	41.0	1.340	2.433	0.681	77.785	42.923	1.404
	V3G1	1.18	0.77	0.65	8.2	4.6	0.111	0.651	0.553	6.979	3.946	0.094
	V5G1	1.00	5.36	0.38	8.1	4.3	0.102	5.363	0.380	8.100	4.349	0.102
ANDESITE												
SLIGHTLY	L11	0.95	3.95	0.05	2.0	1.0	0.016	4.137	0.052	2.083	0.999	0.017
	V2G3	1.00	6.60	0.05	2.2	1.0	0.009	6.600	0.050	2.235	0.984	0.009
	V3G2	1.00	6.60	0.05	2.5	1.1	0.013	6.600	0.050	2.481	1.124	0.013
MODERAT	L2G2	1.00	3.47	0.10	3.9	2.1	0.016	3.472	0.100	3.943	2.061	0.016
	L2G3	1.00	8.33	0.10	4.9	2.4	0.049	8.333	0.100	4.908	2.398	0.049
	V2G2	1.00	3.47	0.10	2.2	8.5	0.284	3.472	0.100	2.191	8.492	0.284
	V2G5	1.00	8.33	0.10	3.9	1.8	0.030	8.333	0.100	3.891	1.839	0.030
	V4G3B	1.46	3.47	0.10	2.6	1.3	0.112	2.374	0.068	1.809	0.919	0.077
HIGHLY	V4G3	1.46	3.47	0.38	2.7	1.4	0.030	2.374	0.260	1.842	0.934	0.021
PYRO												
MOERATE	V4G2	1.46	3.29	0.10	2.8	1.4	0.015	2.249	0.068	1.912	0.983	0.011
	V2G1B	1.00	5.36	0.10	8.2	4.4	0.304	5.363	0.100	8.165	4.375	0.304
HIGHLY	V1G2	0.95	5.36	0.38	8.5	4.6	0.105	5.620	0.398	8.948	4.832	0.110
	V5G2	1.00	1.92	0.38	19.0	10.5	0.328	1.915	0.380	19.015	10.476	0.328
BASALTS												
SLIGHTLY	V7G1	0.30	13.20	0.05	5.6	2.6	0.037	43.849	0.166	18.607	8.646	0.124
	V7G2	0.30	13.20	0.05	6.6	3.2	0.061	43.849	0.166	22.087	10.507	0.204
MODERAT	V2G4	1.00	3.47	0.10	3.4	1.8	0.044	3.472	0.100	3.421	1.767	0.044
	V8	0.95	13.20	0.10	5.7	2.7	0.039	13.833	0.105	5.976	2.785	0.041
HIGHLY	V1G1	0.95	5.36	0.38	21.2	11.5	0.354	5.620	0.398	22.164	12.064	0.371
	V1G3	0.95	5.36	0.38	12.8	6.9	0.181	5.620	0.398	13.364	7.276	0.190
	V1G5	0.95	6.32	0.65	28.1	15.3	0.073	6.622	0.681	29.401	16.034	0.076
							AVG RATES	IRS	WE	FRI	COH	SPA
							AGGLO	6.395	0.199	8.087	4.477	0.113
							TUFF	4.601	0.413	20.862	11.435	0.338
							ANDESITE	5.077	0.098	2.820	2.194	0.057
							PYRO	3.787	0.237	9.510	5.166	0.188
							BASALT	17.552	0.288	16.431	8.440	0.150